Diagenesis and reservoir characteristics of Upper Devonian Leduc dolostones, southern Rimbey-Meadowbrook reef trend, central Alberta.

by

Eva Drivet

Department of Earth and Planetary Sciences
McGill University
Montreal, Canada

December, 1993

A thesis submitted to the Faculty of Graduate Studies and Research in partial
fulfilment of the requirements
for the degree of Master of Science

Name __Drivet Eva__

Earth Sciences , Geology

SUBJECT TERM

| 0 | 3 | 7 | 2 |

U·M·I

SUBJECT CODE

Subject Categories

THE HUMANITIES AND SOCIAL SCIENCES

COMMUNICATIONS AND THE ARTS
Architecture	0729
Art History	0377
Cinema	0900
Dance	0378
Fine Arts	0357
Information Science	0723
Journalism	0391
Library Science	0399
Mass Communications	0708
Music	0413
Speech Communication	0459
Theater	0465

EDUCATION
General	0515
Administration	0514
Adult and Continuing	0516
Agricultural	0517
Art	0273
Bilingual and Multicultural	0282
Business	0688
Community College	0275
Curriculum and Instruction	0727
Early Childhood	0518
Elementary	0524
Finance	0277
Guidance and Counseling	0519
Health	0680
Higher	0745
History of	0520
Home Economics	0278
Industrial	0521
Language and Literature	0279
Mathematics	0280
Music	0522
Philosophy of	0998
Physical	0523

Psychology	0525
Reading	0535
Religious	0527
Sciences	0714
Secondary	0533
Social Sciences	0534
Sociology of	0340
Special	0529
Teacher Training	0530
Technology	0710
Tests and Measurements	0288
Vocational	0747

LANGUAGE, LITERATURE AND LINGUISTICS
Language	
General	0679
Ancient	0289
Linguistics	0290
Modern	0291
Literature	
General	0401
Classical	0294
Comparative	0295
Medieval	0297
Modern	0298
African	0316
American	0591
Asian	0305
Canadian (English)	0352
Canadian (French)	0355
English	0593
Germanic	0311
Latin American	0312
Middle Eastern	0315
Romance	0313
Slavic and East European	0314

PHILOSOPHY, RELIGION AND THEOLOGY
Philosophy	0422
Religion	
General	0318
Biblical Studies	0321
Clergy	0319
History of	0320
Philosophy of	0322
Theology	0469

SOCIAL SCIENCES
American Studies	0323
Anthropology	
Archaeology	0324
Cultural	0326
Physical	0327
Business Administration	
General	0310
Accounting	0272
Banking	0770
Management	0454
Marketing	0338
Canadian Studies	0385
Economics	
General	0501
Agricultural	0503
Commerce Business	0505
Finance	0508
History	0509
Labor	0510
Theory	0511
Folklore	0358
Geography	0366
Gerontology	0351
History	
General	0578

Ancient	0579
Medieval	0581
Modern	0582
Black	0328
African	0331
Asia, Australia and Oceania	0332
Canadian	0334
European	0335
Latin American	0336
Middle Eastern	0333
United States	0337
History of Science	0585
Law	0398
Political Science	
General	0615
International Law and Relations	0616
Public Administration	0617
Recreation	0814
Social Work	0452
Sociology	
General	0626
Criminology and Penology	0627
Demography	0938
Ethnic and Racial Studies	0631
Individual and Family Studies	0628
Industrial and Labor Relations	0629
Public and Social Welfare	0630
Social Structure and Development	0700
Theory and Methods	0344
Transportation	0709
Urban and Regional Planning	0999
Women's Studies	0453

THE SCIENCES AND ENGINEERING

BIOLOGICAL SCIENCES
Agriculture	
General	0473
Agronomy	0285
Animal Culture and Nutrition	0475
Animal Pathology	0476
Food Science and Technology	0359
Forestry and Wildlife	0478
Plant Culture	0479
Plant Pathology	0480
Plant Physiology	0817
Range Management	0777
Wood Technology	0746
Biology	
General	0306
Anatomy	0287
Biostatistics	0308
Botany	0309
Cell	0379
Ecology	0329
Entomology	0353
Genetics	0369
Limnology	0793
Microbiology	0410
Molecular	0307
Neuroscience	0317
Oceanography	0416
Physiology	0433
Radiation	0821
Veterinary Science	0778
Zoology	0472
Biophysics	
General	0786
Medical	0760

EARTH SCIENCES
Biogeochemistry	0425
Geochemistry	0996

Geodesy	0370
Geology	0372
Geophysics	0373
Hydrology	0388
Mineralogy	0411
Paleobotany	0345
Paleoecology	0426
Paleontology	0418
Paleozoology	0985
Palynology	0427
Physical Geography	0368
Physical Oceanography	0415

HEALTH AND ENVIRONMENTAL SCIENCES
Environmental Sciences	0768
Health Sciences	
General	0566
Audiology	0300
Chemotherapy	0992
Dentistry	0567
Education	0350
Hospital Management	0769
Human Development	0758
Immunology	0982
Medicine and Surgery	0564
Mental Health	0347
Nursing	0569
Nutrition	0570
Obstetrics and Gynecology	0380
Occupational Health and Therapy	0354
Ophthalmology	0381
Pathology	0571
Pharmacology	0419
Pharmacy	0572
Physical Therapy	0382
Public Health	0573
Radiology	0574
Recreation	0575

Speech Pathology	0460
Toxicology	0383
Home Economics	0386

PHYSICAL SCIENCES

Pure Sciences
Chemistry	
General	0485
Agricultural	0749
Analytical	0486
Biochemistry	0487
Inorganic	0488
Nuclear	0738
Organic	0490
Pharmaceutical	0491
Physical	0494
Polymer	0495
Radiation	0754
Mathematics	0405
Physics	
General	0605
Acoustics	0986
Astronomy and Astrophysics	0606
Atmospheric Science	0608
Atomic	0748
Electronics and Electricity	0607
Elementary Particles and High Energy	0798
Fluid and Plasma	0759
Molecular	0609
Nuclear	0610
Optics	0752
Radiation	0756
Solid State	0611
Statistics	0463

Applied Sciences
Applied Mechanics	0346
Computer Science	0984

Engineering	
General	0537
Aerospace	0538
Agricultural	0539
Automotive	0540
Biomedical	0541
Chemical	0542
Civil	0543
Electronics and Electrical	0544
Heat and Thermodynamics	0348
Hydraulic	0545
Industrial	0546
Marine	0547
Materials Science	0794
Mechanical	0548
Metallurgy	0743
Mining	0551
Nuclear	0552
Packaging	0549
Petroleum	0765
Sanitary and Municipal	0554
System Science	0790
Geotechnology	0428
Operations Research	0796
Plastics Technology	0795
Textile Technology	0994

PSYCHOLOGY
General	0621
Behavioral	0384
Clinical	0622
Developmental	0620
Experimental	0623
Industrial	0624
Personality	0625
Physiological	0989
Psychobiology	0349
Psychometrics	0632
Social	0451

Short title:

**Diagenesis and reservoir study of
Upper Devonian dolostones,
Alberta subsurface**

"Quelle que soit la puissance du télescope ou du microscope, le problème est toujours le même; il s'agit de se rendre maître d'une apparence, par une vue de l'esprit libre, qui fait naître et renaître ensemble le doute et la preuve"

ALAIN
Propos (Le courage de l'esprit)

GENERAL ABSTRACT

Dolomitization of the Leduc Formation (Upper Devonian) along the southern part of the Rimbey-Meadowbrook trend in central Alberta occurred early by pervasive replacement, and later by minor cementation. Replacive dolomitization postdates submarine cementation and deposition of overlying shales, overlaps stylolitization, and produces $\delta^{18}O$ values indicating precipitation between 45 and 75°C. Therefore, this dolomitization likely originated at burial depths of more than 500 m. Strontium isotope ratios suggest that dolomitizing fluids were slightly more radiogenic than Upper Devonian sea water. Dolomite cements, however, are slightly depleted in oxygen-18, and contain primary fluid inclusions with high homogenization temperatures and salinities reflecting the different fluids responsible for their formation.

The distribution of pore types is governed by depositional facies, whereas effective porosity and permeability are strongly controlled by post-depositional processes. Late-stage cementation (anhydrite, dolomite, calcite, and native sulphur) reduces porosity. This cementation decreases northward, resulting in better reservoirs north of the Medicine River field, above present depths of 3000 m. Replacement dolomitization modified original pore type distribution, improved permeability, and helped retain porosity because dolomites are more resistant to pressure solution than limestones. Burial dissolution of dolomites may have been induced by mixing corrosion, maturation of organic matter, and thermochemical sulphate reduction.

SOMMAIRE

Deux épisodes majeurs de dolomitisation se distinguent au sein de la Formation Leduc (Dévonien Supérieur) située dans la partie sud de l'alignement de récifs Rimbey-Meadowbrook dans l'Aberta centrale: une dolomitisation de remplacement abondante précédant une cimentation mineure par dolomite. Les dolomites de remplacement sont postérieures à la cimentation sous-marine et aux dépôts d'argile sus-jacents. Elles se chevauchent avec les stylolites et ont des signatures isotopiques d'oxygène qui reflètent des températures de précipitation variant entre 45 et 75°C. Par conséquent, la dolomitisation de remplacement a débuté à des profondeurs de plus de 500 m, durant le Dévonien Supérieur ou après. Les rapports isotopiques du strontium indiquent que les fluides de dolomitisation étaient légèrement plus radiogéniques que l'eau de mer du Dévonien Supérieur. Comparés aux dolomites de remplacement, les ciments de dolomite sont appauvris en oxygène-18. Ils renferment des inclusions de fluides primaires qui révèlent des températures d'homogénéisation et des salinités élevées Ces données reflètent la composition différente et les températures plus chaudes des fluides qui ont précipité les ciments de dolomite.

La distribution des différents types de pores est contrôlée par la nature des lithofaciès. Cependant, la porosité et la permeabilité effective sont fortement affectées par la diagénèse. La cimentation tardive (anhydrite, dolomite, calcite, et soufre) a graduellement réduit la porosité. L'abondance des ciments diminue vers le nord, ce qui explique l'amélioration de la qualité des réservoirs au nord de Medicine River, à une profondeur d'enfouissement inférieure à 3000 m. La dolomitisation de remplacement a modifié la distribution originale des pores, a amélioré la perméabilité, et a permis de mieux préserver la porosité durant l'enfouissement, la dolomie étant plus résistante à la pression-dissolution que le calcaire. Des phases de dissolution se sont produites durant et après la dolomitization d'enfouissement, et ont put être engendrées par des processus tels que la corrosion résultant du mélange de fluides avec des compositions et des températures differentes, la maturation de matières organiques, et la réduction thermochimique de sulfate.

TABLE OF CONTENTS

"Origin of Upper Devonian Leduc dolostones, southern Rimbey-Meadowbrook reef trend, Alberta: new textural and geochemical evidence"

"Reservoir characteristics and porosity evolution in Upper Devonian Leduc dolomites, southern Rimbey-Meadowbrook reef trend, Alberta"

LIST OF FIGURES

LIST OF TABLES

LIST OF PLATES

LIST OF APPENDICES

PREFACE

The following statements are made in fulfilment of the "Guidelines Concerning Thesis Preparation" of McGill University.

This research project was initiated in June of 1991 under the supervision of Dr. Eric W. Mountjoy of McGill University. Dr. Mountjoy suggested the project based upon his previous work on subsurface Devonian Leduc dolomites in the Western Canadian sedimentary basin (Laflamme, 1990; Amthor et al., 1993; Chouinard, 1993; Marquez, Ph.D. in progress). Two summers (1991 and 1992) were spent studying cores at the Energy Resources Conservation Board (ERCB) core lab in Calgary, and data were collected by the author, Dr. Mountjoy, and Dr. Amthor from seven fields: Homeglen-Rimbey, Gilby, Medicine River, Sylvan Lake, Lanaway, Garrington, and Bearberry. This manuscript is a synthesis of the author's observations and interpretations of the Leduc dolomites at these locations. Responsibility for the content of this thesis rests with the author, except where indicated in the text. Dr. Mountjoy's name appears as junior author on the manuscripts contained within the thesis, having served as a supervisor, editor, and having assisted in the field during the tenure of this project.

Thesis format

This thesis is comprised of four chapters. Chapter 1 is the general introduction. Chapter 2 is entitled, "Origin of Upper Devonian Leduc dolostones, southern Rimbey-Meadowbrook reef trend, Alberta: new textural and geochemical evidence". It is a synthesis of observations and interpretations regarding the diagenesis, with special emphasis on the origin and timing of dolomitization. Chapter 3 is entitled, "Reservoir characteristics and porosity evolution in Upper Devonian Leduc dolomites, southern Rimbey-Meadowbrook reef trend, Alberta". Depositional facies and pore types are mapped and correlated in the Homeglen-Rimbey field to outline in detail the reservoir characteristics of the Leduc dolostones for this part of the trend. Chapter 3 also focuses on the effect of diagenesis, particularly dolomitization, on porosity evolution and uses the

interpretations in Chapter 2 regarding the origin of dolomites to constrain the environments of porosity generation. As such, chapters 2 and 3 complement one another. The general conclusions of the thesis, Chapter 4, are derived from the specific conclusions in chapters 2 and 3.

Chapters 2 and 3 are written as manuscripts for journal publication, and thus some repetition is unavoidable. An abstract that includes aspects of both chapters precedes this preface. A comprehensive reference list, and appendices are included at the end of the thesis. The descriptions of the wells logged are on file in the Department of Earth and Planetary Sciences, McGill University, c/o Dr. Eric W. Mountjoy.

Original contributions to knowledge

In recent years, the petrography and geochemistry of the dolomitized Leduc buildups and underlying Cooking Lake platform have been studied along the deeper (Laflamme, 1990; Marquez, Ph.D. thesis in progress) and shallower (Machel et al., 1991; McNamara and Wardlaw, 1991; Amthor et al., 1993; Chouinard, 1993) portions of the Rimbey-Meadowbrook reef trend. The field area in this study overlaps geographically with these previously or currently studied fields and consists of carbonate reservoirs buried at depths of 2300 m to 3500 m. Chapter 2 of this dissertation reports new petrographic and geochemical data, (in particular carbon, oxygen, strontium isotopes and fluid inclusions), and integrates information already documented along the reef trend. Chapter 3 presents, for the first time, correlations of depositional facies and facies distribution maps of the extensively dolomitized Leduc Formation in the Homeglen-Rimbey field, and relates them to porosity and permeability. The main contributions of chapters 2 and 3 are:

1. The diagenetic paragenesis for the intermediate burial portion of the Rimbey-Meadowbrook reef trend is established.

2. Six types of dolomite are described including a fine-crystalline dolomite (30 to 60 μm) that has never been reported before and may, in part, represent a precursor dolomite prior to neomorphism. The

origin and timing of these dolomites are established on the basis of their spatial distribution, petrographic characteristics, paragenesis, and geochemistry.

3. The replacement dolomites in the intermediate burial part of the Rimbey-Meadowbrook trend (2300 to 3500 m) are very similar texturally and geochemically to those from the deepest and shallowest portions of the trend, and probably originated in the shallow to intermediate burial environment.

4. New petrographic evidence for dolomite neomorphism are presented. They include: a) the distribution of crystals of Dolomite-R1 (30 to 60 μm) interstitial to and within coarser replacement dolomite crystals (60 to 250 μm); b) textural modification near fractures and pores of replacement dolomite to coarser, nonplanar crystals with undulose extinction; c) bright and dull luminescent bands of replacement dolomites along fractures; and d) zones of dolomite crystals that selectively replace the cloudy core of Dolomite-R2 crystals. The scarcity of these textures suggests that neomorphism of the Leduc dolomites was localised to a few fractures, stylolites, and pores.

5. Late-stage diagenesis include anhydrite and blocky calcite cements, and free sulphur and may be related to thermochemical sulphate reduction reactions.

6. Mapping of the depositional facies and pore systems in the Homeglen-Rimbey field combined with mapping of the main diagenetic cements contribute to the first detailed outline of the reservoir character for this part of the Rimbey-Meadowbrook reef trend.

7. Description of the fracturing and dissolution phases suggests that secondary porosity may have been generated, in part, in the deep burial environment. This result has important implications for hydrocarbon exploration: secondary porosity by deep burial solution

that occurs close to the onset of hydrocarbon maturation and migration is less likely to be further modified than porosity generated in the near surface environment.

General acknowledgements

CHAPTER 1

GENERAL INTRODUCTION

Upper Devonian Leduc carbonate buildups are located in the subsurface of Alberta, along the Rimbey-Meadowbrook reef trend (Fig.1). The Leduc Formation overlies the Cooking Lake platform and is enclosed in basinal shales of the Ireton and Duvernay formations (Fig. 2). The Leduc buildups have been extensively dolomitized, except for a few slightly dolomitized buildups; Golden Spike, Redwater, and Strachan D3B. The limestone Leduc buildups have been discussed in detail, both in terms of their depositional environment and diagenesis (e.g. McGillivray and Mountjoy, 1975; Walls, 1977; Carpenter and Lohmann, 1989; Wendte et al., 1992). Recent studies deal mostly with the petrography and geochemistry of the dolomitized Leduc buildups and underlying Cooking Lake platform along the shallowest and deepest portions of the Rimbey-Meadowbrook reef trend (Laflamme, 1990; McNamara and Wardlaw, 1991; Marquez et al., 1992; Amthor et al., 1993; Chouinard, 1993). They document the presence of two main types of dolomites: a widespread and abundant dolomite that replaced the original limestones, and a later minor dolomite cement that fills pores. On the basis of mass balance calculations, Amthor et al. (1993) concluded that an extensive regional fluid-flow system was necessary for complete dolomitization during early burial of the Rimbey-Meadowbrook reef trend. However, the source of these fluids, the extent of the regional fluid-flow system, as well as a suitable dolomitizing mechanism are still uncertain. The present thesis area overlaps geographically with these previously studied fields and consists of intermediately buried (2300 m to 3500 m) carbonate reservoirs (Figs. 1 and 3; Table 1). Thus, our findings link the information on the diagenesis, in particular on the dolomites, already described updip and downdip of the field area. The objectives of Chapter 2 are: 1) to document new petrographic and geochemical data on the Leduc dolomites in order to better constrain their origin; 2) to examine the effects of increased burial on the distribution of the diagenetic cements; and 3) to investigate potential evidence for thermochemical sulphate reduction related reactions.

Figure 1. Map of the Rimbey-Meadowbrook reef trend showing the distribution of Leduc buildups, extent of dolomitization in the Cooking Lake carbonate platform (modified from Amthor et al., 1993), and the location of the study area. Buildups are dolomitized where the margin of the Cooking Lake platform is dolomitized. Golden Spike and Redwater are situated off the margin and are not dolomitized, except for the westernmost part of Redwater (west of the dotted line). Townships and ranges are indicated and each are 9.7 km (6 miles across). "5th" refers to the fifth meridian (116°W longitude).

Redwater

Morinville

R1 R27

5th

R20

T55

Acheson

Edmonton

Golden Spike

Leduc

T50

West Ireton Shale Basin

East Ireton Shale Basin

Wizard Lake

Western Margin of
Cooking Lake Platform

Bonnie Glen

Westerose

Extent of dolomitized
Cooking Lake

T45

STUDY AREA

Homeglen Rimbey

T40

20 km

Strachan

Medicine River

?

Sylvan Lake

?

Lanaway

Ricinus

Garrington

T35 West

Bearberry

Harmattan

R10

R5

R1

R28

R20

T50

T45

T40

T35

5th

3
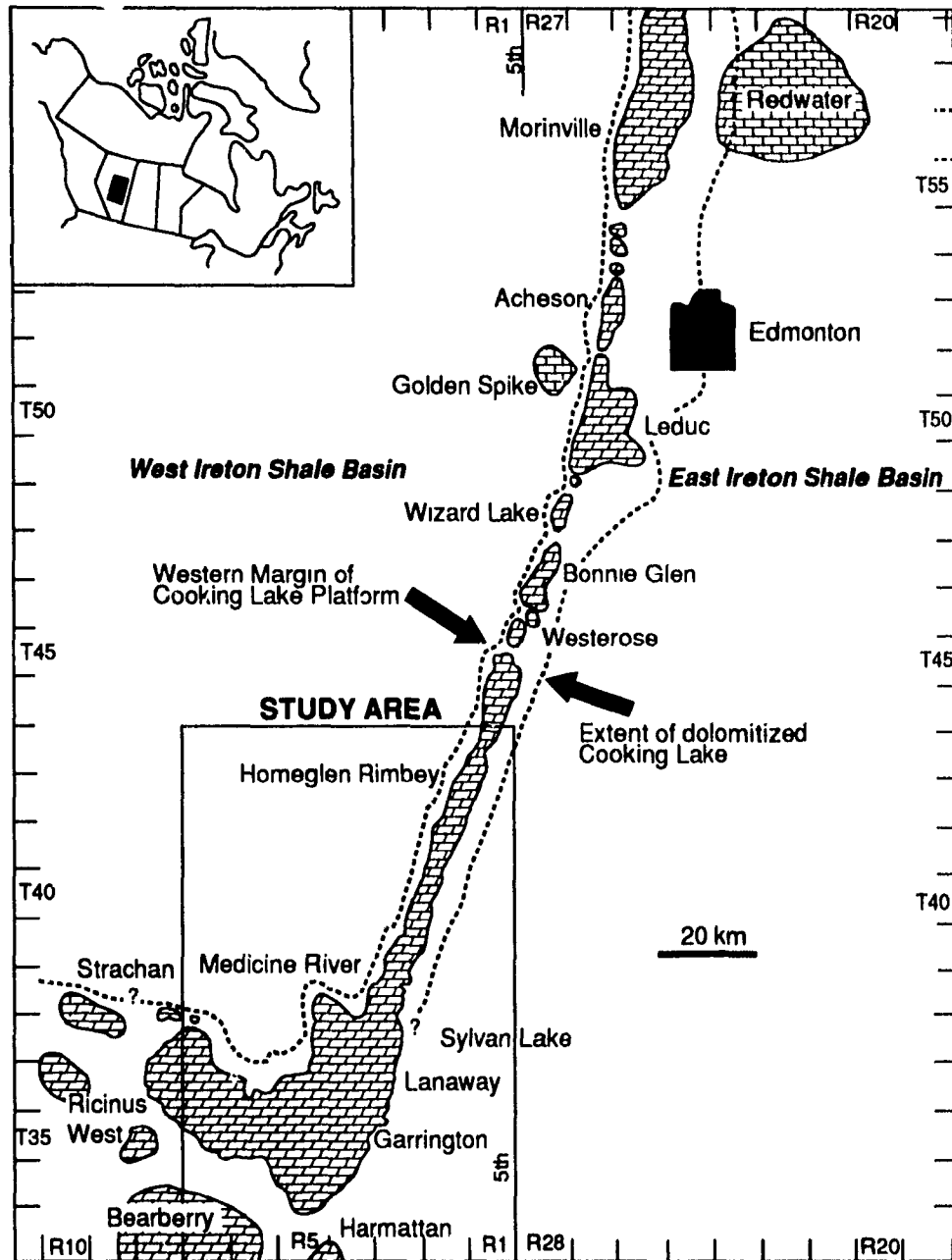
Figure 2. Schematic subsurface Devonian stratigraphy of central Alberta illustrating the relationships of the Cooking Lake Formation platform, overlying Leduc Formation buildups, and adjacent basin sediments (Duvernay Formation source beds and ireton Formation basin fill) (after Stoakes, 1980).

Upper Devonian	Frasnian	West Shale Basin	East Shale Basin	Woodbend Group

Text within diagram:

West Shale Basin

East Shale Basin

Nisku Fm.

Camrose Mbr.

Ireton Fm.

Leduc Fm.

Ireton Fm.

Leduc Fm.

Duvernay Fm.

Duvernay Fm.

Cooking Lake Fm

Majeau Lk. Fm.

Upper Devonian

Frasnian

Woodbend Group

4
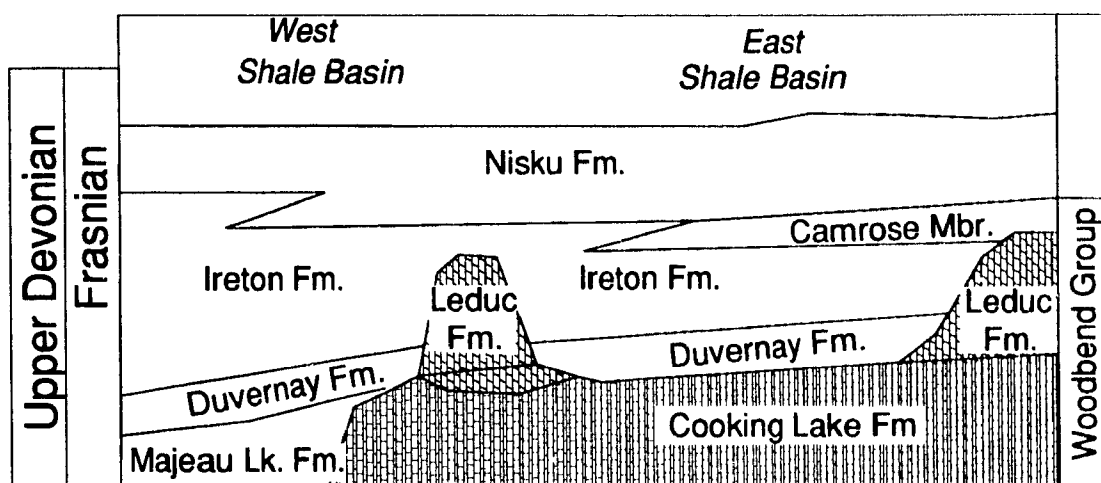
Figure 3. Location of cores studied and cross-sections A-B-C, B-C', and D-D'. Townships and ranges are shown and each are 9.7 km (6 miles) across. 5th refers to the fifth meridian (116°W longitude).

Homeglen Rimbey

C'

C

11-28

D

D'

03-26

11-03

B

14-05

Gilby

T40

T40

14-28

01-30

Medicine River

08-30

10-23

16-11

16-32

Strachan

16-25

11-06

Sylvan Lake

Lanaway

T35

11-10

Garrington

A

5th

T35

Bearberry

Harmattan

R10

R1

R28

Homeglen Rimbey — C' — C — 11-28 — D — D' — 03-26 — 11-03 — B — 14-05 — Gilby — T40 — 14-28 — 01-30 — Medicine River — 08-30 — 10-23 — 16-11 — 16-32 — Strachan — 16-25 — 11-06 — Sylvan Lake — Lanaway — 11-10 — Garrington — A — 5th — T35 — Bearberry — Harmattan — R10 — R1 — R28
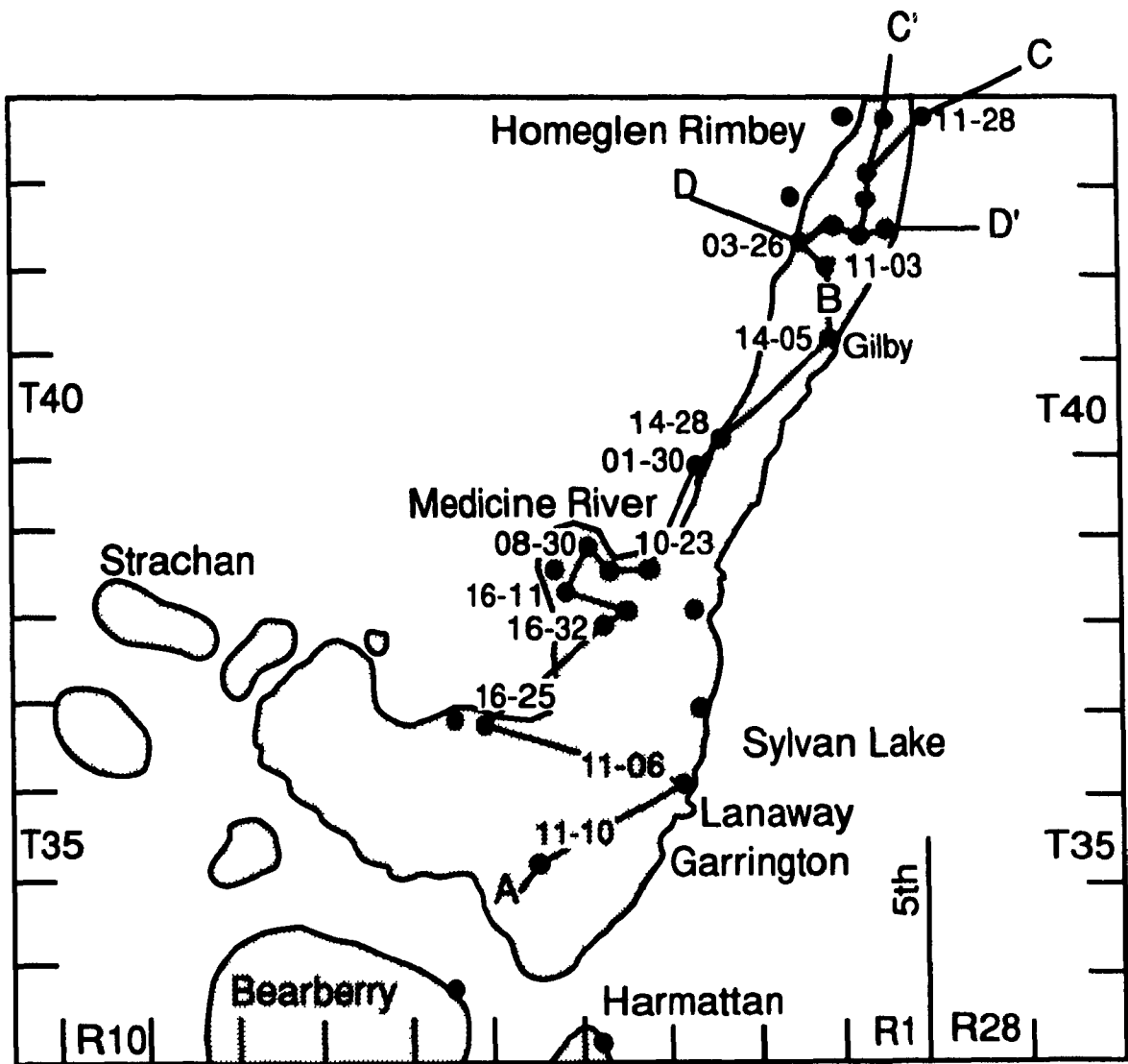
Table 1. List of wells studied. Core intervals are from the Upper Leduc Formation except where indicated by an asterix. Petrographic and geochemical data from wells in bolds are also presented in Amthor et al. (1993).

Location	Well name	Cored intervals (m)
13-09-33-04W5	Mobil Caroline	3383.0 - 3464.2
07-34-33-06W5*	Dome et al. Lobley	3956.3 - 4025.5
11-10-35-05W5	Triad BPX HB Caroline	3352.5 - 3368.5
11-06-36-03W5	Gulf Lanaway	2955.0 - 2991.4
16-25-36-06W5	Chevron Garrington	3458.6 - 3489.4
08-27-36-06W5	Conteira Garrington	3578.3 - 3596.3
10-17-37-03W5	Apache BA Sylvan Lake	2839.2 - 2885.7
16-32-37-04W5	Chevron Sylvan Lake	2981.0 - 3004.4
11-05-38-03W5	Apache BA Sylvan Lake	2781.0 - 2798.1
06-04-38-04W5	Chevron Sylvan Lake	2956.5 - 2989.3
06-20-38-04W5	Chevron Medicine River	3103.0 - 3141.0
10-23-38-04W5	**Suncor et al. Sylvan Lake**	**3007.0 - 3015.0**
08-30-38-04W5	**Chevron Medicine River**	**3105.7 - 3160.0**
16-11-38-05W5	D.W.O. et al Alhambra	2444.5 - 3078.8
08-14-38-05W5	Texaco et al Medicine River	2948.0 - 3300.0
14-28-39-03W5	Sunny Murphy Medicine	2814.0 - 2850.0
01-30-39-03W5	**Chevron et al. Medicine**	**2924.5 - 3000.6**
10-07-40-02W5	Cal. Std. south Gilby	2614.6 - 2646.0
14-05-41-02W5	Chevron Gilby	2512.5 - 2535.8
11-03-42-02W5	**Cal. Std. Gulf Rimbey**	**2374.1 - 2405.8**
06-15-42-02W5	PCP Homeglen Rimbey	2390.0 - 2412.6
07-22-42-02W5	Chevron HRLU Homeglen	2398.0 - 2421.0
07-25-42-02W5**	Calmont Rimbey	2394.5 - 2451.2
09-25-42-02W5	Shell Rimbey	2396.6 - 2443.3
11-25-42-02W5	Imperial Rimbey	2383.5 - 2448.5
03-26-42-02W5	Decalta-Dome Rimbey	2364.9 - 2397.3
11-26-42-02W5	Imperial Rimbey	2400.9 - 2414.3
11-35-42-02W5**	Imperial Rimbey	2516.1 - 2532.0
02-07-43-01W5	BA Reynolds	2305.8 - 2311.6
11-07-43-01W5	BA CPR Reynolds #11	2323.5 - 2397.6
11-20-43-01W5	Chevron Homeglen Rimbey	2363.7 - 2366.8
11-28-43-01W5	Calstan Homeglen Rimbey	2426.1 - 2457.0
03-29-43-01W5	Calstan Homeglen Rimbey	2407.9 - 2442.4
11-29-43-01W5	Chevron Homeglen Rimbey	2290.0 - 2294.4
01-25-43-02W5**	Cal. Std. Rimbey	2446.3 - 2457.0

* Cooking Lake Formation; ** Duvernay/Leduc Formations

The petrophysical characteristics of limestone and partially dolomitized Leduc buildups presented in the literature have shown that their reservoir characteristics are related to depositional facies as well as to diagenesis (e.g. Wendte, 1974; Walls, 1977; Walls and Burrowes, 1985). The Leduc dolomite reservoirs, however, have received little attention due to the difficulties of studying depositional facies in rocks highly altered and modified by dolomitization. A regional study by Amthor et al. (submitted) using core analysis data demonstrates that matrix porosity in Leduc dolostones decreases gradually from township (twp) 46 to 33 with increasing burial depth. Porosity and permeability trends within the Westerose Leduc dolostone buildup, presently buried to depth of about 2000 m, were mapped by McNamara and Wardlaw (1991) using core analyses and nonparametric statistical techniques. They concluded that, in general, permeability and porosity increase from reef flank to reef interior and from upper to lower reef. The Ricinus West gas field is a more deeply buried (4000 m) Leduc dolomite reservoir, in which the depositional facies control the distribution of the pore types despite strong diagenetic overprinting by replacement dolomites (Marquez, 1993). Chapter 3 expands this work with three objectives: 1) to construct a depositional framework and describe the reservoir characteristics of intermediately buried Leduc dolostones; 2) to evaluate the effect of dolomitization and later diagenesis on reservoir character and quality; and 3) to outline the potential processes capable of generating sufficient acidic fluids to account for the dissolution and porosity observed in the replacement dolomites.

CHAPTER 2

Origin of Upper Devonian Leduc dolostones, southern Rimbey-Meadowbrook reef trend, Alberta: new textural and geochemical evidence

Eva Drivet and Eric W. Mountjoy

Department of Earth and Planetary Sciences
McGill University
Montreal, Quebec, Canada
H3A 2A7

ABSTRACT

Upper Devonian Leduc carbonate buildups along the southern part of the Rimbey-Meadowbrook reef trend in central Alberta have been extensively dolomitized and record a complex diagenetic history. The dolomite types occur as replacive and cement. Pervasive replacement dolomitization follows widespread submarine cementation and deposition of the overlying shales, and overlaps with stylolitization. This, combined with $\delta^{18}O$ values of -5.27 to -3.71‰PDB for replacement dolomites, suggests precipitation from fluids between 75 and 45°C, corresponding to burial of 1500 and 500 m respectively, during Late Devonian or later. $^{87}Sr/^{86}Sr$ ratios for replacement dolomites are similar to, or slightly higher (0.70818 to 0.70855) than Upper Devonian seawater (0.7080 to 0.7083), indicating that the dolomitizing fluids were somewhat radiogenic.

Two types of dolomite cements postdate replacement dolomites: a coarse and planar-e(s) Dolomite-C1; and a later very coarse and nonplanar Dolomite-C2 (saddle dolomite). Dolomite-C1 has lower $\delta^{18}O$ values (-7.05 to -3.96‰PDB) than replacement dolomites, and has similar to slightly higher $^{87}Sr/^{86}Sr$ ratios (0.70830 to 0.70950). These geochemical differences reflect the contrasting compositions and temperatures of the fluids from which these dolomites formed. This, combined with the primary fluid inclusions (Th=98 to 142°C; salinity=17.9 to 20.4 wt%NaCl equivalent), indicates that Dolomite-C1 precipitated from hot brines under intermediate to deep burial conditions (>500 to <2800 m) likely during the Carboniferous to Cretaceous. Dolomite-C2 postdates dolomite-C1 and has lower $\delta^{18}O$ values (-9.34 and -8.78‰PDB) and a higher $^{87}Sr/^{86}Sr$ ratio (0.71087), suggesting precipitation from radiogenic fluids with lower oxygen-18 content, and possibly under higher temperature conditions than Dolomite-C1. Blocky calcite with low $\delta^{13}C$ values (-17.9 and -6.53‰PDB), the presence of anhydrite cement, sulphides, and native sulphur, and of 30 to 90 mole% H_2S gases in deeply buried Leduc reservoirs (twp 33 to 39) all support the occurrence of thermochemical sulphate reduction. This mineral assemblage is rare and the mole percent H_2S drops to 1.4 in the northern part of the study area, above present burial depths of about 3000 m.

INTRODUCTION

A series of Leduc carbonate buildups (Woodbend Group, Frasnian age) are located along the Rimbey-Meadowbrook reef trend that extends 480 km in a southwest - northeast direction across central Alberta (Fig. 1). The shallowest reefs (< 2000 m) are located northward in the updip part, with the burial depths increasing southward reaching more than 4300 metres in the Strachan and Ricinus areas (Marquez et al., 1992). The study area includes seven fields located within the intermediate burial portion (2300 to 3500 m) of the reef trend. These fields include: Homeglen-Rimbey, Gilby, Medicine River, Sylvan Lake, Lanaway, Garrington, and Bearberry (Townships 33 to 43, Ranges 1-7 W5), a distance of 130 km along the central and southern part of the Rimbey-Meadowbrook reef trend (Figs. 1 and 3). One well in the Harmattan area was also examined. These fields are completely dolomitized and contain replacement dolomites that sharply crosscut facies and members of the underlying Cooking Lake, and the overlying and adjacent Ireton, and Duvernay formations (Fig. 2).

This paper summarizes research to date on Leduc Formation dolomites of the southern part of the Rimbey-Meadowbrook reef trend. The objectives are: 1) to integrate textural and geochemical data in order to describe the diagenetic evolution of the Leduc dolomitized buildups and constrain the relative timing and origin of dolomitization; and 2) to map the distribution of the diagenetic phases along the reef trend. This work presents new textural and geochemical data for the dolomites and calcites, thus complementing former and current studies dealing with updip and downdip equivalent reservoirs (Amthor et al., 1993; Chouinard, 1993; Marquez, Ph.D. in progress; Prof. Machel and his students at U. of Alberta) (Fig. 1). Furthermore, this paper demonstrates for the first time the variations in the amount and distribution of late-stage cements as a function of burial depth and their possible link to reactions associated with thermochemical sulphate reduction (TSR).

METHODS

This study includes an examination of cores from 35 wells from seven fields (Table 1). Petrography involved the examination of 201 thin sections stained with Alizarin red-S and K-Ferricyanide using the method outlined by Dickson (1965). For crystal size, the apparent maximum dimensions of the dolomite crystals were measured or estimated using Folk's (1962) size scale. The percentage of the main diagenetic cement phases (dolomite cements, anhydrite, calcite, and sulphur) was visually estimated from cores, hand samples, and thin sections from wells distributed along a north-south cross-section of the study area (Fig. 5; Table 2). The results are semi-qualitative and reliability is within about 10% of the estimated value (e.g. 5% cement ± 0.5%). Cathodoluminescence properties of all thin sections were studied using a Nuclide Luminoscope, Model ELM-2, with a beam voltage of 10 Kv and a beam current of 0.5 Ma in a 40-50 mtorr vacuum under an air atmosphere. All thin sections were examined under diffused light, and blue light epifluorescence microscopy (480 to 520 nm).

0.02 to 0.05 mg microsamples of dolomite (74) and calcite (15) were obtained using a modified dental drill, and analyzed for carbon and oxygen isotopes at the University of Michigan. Samples were vacuum roasted at 380°C for one hour to remove organic material, and reacted in anhydrous phosphoric acid at 73 ± 2°C in a reaction vessel connected to a Kiel carbonate extraction device and a Finnigan MAT 251 mass spectrometer. Analyses were corrected for ^{17}O using the procedure of Craig (1957). Carbon and oxygen isotopic values are reported relative to the PDB scale, and have a precision of ± 0.05‰.

Strontium isotopic compositions were analyzed by Steve Whittaker using three separate procedures at three universities, including the University of Saskatchewan (U of S), the University of Alberta (U of A), and L'Université du Québec à Montréal (UQAM). Sr isotopic compositions were determined by dissolving the sample in cold 1.0 N HCl and then treating it with HNO_3 to destroy any organic material present. Sr was separated from the sample by standard elution techniques using HCL on 5 mL cation exchange columns at the U of S, by

co-precipitation with $Ba(NO_3)$ followed by elution on standard 1 mL columns, and by elution with HNO_3 and H_2O on columns containing 50µL of Sr Spec resin. Procedural blanks are (estimated) of less than 150 pg Sr for all methods. The number of samples analyzed at U of S, U of A, and UQAM is 4, 10, and 8 respectively. Sr isotopic compositions were measured using three separate procedures. At the U of S and at the U of A, Sr was loaded as a chloride on Re double filaments and analyzed on a multicollector, respectively. At UQAM, Sr was loaded on Re single filaments with a Ta emitter and analyzed on a multicollector in dynamic mode. Errors associated with these analyses are reported as 2σ values. $^{86}Sr/^{88}Sr$ ratios were normalized to 0.1194. The $^{87}Sr/^{86}Sr$ ratio of NIST Sr 987 determined at the U of S over the interval of this study is 0.710248 ± 27, and at the U of A, 0.71024. At this stage of the study, not enough data were obtained from UQAM to determine the isotopic ratio of NIST Sr 987.

Fluid inclusions in crystal growth zones of dolomite cement were analyzed by Prokopis Kranidiotis using a Fluid Inclusion heating/freezing stage at McGill University based on a USGS design (Werre et al., 1979; Hollister et al., 1981). The procedure is outlined in Coniglio and Williams-Jones (1992). The melting temperature of ice was converted into weight percent NaCl equivalent using equations in Oakes et al. (1990). Reported temperatures are accurate to ± 0.3°C in the subzero range and ± 2°C for the highest temperatures measured.

PETROGRAPHY OF LEDUC DOLOSTONES

Six different dolomite-rock textures are classified according to crystal size, distribution, and crystal boundary shape (planar or nonplanar) using the classification of Sibley and Gregg (1987), and by porosity association (Fig. 4). Based on staining, the dolomites are all non-ferroan. Dolomite-R1, R2, R3, and R4 are replacive, and Dolomite-C1 and C2 (saddle dolomite) are pore-filling (Fig. 4). These dolomites are classified according to the scheme of Amthor et al. (1993) to which Dolomite-R1, a fine-crystalline dolomite, has been added. In order of increasing abundance, the replacement dolomites are: R4, R1, R3, and R2, with

Figure 4. Six dolomite textures observed in the Leduc carbonates of the southern part of the Rimbey-Meadowbrook reef trend compared with the classification scheme of Amthor et al. (1993) (Type 1 to 5 in brackets). "P" is an abbreviation for poie space. Scale bars= 500 μm.

Replacement Dolomite

R1
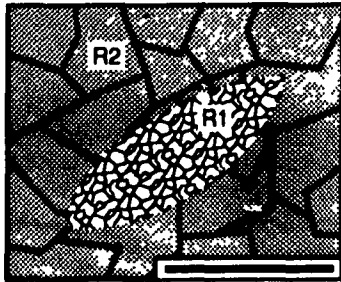
R2 (Type 1)
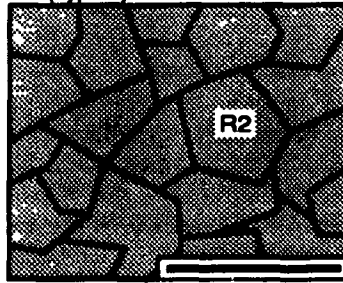
R3 (Type 2)
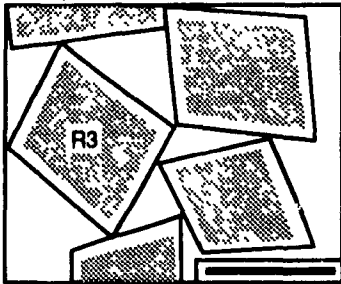
R4 (Type 4)
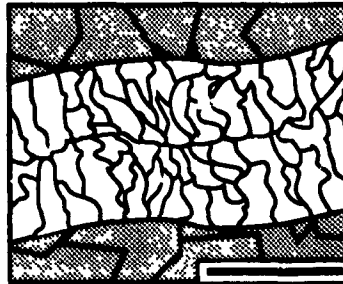
Dolomite Cement

C1 (Type 3)
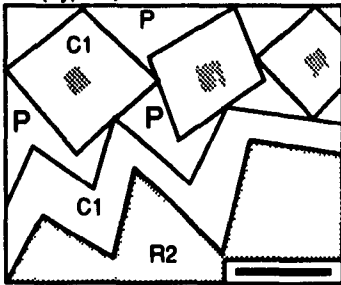
C2 (Type 5)
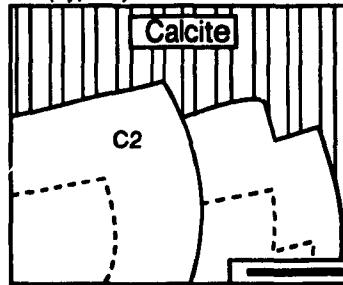
Dolomite-R2 comprising about 80% of the dolomites by volume. Stylolites and later stage cements (anhydrite, calcite, quartz, sulphur, sulphides, and bitumen) were also observed.

Replacement dolomites

R1: Fine-crystalline planar-e(s) dolomite, 35 - 60 µm, is dark-grey to brown and is the least abundant of the dolomite types. It forms dense mosaics of dirty brown and cloudy fine- subhedral to euhedral planar-s (e) crystals that exhibit straight extinction and are coated by dark coloured organic material (Plate 1a). The contacts between Dolomite-R1 and coarser crystalline dolomites are sharp. Locally, however, Dolomite-R1 occurs interstitial to, and is contained within, coarser crystals of Dolomite-R2 (Plate 1d). In such cases, the fine crystals are not in optical continuity relative to the coarser ones, and crystal boundaries and contacts between the two dolomite types are irregular.

R2: Fine- to medium- crystalline planar-s (a) dense dolomite, 60 -250 µm, is light brownish grey, typically cloudy, and is usually fabric destructive (Plates 1a and 2c). Occasionally, the outlines of fossils replaced by Dolomite-R2 are well preserved (see Plates 8a and 8c, Chapter 3). Near fractures and pores, crystals of Dolomite-R2 are coarser, with poorly defined crystal junctions (the majority of which are nonplanar), and exhibit a weak undulose extinction (Plates 1e and 1f) As a matrix replacement, Dolomite-R2 shows little intercrystalline porosity, although it is sometimes associated with zones of fenestral, vuggy, and moldic pores

R3: Coarse-crystalline planar-s (e) dense to porous dolomite, 250 -700 µm, is dark-grey to brown. It occurs either as dense subhedral planar-s cloudy crystals, or as porous euhedral planar-e crystals that are occasionally rimmed by a thin (10 µm) clear zonation (Plate 3a). Euhedral crystals are commonly coated by bitumen (Plate 3a), and their intercrystalline porosity values average 10% based on neutron density logs and core analyses.

Plate 1.   PHOTOMICROGRAPHS OF REPLACEMENT DOLOMITES R1 AND
            R2 IN THE UPPER LEDUC FORMATION: I

A)   Fine crystalline (40-50 μm) planar-e(s) replacement dolomite (R1)
      distributed along a stylolite seam.   The surrounding matrix is
      comprised of fine to medium crystalline (150-200 μm) planar-s(a)
      dense replacement dolomite (R2). 11-07-43-01W5, 2390.0 m, plane
      polarized light. Scale bar 200 μm.

B)   Close up of Plate 1a but under cathodoluminescence light. Both
      replacement dolomites R1 and R2 are characterized by blotchy dull
      orange-red luminescence. Scale bar 300 μm.

C)   Close up of Plate 1b under fluorescence microscopy. Replacement
      dolomites R1 and R2 exhibit green fluorescence.   The bright
      fluorescent zone that surrounds crystals of Dolomite-R1 represents
      organic material distributed within the stylolite seams. Scale bar 75
      μm.

D)   Patches of fine replacement dolomite (R1) are distributed within
      coarser replacement dolomite (R2). The coarse crystals are not in
      optical continuity with the finer ones. 08-30-38-04W5, 3135.6 m,
      cross-polarized light. Scale bar 400 μm.

E)   Fracture filled with native sulphur (S) that crosscuts replacement
      dolomite (R2). The Dolomite-R2 crystals surrounding the fracture are
      characterized by irregular non-planar crystal forms and exhibit a
      weak undulose extinction. These crystal morphologies are unusual
      and only occur near fractures filled with native sulphur. 08-27-36-
      06W5, 3593.7 m, cross-polarized light. Scale bar 1 mm.

F)   Close up of Plate 1e shows in more details the irregular non-planar
      crystal boundaries of Dolomite-R2 adjacent to the fractures. Cross-
      polarized light. Scale bar 300 μm.
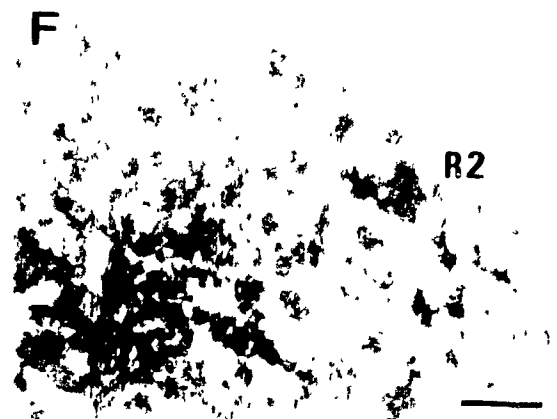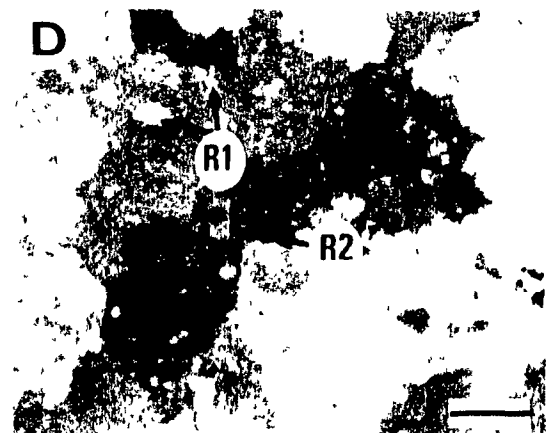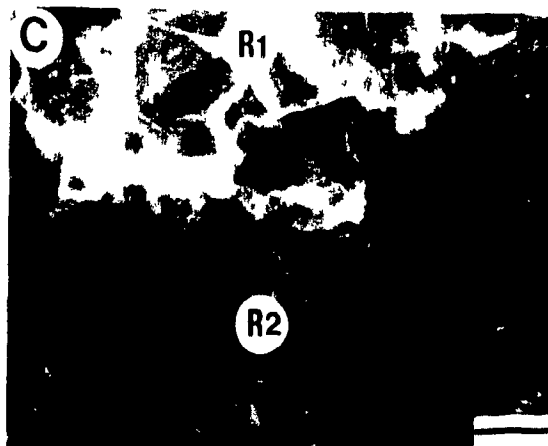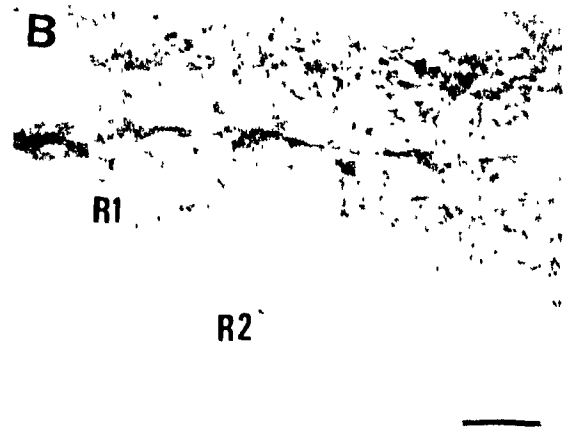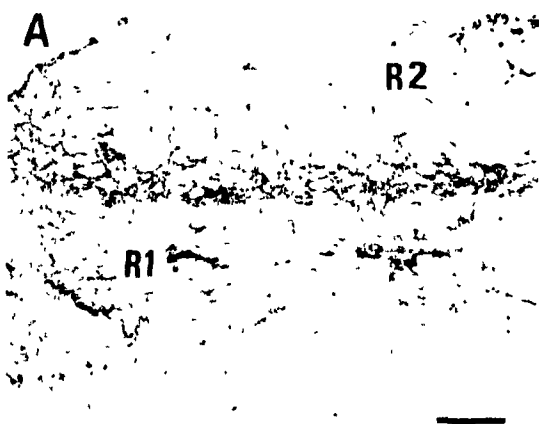
Plate 2.   PHOTOMICROGRAPHS OF REPLACEMENT DOLOMITES R1 AND
            R2 IN THE UPPER LEDUC FORMATION: II

A,B)   Paired cross-polarized and cathodoluminescence views of
        replacement Dolomite-R2 adjacent to thin fractures.   Near the
        fractures, the crystals of replacement dolomite are rimmed by a thin
        zone of bright luminescence whereas the dolomite crystals away from
        the fractures lack zonations. 16-32-37-04W5, 2989.2. Scale bars in
        A) and B) are 470 and 330 μm respectively.

C,D)   Paired plane-polarized and cathodoluminescence views of
        replacement Dolomite-R2. Adjacent to the fracture, the edges of the
        Dolomite-R2 crystals are clearer under plane light, and exhibit a
        duller luminescence compared to the crystals of replacement
        dolomite away from the fracture zone. 16-32-37-04 W5, 2989.2 m.
        Scale bar 330 μm.

E,F)   Paired plane-polarized and cathodoluminescent views of altered
        Dolomite-R2 exhibiting patchy replacement of brightly red
        luminescent Zone 1 dolomite by dull red luminescent Zone 2
        dolomite, and overgrowth by bright red luminescent Zone 3 dolomite
        (arrows). These zonations are not characteristics of Dolomite-R2 and
        are only observed in this thin section locally. 07-22-42-02W5, 2402.5
        m. Scale bar 330 μm.
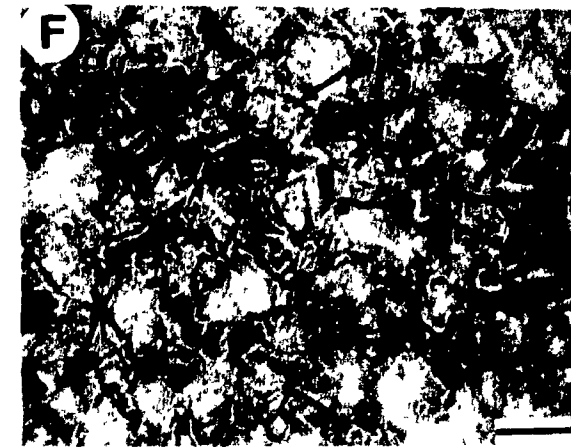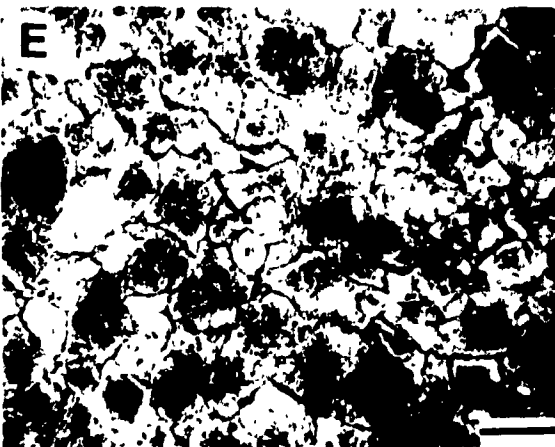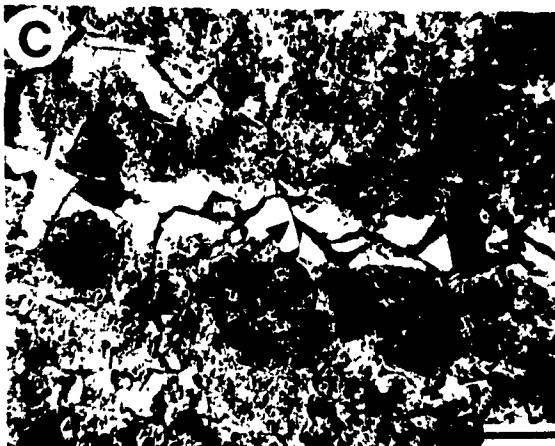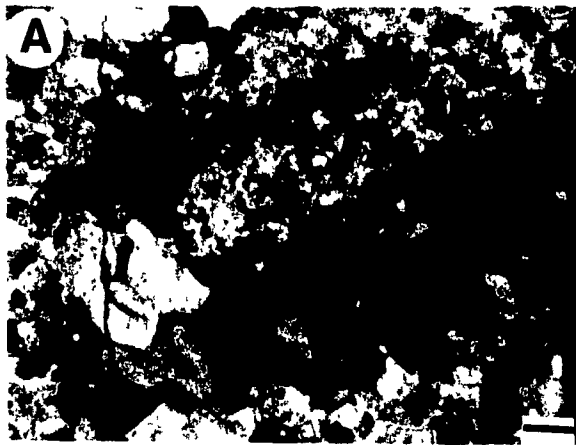
Plate 3. CORE AND PETROGRAPHIC CHARACTERISTICS OF REPLACEMENT DOLOMITES R3 AND R4 IN THE UPPER LEDUC FORMATION

A) Photomicrograph of coarse crystalline planar-e replacement dolomite (R3) with intercrystalline (I) porosity partially occluded by bitumen (black coating). The cloudy core of the dolomite crystal is rimmed by a thin clear zonation of dolomite cement. 11-07-43-01W5, 2397.4 m, plane-polarized light. Scale bar 1 mm.

B) Close up of Plate 3a under cathodoluminescence. The clear zonations observed under plane light exhibit dull red luminescence, whereas the cloudy core is characterized by brighter red colours. Scale bar 310 µm.

C) Close up of Plate 3b under fluorescence. The dull red luminescent rims exhibit dark green fluorescence whereas the brighter red cloudy core is represented by yellowish green fluorescence. Scale bar 75 µm.

D) Photomicrograph of replacement of fibrous calcite cement by Dolomite-R4. The coarse fibrous crystals that radiate out from the pore boundaries are readily recognized despite dolomitization. 08-27-36-06W5, 3593.0 m, cross-polarized light. Scale bar 1.8 mm.

E) Replacement of isopachous cement by Dolomite-R4. Interparticle porosity is observed between the allochems. 03-29-43-01W5, 2320.8 m. Scale bar in centimetres.

F) Photomicrograph of the isopachous cement observed in Plate 3e under plane-polarized light. The primary fabrics have been completely obliterated by replacement dolomitization (R4). Only the outline of allochems (A) is observed under thin section. Scale bar 2 mm.

G) Close up of Plate 3f under cathodoluminescence (dashed area in Plate 3f). The luminescence of Dolomite-R4 is homogeneous dull red. Scale bar 300 µm.

H) Close up of Plate 3g under fluorescence. The fluorescence of Dolomite-R4 is homogeneous green. Scale bar 75 µm.
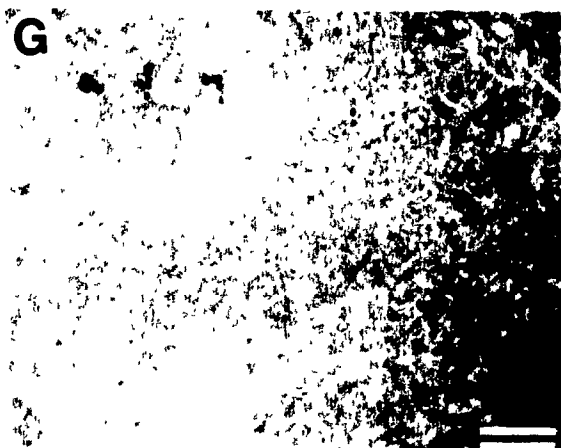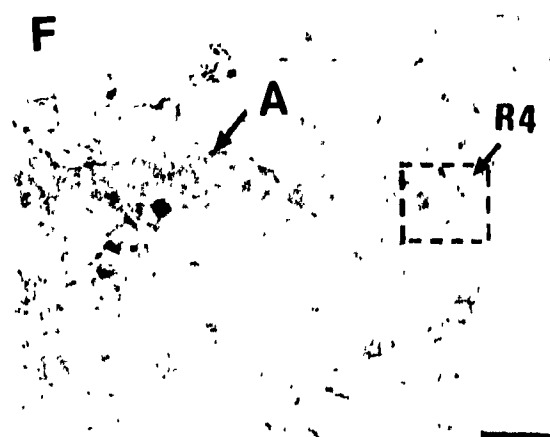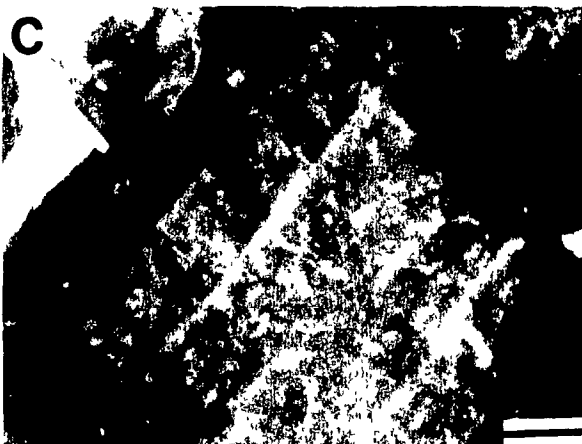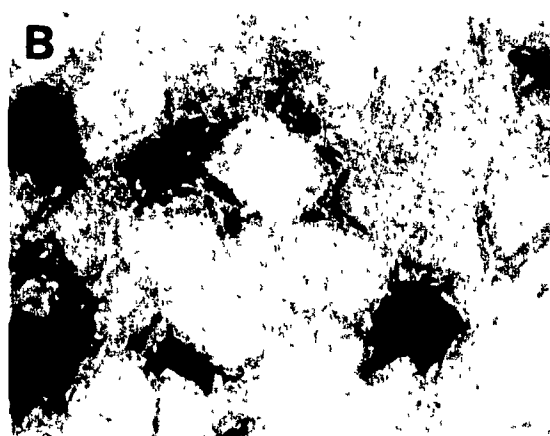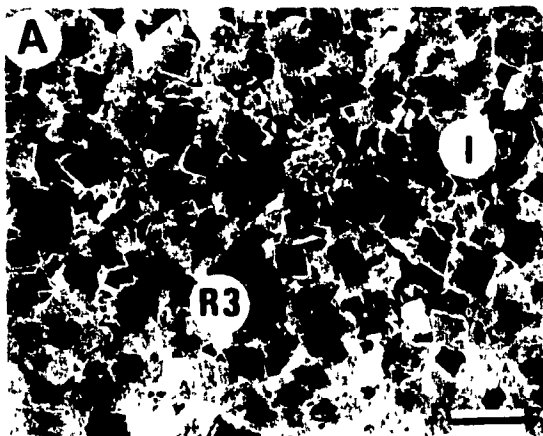
R4: Coarse-crystalline nonplanar anhedral dolomite mimics the crystal habits of fibrous and isopachous calcite cements in partially (e.g. flank well 10-23, 3014.2 m) to completely dolomitized cores (e.g. buildup interior wells 6-20, 3124.0 m; 11-5, 2796.6 m). It is characterized by coarse fibrous calcite crystals (100 μm to 1mm long, and 25 to 100 μm wide) that radiate out from the boundaries of fossils and large pores. Despite dolomitization, sweeping extinction and sutured crystal contacts are partially preserved (Plate 3d). Dolomite-R4 also replaces isopachous calcite cement, and occurs as light beige equant crystals rimming interparticle porosity in *Amphipora* and *Thamnopora* grainstones (Plates 3e and 3f). The microscopic textural features of the precursor calcite cement have been completely obliterated, and the crystal boundaries are poorly defined. Dolomite-R4 differs from calcite fibrous and isopachous cements by showing irregular and poorly defined crystal boundaries.

Cathodoluminescence of all replacement dolomites is generally characterized by a homogeneous to blotchy dull orange-red colour (Plates 1 to 3). Bright and dull luminescent zonations in crystals of Dolomite-R2 occasionally occur near fractures (Plates 2a to 2d). In this case, the dolomite crystals are coarser and less cloudy compared to the crystals of replacement dolomite distributed away from the fracture zones. Unusual zonations in replacive Dolomite-R2 are observed in one sample (well 07-22-42-02W5, 2402.5 m) with near to complete replacement of the core (Zone 1) by Zone 2 dolomite with subsequent replacement and overgrowth by Zone 3 dolomite (Plates 2e and 2f). In general, all replacement dolomites are characterized by green fluorescence (Plates 1 to 3). When zoned, the cloudy cores of replacement dolomites usually fluoresce yellowish green and the clear rims fluoresce dark green (e.g. Plate 3c). Primary fabrics are rarely observed under fluorescence.

Dolomite cements

C1: Coarse-crystalline planar-e (s) dolomite cement, 250 - 800 μm, is white to light beige and locally comprises up to 15% of Leduc dolomites (e.g. core 11-06, 2974.8 m). Crystals are coarse euhedral to subhedral planar-e (s), either clear, or with cloudy cores and clear rims. They exhibit straight extinction (Plate 4a), and contain fluid inclusions within well defined crystal growth zones (Plate 4f).

C2: Very coarse-crystalline nonplanar saddle dolomite cement, 720 μm - 1.12 mm, is white, occurs in vugs in minor amounts (< 1%), and postdates Dolomite-C1 (Plate 5a). It is observed in only four wells, one from the Cooking Lake (07-34-33-06W5, 3969.7 m), and three from the Upper Leduc (6-20-38-04W5, 3104.7 m; and 8-30-38-04W5, 3107.7 m; 03-29-43-01W5, 2374.7 m). Crystals are euhedral to subhedral, have a slightly curved to a typical saddle shape, and exhibit sweeping extinction (Plates 5a and 5b). Dolomite-C2 is scarcer and finer crystalline in the study area than in the southernmost part of the Rimbey-Meadowbrook reef trend where it is characterized by crystal sizes ranging between 1 and 5 mm (Marquez, pers. comm., 1993).

Cathodoluminescent and fluorescent zones occur locally in dolomite cement C1, with inclusion-rich cores exhibiting dull red luminescence and yellowish green fluorescence. The clear rims have a brighter red luminescence and a dark green fluorescence (Plates 4a to 4c). Up to five cathodoluminescent zones (alternating bright and dull red) and fluorescent zones (alternating dark and yellow green) are recognized (Plates 4d and 4e). However, these zones cannot be correlated from sample to sample because they are too rare. In contrast, Dolomite-C2 luminesces dull red, fluoresces dark green, and never contains any crystal zonations (Plates 5a to 5d).

Later-diagenetic phases

Wispy and high amplitude stylolites are present throughout most cores, and increase in abundance within and near green shaly layers. In general, stylolites crosscut replacement dolomites (Plate 6a). However, locally, patches and rhombs

Plate 4.   PHOTOMICROGRAPHS OF DOLOMITE CEMENT C1 IN THE
             UPPER LEDUC FORMATION

A,B,C)   Cross-polarized, cathodoluminescence, and fluorescence
             views of dolomite cement-C1 and blocky calcite (Ca) that fill
             porosity in replacement dolomite-R2 (R2). 16-25-36-06W5,
             3489.2 m. Scale bars for A), B), and C) are 680 μm, 330
             μm,and 75 μm respectively.

D,E)   Paired plane-polarized and cathodoluminescence views of
             Dolomite-C1 precipitated following replacement dolomite R2,
             and overlained by blocky calcite (Ca). This rare example
             shows five zones in Dolomite-C1 (labelled 1 to 5 in the photo).
             Zone 1 replaces and overgrows replacement dolomite R2. 08-
             14-38-05W5, 3004.9 m. Scale bar 330 μm.

F)   Primary fluid inclusions (arrow) in dolomite-C1 are distributed
             within the crystal growth zones and thus are interpreted to be
             of primary origin. 11-03-42-02W5, 2390.4 m. Scale bar 40
             μm.
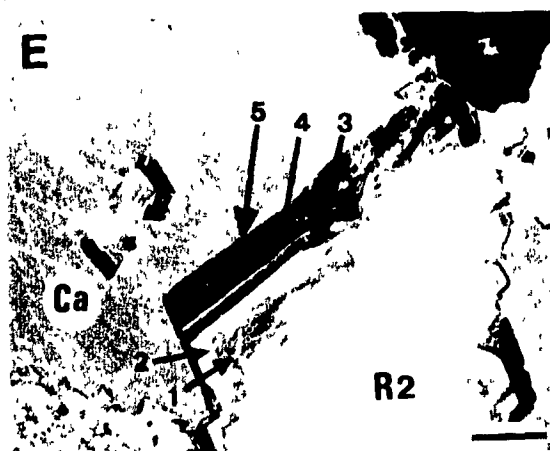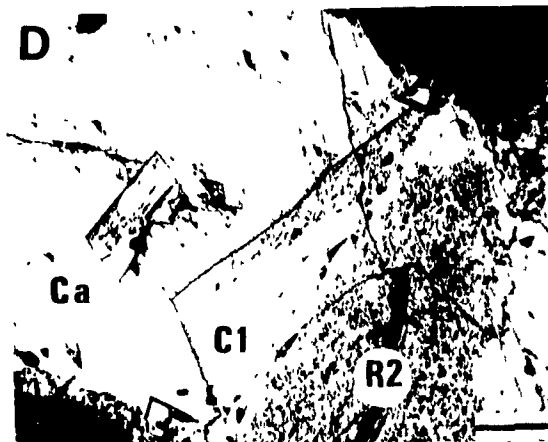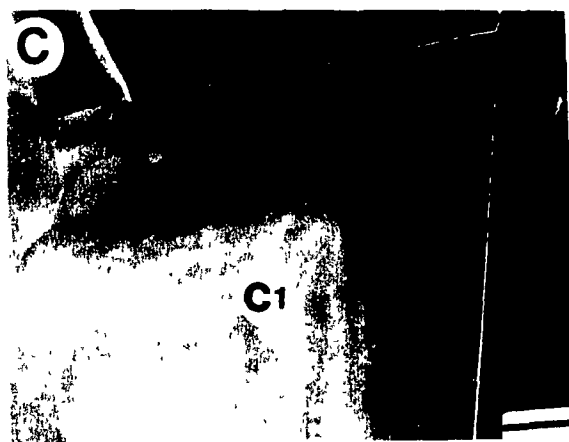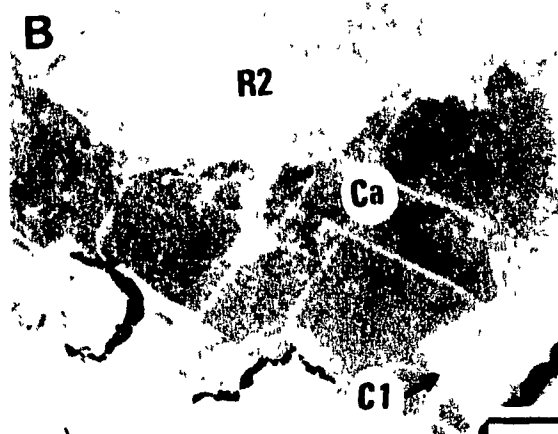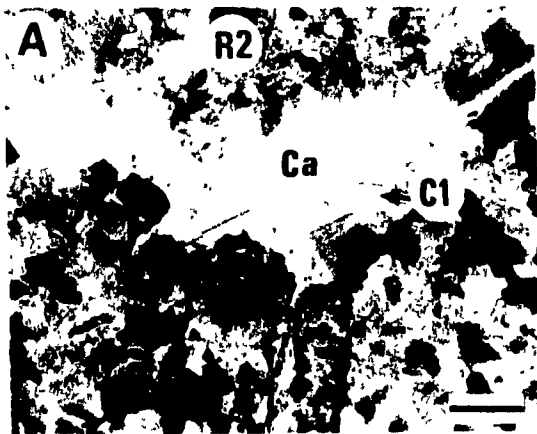
Plate 5.   PHOTOMICROGRAPHS OF DOLOMITE CEMENT C2 IN THE
UPPER LEDUC FORMATION

A,B,C,D)   Plane light, cross-polarized light, cathodoluminescence, and
fluorescence views of saddle dolomite cement (C2) and
Dolomite-C1 that fill a pore in replacement dolomite.
Compared to Dolomite-C1, Dolomite-C2 is coarser, has a
similar dull red luminescence but never contains any
zonations, and is characterized by dark green fluorescence.
03-29-43-01W5, 2374.7 m. Scale bars for A), B), C), and D)
are 1.75 mm, 1 mm, 330 μm, and 75 μm respectively.
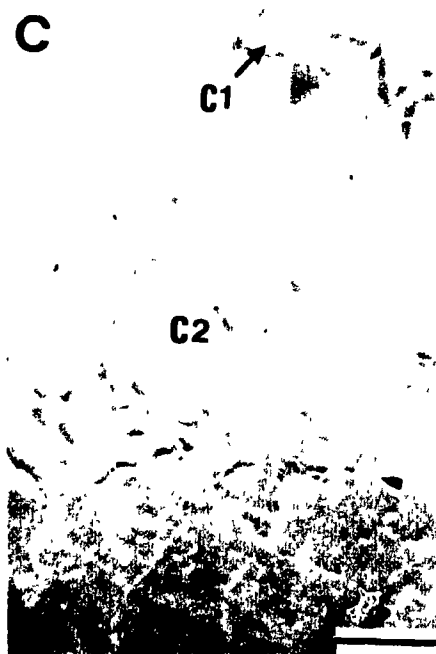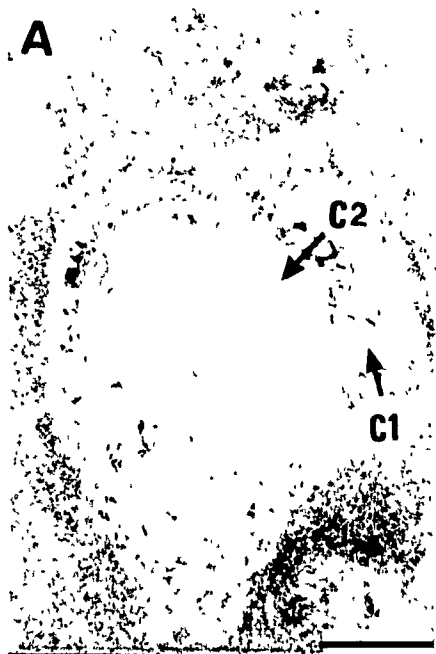
of replacement dolomite are optically continuous across stylolites (Plate 6b) and therefore postdate them. Dolomite and anhydrite cements occur along stylolites and sometimes are crosscut by stylolites (Plates 6c and 6d).

Anhydrite occurs both as cement and replacive phases. Anhydrite cements overlie Dolomite-C1, and are commonly coated by bitumen (Plates 7a and 7b). The replacement of dolomite by aphanocrystalline to very coarse anhydrite is indicated by the presence of: a) remnants of dolomite in anhydrite; b) angular clasts of matrix dolomites surrounded by anhydrite (Plate 10a); and c) corrosion of crystals of replacement dolomite and dolomite cement by anhydrite (Plates 10e and 10f). The common occurrence of uncorroded crystals of replacement dolomite and dolomite cement adjacent to anhydrite (Plates 10g and 10h) suggests that anhydrite cement is much more abundant than anhydrite replacement.

Blocky calcite cement constitutes a volumetrically minor percentage of the rocks but may reach up to 15% locally. Usually crystals are limpid to translucent, anhedral, and coarse (100 μm to 5 mm). This calcite fills vuggy, moldic, and fenestrae pores following dolomite and anhydrite cements (Plate 4a). Replacement of Dolomite-C1 by blocky calcite (dedolomitization) occurs locally in two wells (8-30-38-4 W5 and 11-3-42-2 W5) (Plate 7f).

Bitumen, quartz, sulphur, and sulphides are volumetrically minor. Bitumen coats replacement dolomites, dolomite cements, and anhydrite (Plates 7b and 7c). Coarse (up to 1 cm across) euhedral crystals of quartz that contain fluid inclusions occur in two Leduc buildup interior wells (11-06-36-03W5, 2962.9 m; and 11-03-42-02W5, 2393.7 m) and one well from the Cooking Lake Formation (07-04-34-33-06W5, 3976.0 m). This cement postdates blocky calcite cement (Plate 7g).

Locally, sulphides (probable pyrite) occur within crystal zonations of Dolomite-C1 (Plates 7d and 7e). They also form thin geopetals above dolomite cement that rims replacement dolomite clasts in a few brecciated intervals (Plate 10a). Sulphides predate anhydrite cements, although locally, specks of pyrite float in anhydrite. Sphalerite and galena postdate blocky calcite. Native sulphur occurs in pores and thin late-stage fractures that crosscut blocky calcite cement (Plate 7h).

Plate 6.   PHOTOMICROGRAPHS OF STYLOLITES IN THE UPPER LEDUC
           FORMATION

A)   Stylolites filled with insoluble material, truncate replacement
      Dolomite-R2.   06-20-38-04W5, 3104.4 m, plane polarized light.
      Scale bar 800 μm.

B)   The arrows point to crystals of replacement dolomite (R2) that
      continue across and truncate the stylolite (S).   16-32-37-04W5,
      3002.5 m, cross-polarized light.   Scale bar 225 μm.

C)   Crystals of dolomite cement (C1) adjacent to a stylolite (S) indicate
      that in this case, dolomite cementation overlapped with stylolitization.
      11-03-42-02-W5, 2395.0 m, plane polarized light.   Scale bar 290 μm.

D)   Stylolite (S) truncates crystals of anhydrite cement (A).   03-29-43-
      01W5, 2361.3 m, cross-polarized light.   Scale bar 455 μm.
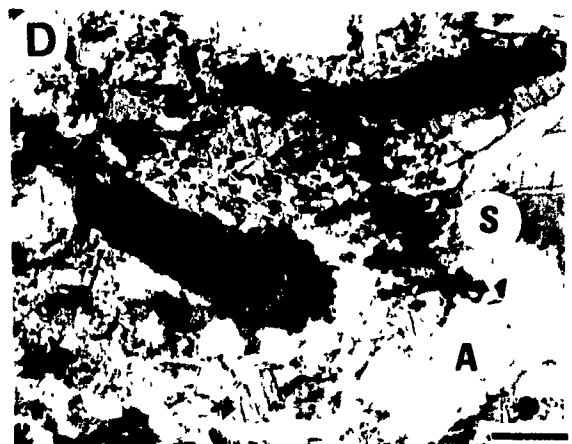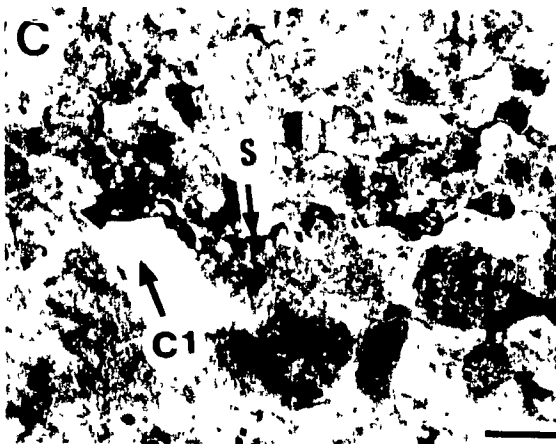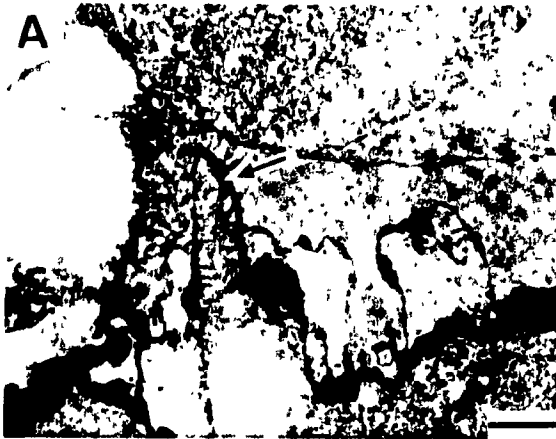
Plate 7.   PHOTOMICROGRAPHS ILLUSTRATING THE PARAGENETIC SEQUENCE OF THE LATER DIAGENETIC PHASES IN THE UPPER LEDUC FORMATION

A)   Anhydrite (A) and Dolomite-C1 cements occlude a pore. 16-11-38-05W5, 3070.5 m, cross-polarized light. Scale bar 2 mm.

B)   Bitumen (black material) coats crystals of anhydrite cement (A). 03-29-43-01W5, 2327.7 m, plane-polarized light. Scale bar 260 μm.

C)   Bitumen (black material) coats crystals of Dolomite-C1. 11-26-42-02W5, 2407.4 m, plane polarized light. Scale bar 355 μm.

D,E)   Paired plane light and fluorescent views of specks of sulphides, probably pyrite, trapped within the crystal zones of Dolomite-C1. The specks do not fluoresce, whereas Dolomite-C1 exhibits green fluorescence. 11-03-42-02W5, 2394.8 m. Scale bar 75 μm.

F)   Inclusions of dolomite cement (C1) within blocky calcite cement (Ca) (stained with Alzarin red-S) indicate dedolomitization. This texture occurs along fractures that crosscut a stylolite (S) 11-03-42-02W5, 2384.4 m, plane-polarized light. Scale bar 520 μm.

G)   Quartz (Q) occludes a pore following coarse blocky calcite (Ca) cement. 11-06-36-06W5, 2962.8 m, plane-polarized light. Scale bar 2.5 mm.

H)   Crystal of blocky calcite (Ca) corroded by native sulphur (S). Native sulphur fills a fracture that cuts replacement Dolomite-R2 and extends into the pore partially filled by coarse calcite. 08-27-36-06W5, 3593.7 m, cross-polarized light. Scale bar 300 μm.
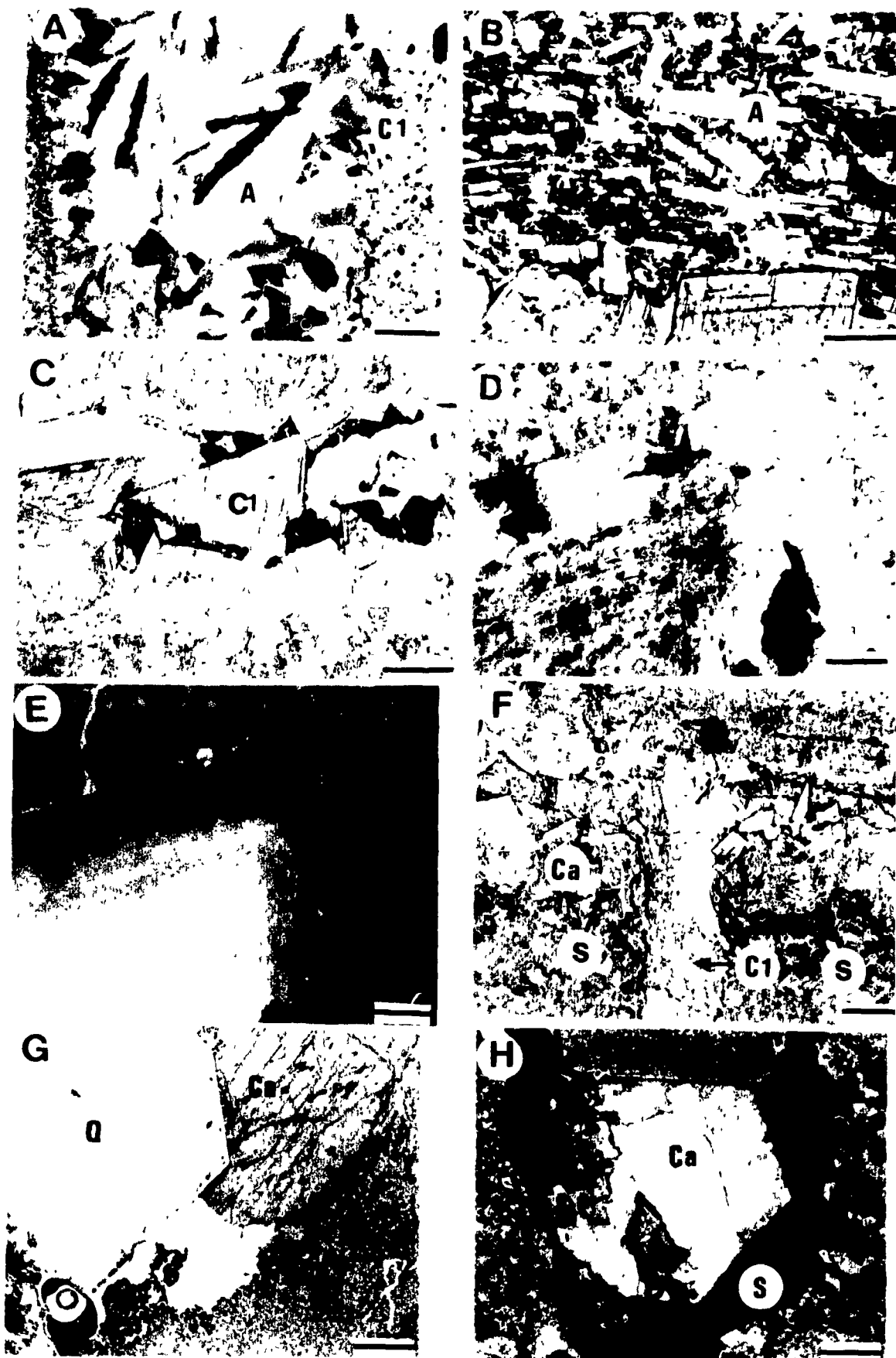
Distribution of replacement dolomites and later-diagenetic phases

The regional distribution of replacement dolomites is similar to that reported in Amthor et al. (1993) for the updip part of the Rimbey-Meadowbrook reef trend. Replacement dolomitization in the Leduc Formation buildups of the study area is pervasive and fabric destructive. In the off-reef well 10-07-40-02W5, the overlying Ireton Formation is completely dolomitized. This, combined with the fact that basal Duvernay limestones are completely dolomitized along the Leduc-Acheson-Morinville buildups (Andrichuk, 1958; Amthor et al., 1993), indicates that massive replacement dolomitization postdates deposition of the Ireton and Duvernay Formations, the basinal equivalents of the upper and lower parts of the Leduc Formation buildups respectively.

Dolomite-R1 occurs locally in flank wells and some buildup interior wells where it replaces patches of fine carbonate mud distributed in stylolite seams (Plate 1a), geopetal fillings, breccia clasts, sedimentary laminae, and burrows. Dolomite-R2 is widespread throughout the buildups, replacing both the matrix and allochems (pellets, skeletal fragments). Dolomite R3 occurs most abundantly in skeletal grainstones (see Plates 8e and 8f, Chapter 3). Dolomite-R4 replaces fibrous and isopachous calcite cements, and thus its distribution is related to these early stage calcite cements. As a result, Dolomite-R4 is commonly observed in *Amphipora* and *Thamnopora* grainstones that are most abundant in the buildup interior (Figs. 13 and 14). These observations suggest that despite fabric destructive dolomitization, the distribution of the different replacement dolomite types is in part related to the original texture of the limestone precursor.

The general distribution and relative abundance of the later diagenetic cements, including anhydrite, dolomite (C1 and C2), calcite, and sulphur, is mapped along the reef trend (Table 2; Figs. 5 and 6). Calcite and dolomite, and native sulphur occur in minor amounts (less than 2%). Of all the cements, anhydrite constitutes the most pervasive and volumetrically important, filling intraclast pores in brecciated dolomites, vugs, molds, and fractures. A northward increase in average porosity values from 2 to 7% (Amthor et al., submitted)

Table 2. Average percentage of anhydrite, dolomite, calcite, and sulphur cements for different Upper Leduc wells along the southern part of the Rimbey-Meadowbrook reef trend, central Alberta. These percentages are based on visual estimates in cores, hand samples, and thin sections.

Location	Anhydrite	Dolomite	Calcite	Sulphur
13-09-33-04W5	7.2	1.5	0.0	0.0
11-10-35-05W5	5.2	0.1	0.0	0.0
11-06-36-03W5	6.4	1.3	0.8	0.1
16-25-36-06W5	5.9	1.0	1.5	0.5
08-27-36-06W5	4.1	0.6	0.2	0.6
16-32-37-04W5	4.8	0.8	0.2	0.0
06-04-38-04W5	4.9	0.3	0.0	0.0
06-20-38-04W5	3.5	0.9	0.0	0.0
10-23-38-04W5	7.5	0.0	0.5	0.0
08-30-38-04W5	4.3	0.5	0.1	0.0
16-11-38-05W5	5.8	1.3	0.0	0.0
14-28-39-03W5	5.0	0.4	0.2	0.0
01-30-39-03W5	2.5	0.0	0.0	0.0
14-05-41-02W5	4.0	0.0	0.0	0.0
11-03-42-02W5	0.0	0.8	0.6	0.0
07-25-42-02W5	0.0	0.5	0.5	0.0
11-25-42-02W5	0.4	1.3	0.1	0.0
03-26-42-02W5	2.5	0.0	0.0	0.0
11-07-43-01W5	0.0	0.9	0.2	0.0

Figure 5. South-north cross section A-B-C along the study area (see Fig. 3 for location) showing general distribution of anhydrite, dolomite (C1 and C2) and blocky calcite cements, and native sulphur. The abundance of these diagenetic phases decreases updip with decreasing burial depth. North of the Medicine River field (above present burial depths of about 3000 m), these phases are rare to absent (e.g. wells 01-30, 03-26, 07-25, and 11-07).

Top of Leduc

A   Lanaway   Medicine River

11-10 11-06 16-25 08-27 16-32 06-04 16-11 08-30 06-20 10-23

meters
0
20
40

Gilby   B   Homeglen-Rimbey   C

01-30 14-28 14-05 11-03 03-26 11-25 07-25 11-07 03-29 11-28

- Anhydrite
- Dolomite cements
- Calcite
- Native sulphur
- Lack the above phases

27
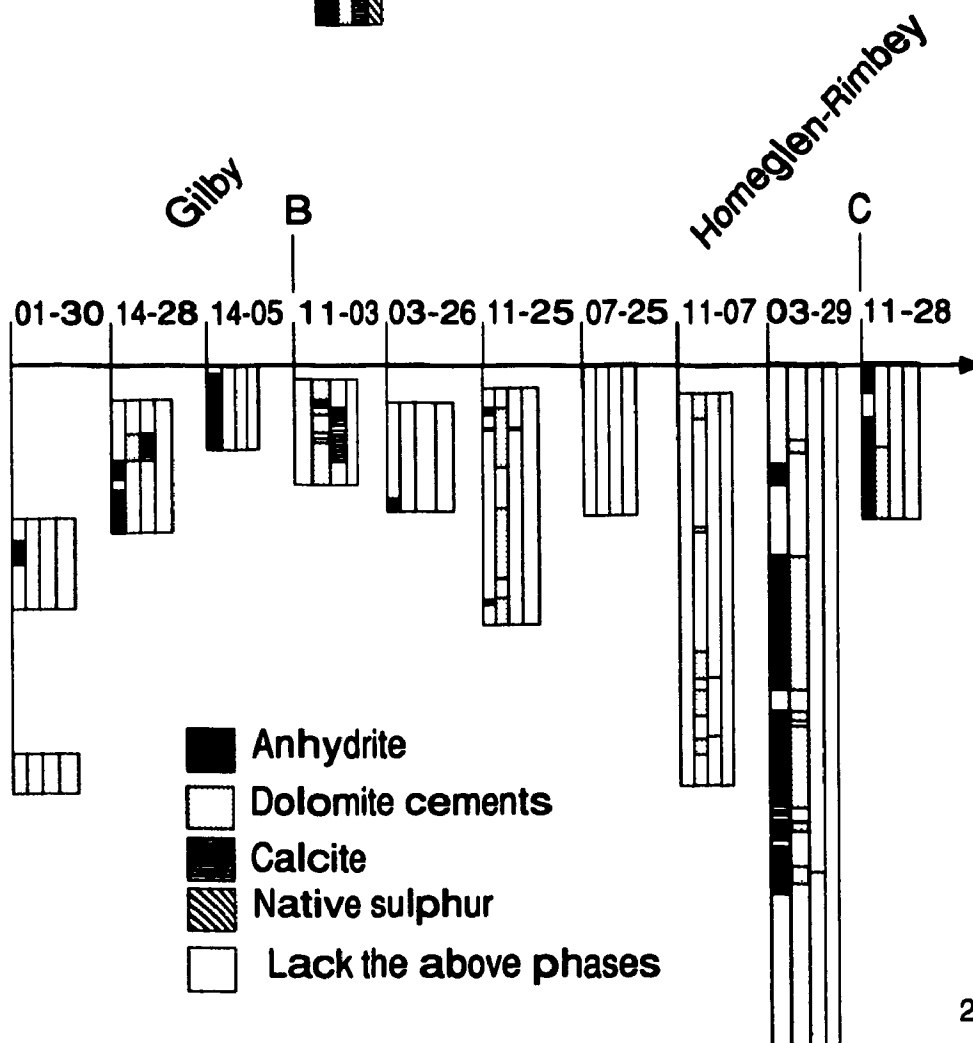
Figure 6. Generalized variation in porosity along the Rimbey-Meadowbrook reef trend (Amthor et al., submitted), and estimated percentages of late-stage anhydrite, dolomite (C1 and C2) and blocky calcite cements, and native sulphur. These cements reduce average porosity from about 7% at depths of about 2300 m to 2% at depths of 3500 m.

SW   Dolomitized Buildups   NE

Harmattan
Field (3500 m)

Homeglen-Rimbey
Field (2300 m)

TOTAL AVERAGE POROSITY BEFORE CEMENTATION

12.5%   12.5%

0

5%

10%
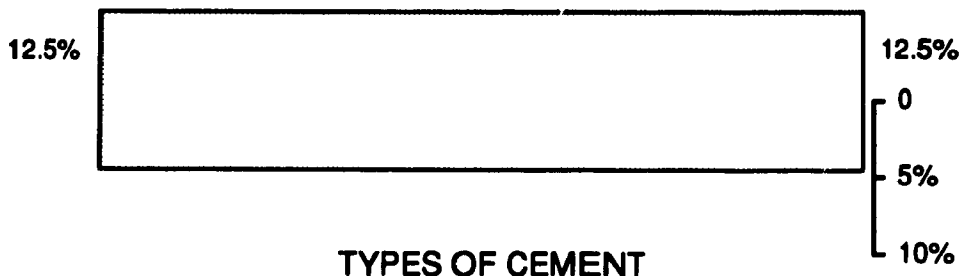
TYPES OF CEMENT

Anhydrite
(in part replacive)

7%   4%

Dolomite

1.5%   1%

Calcite

1.5%   0.5%

Native sulphur

0.5%   0%
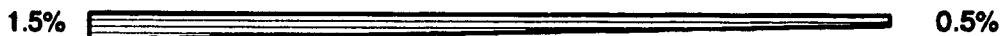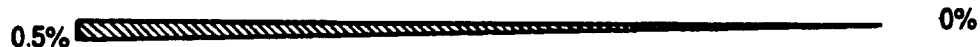
PRESENT AVERAGE MATRIX POROSITY

2%   7%

28
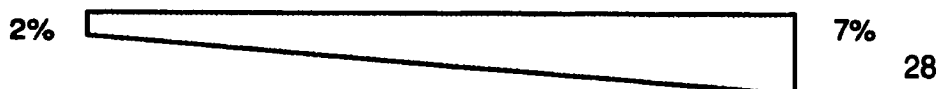
coincides with a decrease in the total amount of cements from 10.5 % in the Garrington area (township 35) to 5.5% in the Homeglen Rimbey field (twps 42 and 43) (Fig. 6). Native sulphur and calcite cement occur locally in the southern part of the study area (twp 33 to 37) at depths greater than 3000 m, and are rare to absent in the northern part (twp 38 to 43) (Figs. 5 and 6). Estimated percentages of anhydrite and dolomite cements decrease northward along the trend (Figs. 5 and 6), and only a trace of theses phases occurs north of the study area (Amthor et al., 1993; Machel, pers. comm., 1993).

GEOCHEMISTRY OF DOLOMITES AND CALCITES

Oxygen and carbon isotopic values for all replacement dolomites (R1 to R4) range from $\delta^{13}C$= 0.29 to 3.80 ‰PDB, and $\delta^{18}O$= -5.27 to -3.71 ‰PDB (Table 3a; Fig. 7a). Given the large number of analyzed replacement dolomites (n=44), and their widespread spatial distribution, there is a relatively narrow range of isotopic composition. Replacement dolomites have lower $\delta^{18}O$ values compared to hypothetical Upper Devonian marine dolomites, estimated by Amthor et al. (1993) to vary from $\delta^{18}O$= 0 to -2.5 ‰SMOW, assuming $\delta^{18}O$ value for Devonian marine calcites of -4.0 ‰PDB (Fig. 7a). The oxygen and carbon isotopic composition of Dolomite-C1 (n=28) mostly overlaps with that of replacement dolomites except for three values that have lighter ^{18}O (-6.07, -6.21, and -7.05‰PDB) (Fig. 7b). Crystals of Dolomite-C2 (saddle dolomite) in the Leduc Formation are rare in the study area and are difficult to separate from Dolomite-C1 since the two occur close together. As a result, only two samples of saddle dolomite were analyzed, both from the Cooking Lake Formation. These samples are lower in $\delta^{18}O$ values (-9.34 and -8.78 ‰PDB) than all other dolomite types (Fig. 7b). The oxygen and carbon isotopic values for blocky calcite cement range from $\delta^{13}C$= -17.9 to 3.48 ‰PDB, and $\delta^{18}O$= -9.51 to -4.61 ‰PDB (Table 3b; Fig. 7b). Samples with lighter carbon and oxygen isotopes ($\delta^{13}C$= -17.9 and -6.53 ‰PDB, and $\delta^{18}O$= -8.02 and -7.71 ‰PDB) were collected from cores that contain native sulphur. Calcite cement with low oxygen isotopic values (-9.51 to -7.94‰PDB) and with carbon isotopic

Table 3a. Carbon, oxygen, and strontium isotopic data of replacement dolomites, and dolomite cements from the Upper Devonian Leduc Formation, southern part of the Rimbey-Meadowbrook reef trend. Mean values are indicated in bold.

Dolomite types	Well location	Depth (m)	$\delta^{13}C$ (PDB)	$\delta^{18}O$ (PDB)	$^{87}Sr/^{86}Sr$ $\pm 2\sigma$
Replacement dolomite R1	11-10-35-05W5	3364	0.29	-3.71	
	16-25-36-06W5	3470	3.58	-4.55	
	08-27-36-06W5	3583	3.71	-4.57	
	08-27-36-06W5	3593	3.73	-4.57	
	16-11-38-05W5	3071	2.13	-4.29	
	11-07-43-01W5	2390	2.15	-4.39	
	03-29-43-01W5	2375	2.76	-5.04	
			2.69	**-4.45**	
Replacement dolomite R2	11-10-35-05W5	3364	0.43	-3.71	0.70834 ± 5
	11-06-36-03W5	2973	2.04	-4.08	0.70871 ± 2
	08-27-36-06W5	3583	3.64	-4.62	
	08-27-36-06W5	3593	3.47	-4.90	
	10-17-37-03W5	2863	2.13	-4.25	
	16-32-37-04W5	2982	1.29	-4.98	
	16-32-37-04W5	2988	1 48	-4.64	
	16-32-37-04W5	2988	1.70	-3.76	
	16-32-37-04W5	2989	1.51	-4.28	0.70912 ± 4
	16-32-37-04W5	2991	1.58	-4.06	
	16-32-37-04W5	3004	2.17	-4.11	0.70818 ± 4
	06-04-38-04W5	2961	1.18	-4.54	
	08-30-38-04W5	3135	3.67	-4.06	
	16-11-38-05W5	3071	2.28	-4.48	0.70855 ± 5
	14-28-39-03W5	2823	2.33	-4.25	
	14-28-39-03W5	2834	3.13	-4.33	
	14-05-41-02W5	2514	1.57	-4.27	
	11-03-42-02W5	2384	1 96	-4.73	
	11-03-42-02W5	2390	1.59	-4.80	
	11-03-42-02W5	2395	2.02	-4.44	
	07-22-42-02W5	2402	1.96	-5.27	0.70856 ± 2
	11-25-42-02W5	2429	2.36	-4.68	
	11-07-43-01W5	2390	2.09	-4.76	
	11-28-43-01W5	2445	2.86	-4.77	
	03-29-43-01W5	2375	2.67	-5.06	
	03-29-43-01W5	2382	2.55	-4 44	0.70826 ± 2
	03-29-43-01W5	2441	3.33	-4.73	
			2.18	**-4.48**	**0.70850**

Dolomite types	Well location	Depth (m)	δ^{13}C (PDB)	δ^{18}O (PDB)	^{87}Sr/^{86}Sr ±2σ
Replacement dolomite R3	16-32-37-04W5	2982	1 19	-4 60	
	06-04-38-04W5	2961	1.28	-4.43	
	11-03-42-02W5	2375	1.30	-5 18	
	03-29-43-01W5	2375	2.68	-5.20	
	03-29-43-01W5	2441	3.34	-5.03	
			1.96	**-4.89**	
Replacement dolomite R4	08-27-36-06W5	3583	3.80	-4 11	
	08-27-36-06W5	3583	3.24	-4.43	
	08-27-36-06W5	3593	3.66	-4 76	
	16-32-37-04W5	2991	1.74	-4.21	
	06-20-38-04W5	3124	3.51	-4.93	
			3.19	**-4.49**	
Dolomite cement C1	11-06-36-03W5	2973	2.33	-4.31	
	11-06-36-03W5	2975	1.97	-4.07	
	11-06-36-03W5	2991	2.55	-4.00	
	16-25-36-06W5	3487	3 08	-5.50	
	10-17-37-03W5	2863	1.99	-4 64	
	10-17-37-03W5	2863	1.97	-3.96	
	16-32-37-04W5	3002	0.31	-4.00	
	06-20-38-04W5	3105	2.78	-4.67	0.70903 ± 1
	08-30-38-04W5	3159	1.17	-6.21	0.70950 ± 1
	16-11-38-05W5	3070	2.13	-3.96	
	14-28-39-03W5	2823	2.75	-4.84	0.70883 ± 2
	11-03-42-02W5	2384	1.82	-4.39	
	11-03-42-02W5	2384	1.98	-4.53	
	11-03-42-02W5	2384	2.00	-4 89	
	11-03-42-02W5	2390	1.73	-4.81	0.70830 ± 2
	11-03-42-02W5	2395	1.36	-5 37	0.70834 ± 2
	11-03-42-02W5	2395	2.01	-4.92	
	11-25-42-02W5	2420	1.17	-7.05	0 70862 ± 2
	11-25-42-02W5	2429	2.19	-4.57	
	11-25-42-02W5	2429	2.11	-4.29	
	11-35-42-02W5	2527	2.39	-5.57	0.70876 ± 1
	11-28-43-01W5	2445	2.61	-5.04	
	11-28-43-01W5	2445	2.77	-4.55	
	11-28-43-01W5	2445	2.94	-5 18	
	03-29-43-01W5	2375	2.02	-6.07	
	03-29-43-01W5	2382	2.53	-4.07	0.70834 ± 2
	03-29-43-01W5	2382	2.49	-4.37	

Dolomite types	Well location	Depth (m)	$\delta^{13}C$ (PDB)	$\delta^{18}O$ (PDB)	$^{87}Sr/^{86}Sr$ ±2σ
Dolomite cement C1	03-29-43-01W5	2382	2.42	-4.34	
			2.13	**-4.79**	**0.70871**
Dolomite cement C2	*07-34-33-06W5	39697	4.16	-8.78	
	*07-34-33-06W5	39697	3.48	-9.34	0.71087 ± 1
			3.82	**-9.06**	**0.71087**

Table 3b. Carbon, oxygen, and strontium isotopic data of coarse blocky calcite cements from the Upper Devonian Leduc Formation, southern part of the Rimbey-Meadowbrook reef trend. Four types of calcite cements are distinguished on the basis of their association with other diagenetic phases. Mean values for each types are indicated in bold.

Types of coarse blocky calcite cements	Well location	Depth (m)	$\delta^{13}C$ (PDB)	$\delta^{18}O$ (PDB)	$^{87}Sr/^{86}Sr$ ±2σ
Postdate replacement dolomites	01-30-39-03W5	2935	1.98	-7.80	0.70825 ± 1
	01-30-39-03W5	2993	3.48	-5.16	
			2.73	**-6.48**	
Postdate dolomite cement C1	10-23-28-04W5	3008	-0.61	-7.24	
	14-28-39-03W5	2823	1.67	-4.61	0.70876 ± 1
	11-03-42-02W5	2381	0.98	-5.41	
	11-03-42-02W5	2384	-1.14	-7.82	
	11-25-42-02W5	2420	1.70	-4.83	0.70873 ± 2
	11-07-43-01W5	2390	1.67	-9.31	
			0.71	**-6.53**	**0.70874**
Distributed near pores filled with native sulphur	11-06-36-03W5	2963	-6.53	-7.71	
	16-25-36-06W5	3460	-17.9	-8.02	
	16-25-36-06W5	3489	0.26	-9.12	0.70894 ± 2
	08-27-36-06W5	3578	-2.58	-5.95	
			-6.74	**-7.70**	**0.70894**
Distributed near sulphides	11-03-42-02W5	2384	-1.78	-7.94	
	11-03-42-02W5	2395	1.23	-9.10	0.70874 ± 2
	11-07-43-01W5	2390	1.83	-9.51	
			0.42	**-8.85**	**0.70874**

Figure 7. A. Cross plot of $\delta^{13}C$ and $\delta^{18}O$ values for replacement dolomites (R1 to R4) from different Leduc buildups along the southern part of the Rimbey-Meadowbrook reef trend (Table 3a). Replacement dolomites (R1 to R4) form a relatively tight cluster, slightly depleted in oxygen-18 relative to a hypothetical dolomite precipitated in equilibrium with Upper Devonian seawater (see Amthor et al., 1993 for reference values). B. Cross plot of $\delta^{13}C$ and $\delta^{18}O$ values for replacement dolomites (R1 to R4), dolomite cements (C1 and C2), and blocky calcite cement from different Leduc buildups along the southern part of the Rimbey-Meadowbrook reef trend (Tables 3a and 3b). $\delta^{18}O$ values of dolomite cement C1 overlap and are slightly lower than those of replacement dolomites. Dolomite cement C2 is significantly more negative in $\delta^{18}O$ values than all the other dolomite types. $\delta^{18}O$ and $\delta^{13}C$ values of blocky calcite overlaps with those of the dolomites, with some $\delta^{13}C$ being much lower.

A)
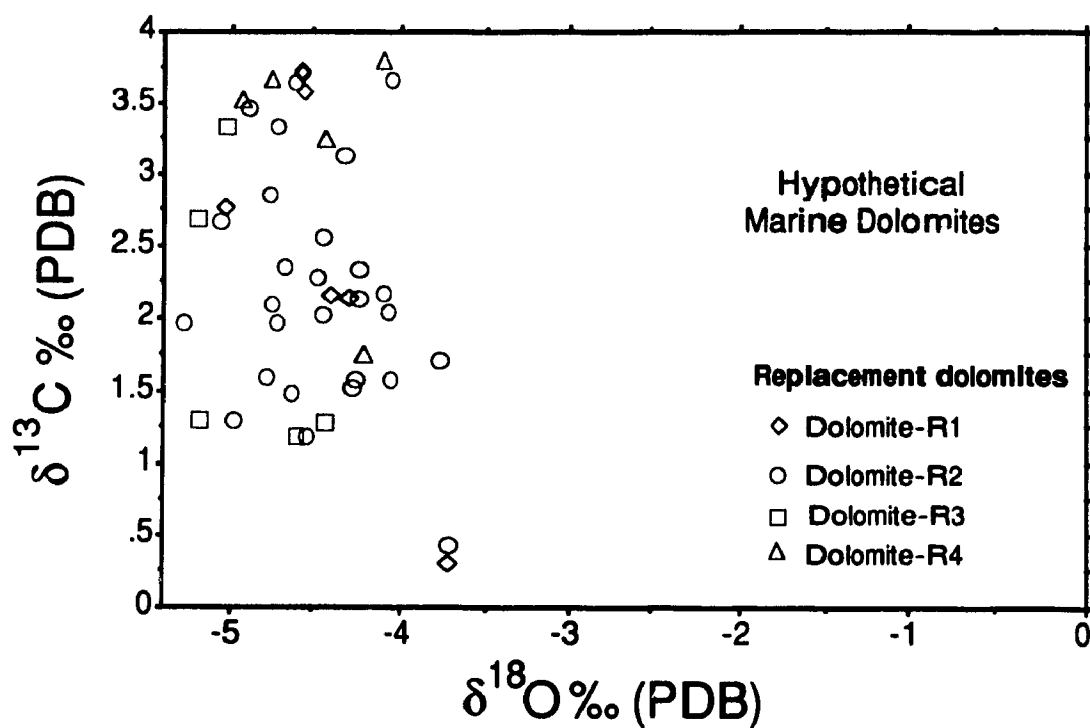
B)
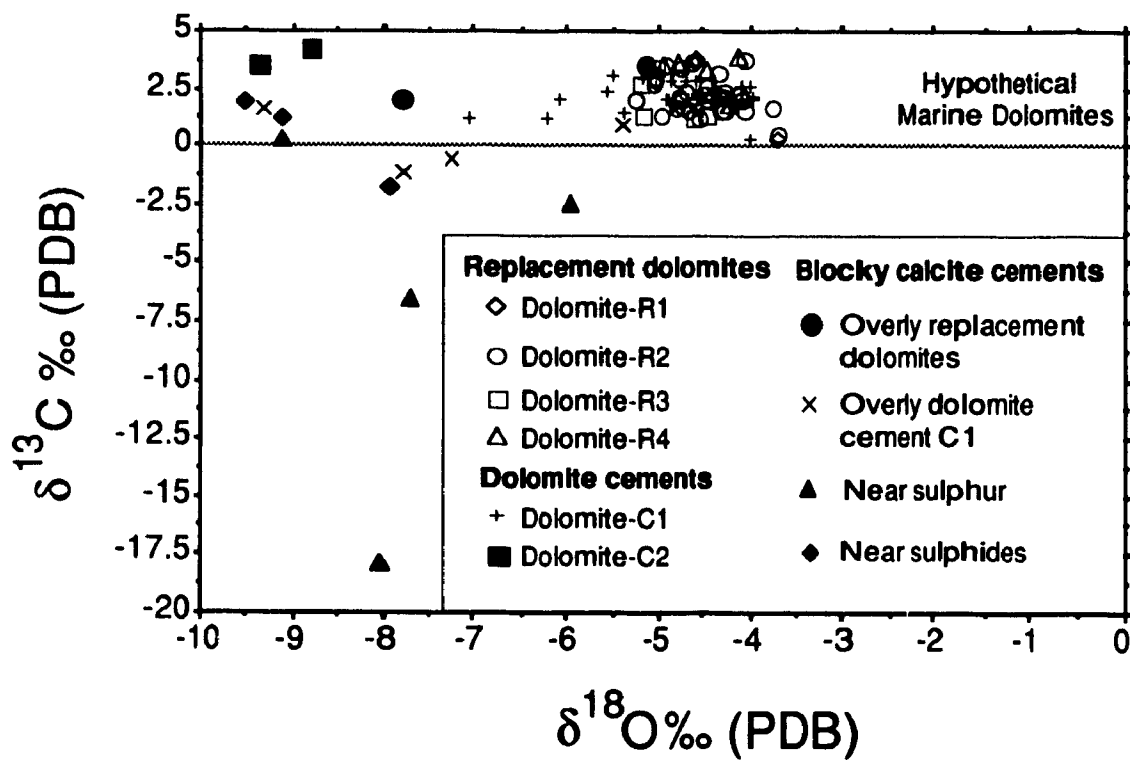
Figure 8. Cross plot of $^{87}Sr/^{86}Sr$ and $\delta^{18}O$ for replacement dolomite (R2), dolomite cements (C1 and C2), and blocky calcite cement from different buildups and positions within the buildups (Tables 3a and 3b). No clear trend is observed. However, in general dolomite cements have higher $^{87}Sr/^{86}Sr$ ratios and lower $\delta^{18}O$ values than the replacement dolomites, and lower $^{87}Sr/^{86}Sr$ ratios and higher $\delta^{18}O$ values relative to blocky calcite.
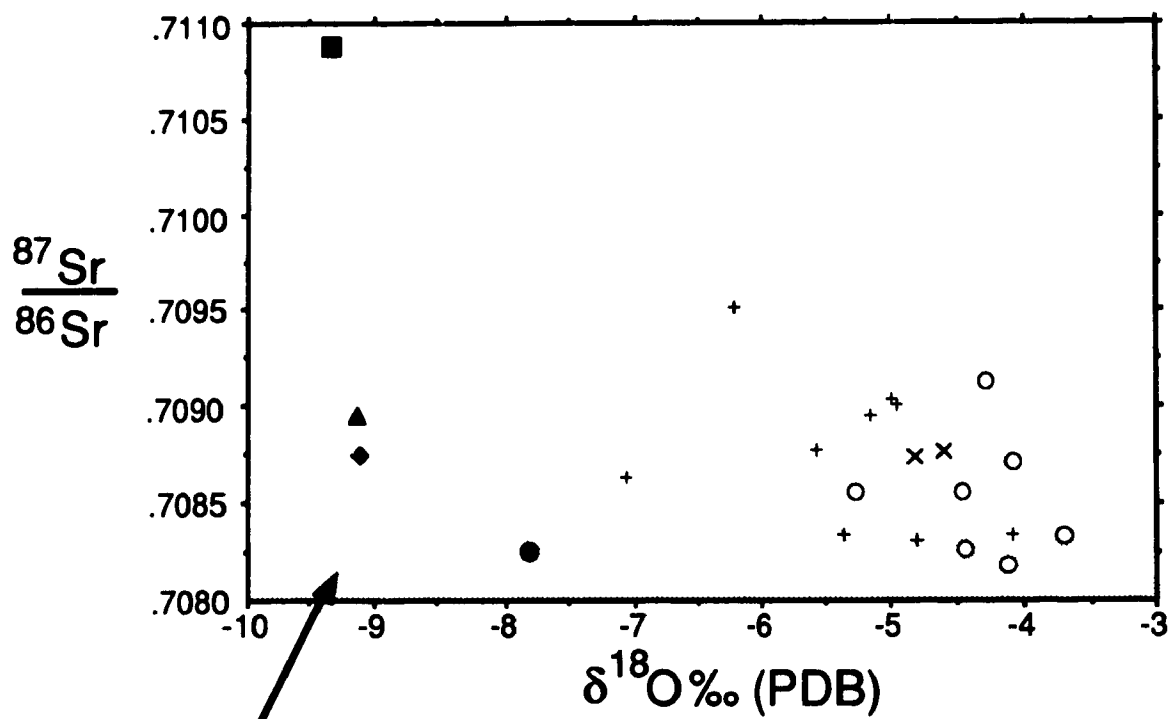
$^{87}Sr/^{86}Sr$ range for Upper Devonian
seawater (Burke et al., 1982)

Dolomites
o Dolomite-R2
+ Dolomite-C1
■ Dolomite-C2

Blocky calcite cements
● Postdate replacement
   dolomites
× Postdate dolomite
   cement C1
▲ Near sulphur
◆ Near sulphides

signatures near to zero (-1.78 to 1.83‰PDB) occur in pores near fractures that are filled with sulphides.

Strontium isotopes were measured from seven samples of Dolomite-R2 that have values ranging between 0.70818 and 0.70912 (Table 3a; Fig. 8). Eight samples of Dolomite-C1 (0.70830 to 0.70950) overlap and are slightly more radiogenic than for the replacement dolomites. The $^{87}Sr/^{86}Sr$ ratios of calcite cements (0.70873 to 0.70894) overlap and are more radiogenic than those of Dolomite-C1 (Fig. 8). These trends, however, are not as well defined as those for the Presqu'ile Barrier (Qing and Mountjoy, 1992).

FLUID INCLUSIONS

Twenty seven primary liquid-vapour fluid inclusions within the crystal growth zones of Dolomite-C1 (Plate 4f) have been analyzed. These inclusions are 7 to 15 μm in length, 3 to 8 μm in width, and contain an aqueous liquid and a small vapour bubble (about 1.5 μm in diameter). The studied inclusions are interpreted to be primary because they are distributed along lineations that follow the orientation of the crystal zonations of Dolomite-C1, and never crosscut the crystal faces (Plate 4f). They have homogenization temperatures between 98 and 129°C, with three other inclusions giving temperatures between 140 and 142°C (Table 4; Fig. 9a; Appendix 1). Ice melting temperatures of these inclusions (-18.3 to -14.7°C) indicate high salinities (17.9 to 20.4 wt.% NaCl equ.). An additional six inclusions were measured in the cloudy core of replacement dolomite crystals. These inclusions are, in some cases, very close to a rim of clear dolomite cement that surrounds the cloudy core, making it difficult to determine whether they were within replacement dolomite or dolomite cement. Homogenization temperatures obtained range from 100 to 122°C (mean= 113°C), and salinities are between 19.5 and 19.8 wt% NaCl equivalent (mean= 19.7) (Fig. 9b). These values from the cloudy cores of replacement dolomites are very similar to the ones derived for the primary inclusions in the Dolomite-C1.

Table 4. Summary of fluid inclusion microthermometric data (ranges, means, standard deviation (±), number of analyses (n)) for fluid inclusions in dolomite cement C1 from the Leduc Formation. See appendix I for more details. The majority of the inclusions studied are liquid primary inclusions that occur within growth zones of dolomite cement (Dol-C1). Six inclusions measured in 03-29-43-01W5 were located in the cloudy core of replacement dolomite crystals (250μm). In some cases, these inclusions are very close to a rim of clear dolomite cement which surrounds the cloudy core. (T_f: freezing temperature; T_m(ice): final ice melting temperature; T_h: homogenization temperature).

Dolo. Type	Location	Depth	T_f(°C)	T_m(ice) (°C)	Salinity (wt% NaCl eq.)	T_h (°C)
Dol-C1	08-30-38-04W5	3159	-73 to -56 (-68±4 n=10)	-17.8 to -16.8 (-17±0.3 n=8)	19.4 to 20.1 (20±0.2 n=8)	98 to 121 (110±8 n=12)
Dol-C1	11-03-42-02W5	2390	-70 to -56 (-66±5 n=17)	-18.3 to -17.4 (-18±0.4 n=7)	19.9 to 20.4 (20±0.2 n=6)	110 to 142 (122±11 n=11)
Dol-C1	03-29-43-01W5	2382	-66 to -61 (-64±2 n=7)	-15.4 to -14.7 (-15±0.3 n=6)	17.9 to 18.4 (18±0.2 n=6)	114 to 140 (126±8 n=7)
Dol-R2 (?)	03-29-43-01W5	2382	-71 to -68 (-69±1 n=6)	-17.4 to -17 (-17±0.2 n=6)	19.5 to 19.8 (20±0.2 n=6)	100 to 122 (113±8 n=6)

Figure 9. A. Histograms for 36 aqueous liquid-vapour primary fluid inclusions in Dolomite-C1 cement from wells 08-30-38-05W5, 11-03-42-02W5, and 03-29-43-01W5 (Table 4; Appendix 1) showing homogenization temperatures (T_h), ice melting temperatures (T_m(ice)), and corresponding salinities in weight percent NaCl equivalent. B. Histograms for six fluid inclusions measured in one sample from well 03-29-43-01W5, 2382 m, (Table 4) showing homogenization temperatures (T_h), ice melting temperatures (T_m(ice)), and corresponding salinities in weight percent NaCl equivalent of aqueous liquid-vapour primary fluid inclusions in cloudy cores of replacement Dolomite-R2 along the boundary with the clear rim of dolomite cement C1. Because of their proximity to the rims of dolomite cement C1, it is questionable whether these inclusions belong to the replacement dolomites or the later cements.

A) Primary fluid inclusions in Dolomite-C1
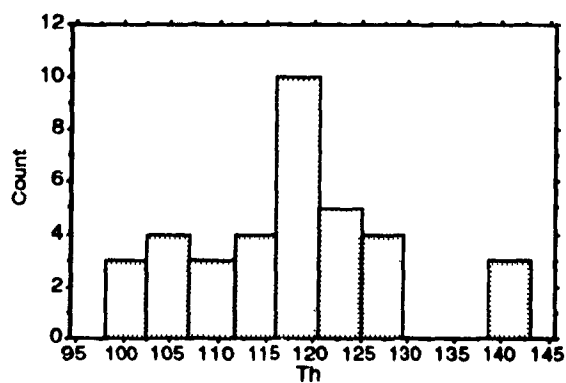
B) Fluid inclusions in Dolomite-R2 or Dolomite-C1?
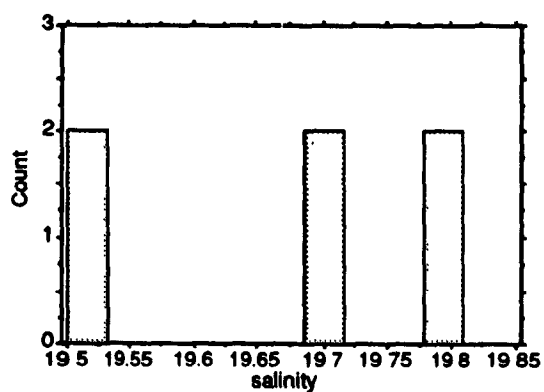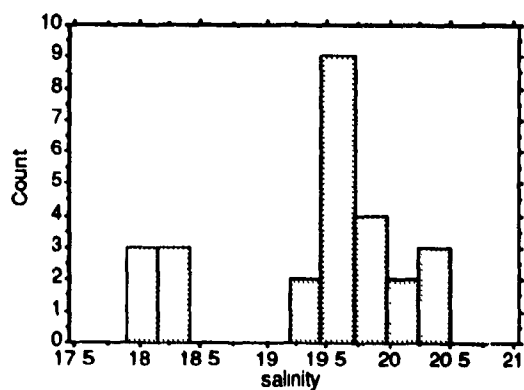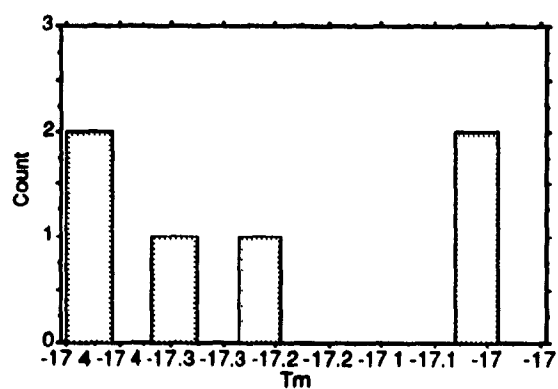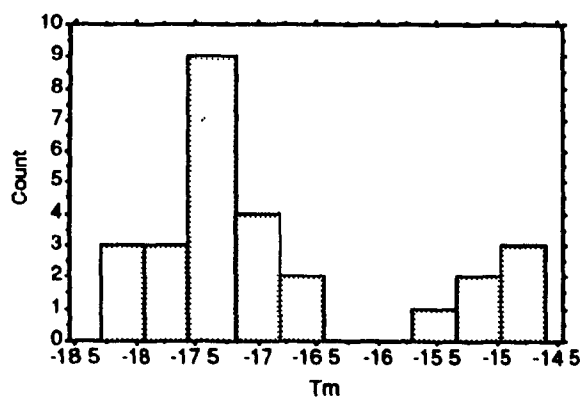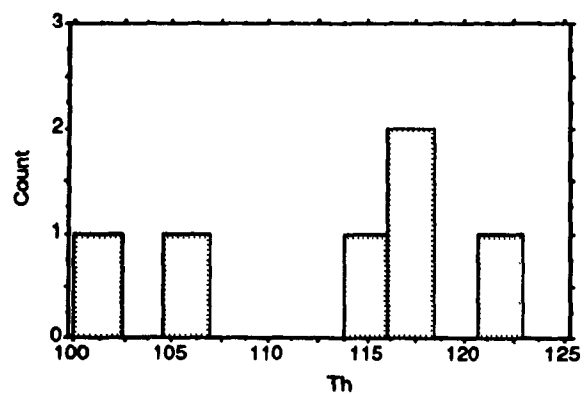
PARAGENETIC SEQUENCE AND TIMING OF DOLOMITIZATION

Diagenesis in the Leduc dolomite buildups is complex (Fig. 10). Most early diagenetic features, best recognised in limestone buildups, have been modified and/or obliterated by later diagenesis, especially replacement dolomitization. Dolomite-R4 replaces isopachous and fibrous calcite cements (Plates 3d to 3h), indicating that replacement dolomitization postdates early submarine cementation. Replacement dolomites (R1 to R3) extend into underlying and overlying formations, implying that dolomitization postdates deposition of the Ireton and Duvernay shales. In general, replacement dolomites are crosscut by stylolites (Plate 6a), indicating that dolomitization took place prior to some stylolitization. Locally, crystals of replacement dolomites overlap and are optically continuous across some stylolites (Plate 6b). This suggests that some replacement dolomitization or later neomorphism of replacement dolomites have postdated stylolitization. Replacement dolomites predate bitumen (Plate 3a) and thus originated prior to the generation and migration of hydrocarbons (Late Cretaceous to Early Tertiary) (Deroo et al, 1977; Creaney and Allan, 1992). This, combined with the fact that replacement dolomites crosscut facies and surrounding formations, broadly constrains the timing of replacement dolomitization to be Late Devonian or younger.

Dolomite-C1 fills pores in matrix dolomites (R1 to R3) (Plate 4a) and therefore postdates replacement dolomitization. Dolomite-C2 occludes the remaining pores in these dolomites (Plate 5a), and represents the latest phase of dolomite cementation. Dolomite cements (C1 and C2) are coated by bitumen (Plate 7c) indicating that they precipitated before oil migration. The occurrence of sulphides within Dolomite-C1 crystals (Plates 7d and 7e) suggests that some dolomite cementation overlapped with pyritization.

Anhydrite cementation postdates Dolomite-C1 (Plate 7a), and precedes blocky calcite cements. Stylolites locally crosscut anhydrite cements (Plate 6d) indicating that they continued after anhydrite cementation. Replacement of dolomites (R1 to R4 and C1) by anhydrite is observed in several brecciated

Figure 10. Paragenetic sequence of Leduc Formation in the study area. The terms shallow, intermediate, and deep burial are defined relative to stylolitization. Intermediate burial represents the onset of stylolitization (> 500 m from Dunnington, 1967; Lind, 1993), and shallow and deep burial define pre- and post-incipient stylolitization corresponding to depths of approximately < 500 m and > 1500 m respectively.

Paragenetic sequence of the Leduc dolostones

DIAGENETIC EVENT	EARLY → LATE			
Isopachous calcite cementation	▅▅▅ ▪			
Submarine cementation	▅▅▅			
Stylolitization		▪ ▪▪ ▅▅	▪ ▪ ▪ ▪▪▅▅▅	▪ ▪ ▪ ▪
Replacement dolomitization		▪ ▪ ▪ ▪▅▅▅▅	▅ ▪ ▪ ▪	
Dolomite cementation				▅▅▅ ▪
Anhydrite cementation and replacement				▪ ▪▪▅▅▅
Calcite cementation				▪ ▪▪ ▅▅▅
Quartz cementation				▪ ▪▪▅▅
Bitumen emplacement				▅▅▅▅
Sulphur and sulphides emplacement				▅▅▅

Sea floor Shallow Burial (< 500 m) Intermediate Burial (500-2000 m) Deep Burial (> 2000 m)
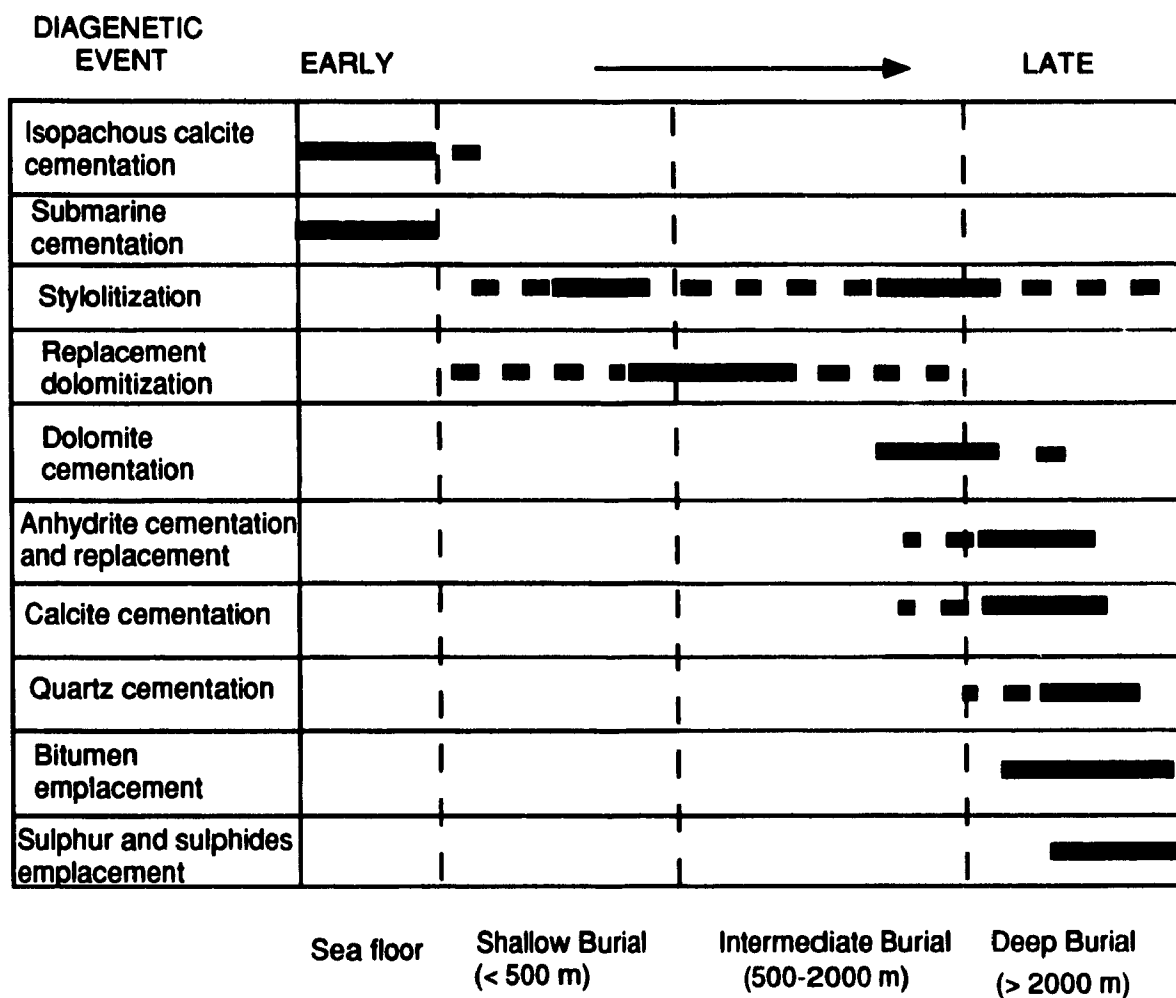
intervals (Plates 10e and 10f) and probably overlapped with the anhydrite cement that occurs in the breccia pores on top of Dolomite-C1. Blocky calcite precipitated after Dolomite-C1 since it fills pores on top of Dolomite-C1 (Plate 4a), and locally replaces Dolomite-C1 (Plate 7f). The relative timing between blocky calcite and Dolomite-C2 could not be resolved since the two were not observed together. Quartz, sulphides, and native sulphur postdate blocky calcite cementation (Plates 7g and 7h). However, the relative timing between quartz and sulphur-bearing minerals could not be determined.

ORIGIN OF LEDUC DOLOSTONES

Two main stages of dolomitization are recognized within the Leduc Formation: 1) replacement dolomites (R1 to R4); and 2) dolomite cements (C1 and C2). The origin of these dolomites is debatable and several models have been proposed, ranging from sea floor to burial dolomitization (see Machel and Mountjoy, 1987; Amthor et al., 1993). In the following sections, petrographic and geochemical data are integrated to constrain the environment of dolomitization and dolomite cementation. Prior to interpreting the origin of the Leduc dolostones, the possibility that replacement dolomites have undergone neomorphism is evaluated.

Neomorphism

Recently, several examples of both recent and ancient neomorphosed dolomites have been documented (e.g. Gregg and Sibley, 1984; Gregg and Shelton, 1990; Kupecz et al., 1991; Kupecz and Land, 1991; Gregg et al., 1992; Mazzullo, 1992; Montañez and Read, 1992). Other dolomites, however, have been interpreted to be unaltered chemically and texturally since their formation (e.g. Lee and Friedman, 1987; Amthor et al., 1993). These different opinions arise from the difficulty of distinguishing subtle changes in textural and geochemical compositions relative to inferred preexisting phases. Mazzullo (1992) reviewed the main criteria for recognizing neomorphism: (1) an increase in the ordering and stoichiometry of crystals; (2) changes in crystal texture (mainly an increase in

crystal size correlated with an increase in nonplanar crystal boundaries); (3) homogeneous and blotchy cathodoluminescence; and (4) changes in oxygen and strontium isotopic and major and trace element compositions (primarily Sr and Na).

In this study, the following observations suggest that replacement dolomites did not result from recrystallization of an earlier dolomite: 1) early seawater related dolomites are minor to nonexistent in undolomitized (e.g. Golden Spike; Walls, 1977), partially and completely dolomitized Leduc buildups; 2) reworked clasts in partially dolomitized debris-flow deposits of buildup-slope facies are entirely limestone (e.g. well 01-30-39-03 W5), indicating that matrix dolomitization postdates deposition and that the clasts were not dolomitized at an early stage; 3) replacement dolomites grade directly into limestones and crosscut the underlying Cooking Lake Formation and overlying Ireton Formation; 4) there is no evidence for a Devonian regional meteoric recharge in Leduc Formation buildups and the underlying Cooking Lake platform, that could have resulted in alteration; 5) textural relationships indicate that replacement dolomitization took place after submarine cementation (isopachous and fibrous calcite cements), and overlaps and postdates early stylolitization; and 6) the presence of allochem ghosts in medium to coarse-crystalline replacive Dolomite-R2 (Plates 8f and 8g) may be evidence of direct replacement of limestone rather than neomorphism of a precursor dolomite (Lee and Friedman, 1987; Sibley and Gregg, 1987); the absence of allochem ghosts, however, does not necessarily imply that recrystallization has occurred (Mazzullo, 1991). The above six points together with geochemical data (discussed later) suggest that most Leduc replacement dolomites formed at shallow to intermediate burial depths, and since then, have undergone minor recrystallization.

Local recrystallization of matrix dolomites near fractures, stylolites, and pores is suggested by the following textural features observed in about 15 out of the 201 thin sections studied: 1) a few planar-s crystals of Dolomite-R1 (30 to 60 µm) are distributed interstitial to and within coarser planar to nonplanar-s replacement dolomite crystals (60 to 250 µm), with the finer dolomite crystals in optical discontinuity with the coarser ones (Plate 1d); 2) occasionally, near

fractures and pores, crystals of replacement dolomite are coarser, nonplanar, and exhibit undulose extinction (Plates 1e and 1f); 3) the presence of bright and dull luminescent bands of replacement dolomites along fractures (Plates 2a to 2d); and 4) the unusual occurrence of crystal zonations in Dolomite-R2 with replacement of relict cores (Zone 1 in Plate 2f) by Zone 2, and the minor replacement of Zone 2 by Zone 3 dolomite (Plates 2e and 2f). Point (1) may be explained by local recrystallization of fine-crystalline dolomites to coarser crystals resulting in a mixture of fine and coarser replacement dolomites. Another explanation, however, may be that the fine-crystalline dolomites represent a relict of the earliest stage dolomites and have not been modified by the later replacement dolomitization events. The presence of fine-crystalline (10-30 μm) isolated dolomite rhombs has been reported locally within the limestone matrix of the Cooking Lake platform that underlies the Leduc Formation (Chouinard, 1993) and in the Leduc Formation at Golden Spike (Walls, 1977). The origin of these rhombs is uncertain but they may have formed on the seafloor or just below it during early burial, similar to what occurs in today's oceans (Tucker and Wright, 1990). These rhombs were probably present in the completely dolomitized Leduc buildups and were not necessarily modified by later stage replacement dolomitization. The textural relationships described in points 2 to 4, however, suggest that neomorphism took place at least locally.

Controls on textural attributes

Replacement dolomites in the Leduc Formation exhibit a wide range of crystal sizes from 30 to 700 μm. Aside from the textural changes associated with fractures, pores, and stylolites as noted above, the crystal size of replacement dolomites appears to be controlled mainly by the primary facies. Commonly, fine-crystalline replacement Dolomite-R1 is distributed along stylolites, geopetals, and sedimentary laminations (Plate 1a). This, combined with the fact that the contacts between Dolomite-R1 and coarser replacement dolomites are generally sharp, suggests that Dolomite-R1 was fabric selective and that the finer crystal size is a

function of the precursor lithofacies being replaced. Dolomite-R3 is usually associated with intercrystalline porosity and is commonly distributed as patches that resemble burrows, and as layers resembling sedimentary grainstones (see Plate 8e, Chapter 3). When the dolomitizing fluids replaced porous and permeable facies such as burrows and grainstones, the resultant dolomite crystals would have grown coarser and more euhedral into the surrounding pore. Thus, the crystal distribution, morphology, and size of Dolomite-R3 may have been controlled by the primary facies. Alternatively, dissolution of the crystal surface may have been so slow that angular dissolving surfaces may result in euhedral crystal forms (Berner, 1978), similar to the Dolomite-R3. In summary, the textural attributes of replacement dolomites appear in general to be controlled by primary fabrics and porosity. It is difficult to determine the extent to which earlier textures and original geochemical signatures have been modified by neomorphism. The available data discussed in the above section suggest that it is local and minor.

Origin of replacement dolomites

Sea floor diagenesis cannot be recognized in the study area due to obliteration by replacement dolomitization. However, evidence from the undolomitized Leduc buildups such as the Golden Spike (McGillivray and Mountjoy, 1975; Walls, 1977) and Strachan (Marquez, Ph.D. in progress) indicate that the extent of seafloor dolomitization was probably minor. Replacement dolomites overlap and postdate stylolitization (Plates 6a and 6b; Fig. 11). Observations by Dunnington (1967) suggest that stylolites formed in limestones at depths between 500 and 700 m. A study by Lind (1993) of a continuous limestone core from the Ontong Java Plateau indicates that stylolites first appear at 470 m and are common below 830 m. Using these estimates as guides for the onset of stylolitization, the replacement dolomites associated with stylolitization probably precipitated at depths greater than 500 m in the shallow burial environment.

Several workers integrate textural data with oxygen isotopic compositions to estimate the depth at which dolomitization occurred (e.g. Land, 1985; Machel

and Anderson, 1989; Qing and Mountjoy, 1989; Amthor et al., 1993). There are several important assumptions involved, one being that the original isotopic signature of the dolomites has not been modified later. As noted earlier, small portions of replacement dolomites have been recrystallized near fractures, stylolites, and pores. Samples for isotope analyses were carefully selected to avoid these zones of alteration, and the following calculations are made assuming that neomorphism was not significant.

Additional assumptions used to estimate the paleotemperature at which replacement dolomites precipitated include: 1) the $\delta^{18}O$ values for marine components and cements ($\delta^{18}O_{calcite}$) deposited in Devonian seawater vary between -4 and -3‰PDB (Amthor et al., 1993), and for each of these $\delta^{18}O_{calcite}$ values, calculations were made for temperature of Devonian seawater equal to 25° and 35°C; 2) the diagenetic fluids were principally derived from Frasnian seawater; and 3) the $\delta^{18}O$ values of formation waters have not been modified significantly during early burial.   Following the procedure of Friedman and O'Neil (1977) and Land (1980, 1983, 1985) (Appendix 2), the precipitation temperatures for the Leduc replacement dolomites in the study area vary from 45 to 75°C (Table 5). Assuming that surface paleotemperatures were close to 30°C (relatively warm), and the present geothermal gradient of 30°C/km has not changed significantly since Late Devonian, 45° and 75°C correspond to burial depths of about 500 m and 1500 m respectively.   These depths would have been reached towards the end of the Devonian or later (Fig. 11). The minimum burial depth estimate (500 m) suggests that replacement dolomitization was initiated in the shallow burial environment between the Late Devonian and Early Carboniferous, which is consistent with the textural relationships. Similar interpretations are presented by several authors for Leduc replacement dolomites from other fields (e.g. Laflamme, 1990; Amthor et al. 1993), and from similar dolomites from other Devonian formations in the Western Canadian Sedimentary Basin (Machel and Anderson, 1989; Qing and Mountjoy, 1989; Kaufman et al., 1991).

Table 5. Paleotemperature estimates for precipitation of replacement dolomites in the Leduc Formation using measured minimum and maximum oxygen isotopic values and assuming different $\delta^{18}O$ values for Devonian marine components (-3 ‰ and -4 ‰PDB), and different temperatures for Devonian seawater (25° and 35°C).

Assuming temperature of Devonian seawater= 25°C

		Temperature (°C) of dolomite precipitation for:	
		$\delta^{18}O_{calcite}$= -3 ‰PDB	$\delta^{18}O_{calcite}$= -4 ‰PDB
	Estimated $\delta^{18}O_{fluid}$	-0.6 ‰SMOW	-1.7 ‰SMOW
Measured $\delta^{18}O_{dolomite}$	-5.20 (min.)	61	54
	-3.71 (max.)	52	45

Assuming temperature of Devonian seawater= 35°C

		Temperature (°C) of dolomite precipitation assuming:	
		$\delta^{18}O_{calcite}$= -3 ‰PDB	$\delta^{18}O_{calcite}$= -4 ‰PDB
	Estimated $\delta^{18}O_{fluid}$	1.3 ‰SMOW	0.34 ‰SMOW
Measured $\delta^{18}O_{dolomite}$	-5.20 (min.)	75	68
	-3.71 (max.)	64	58

Figure 11. Burial-temperature-time plot for Leduc buildups in the Homeglen-Rimbey and Garrington fields, constructed assuming a geothermal gradient of 30°C/km (Hudson and Anderson, 1989) and a surface temperature of 30°C (Walls et al., 1979). The inferred burial depths, temperatures, and timing of replacement dolomitization and dolomite cementation are also plotted. See text for detailed explanations.

Burial Plot
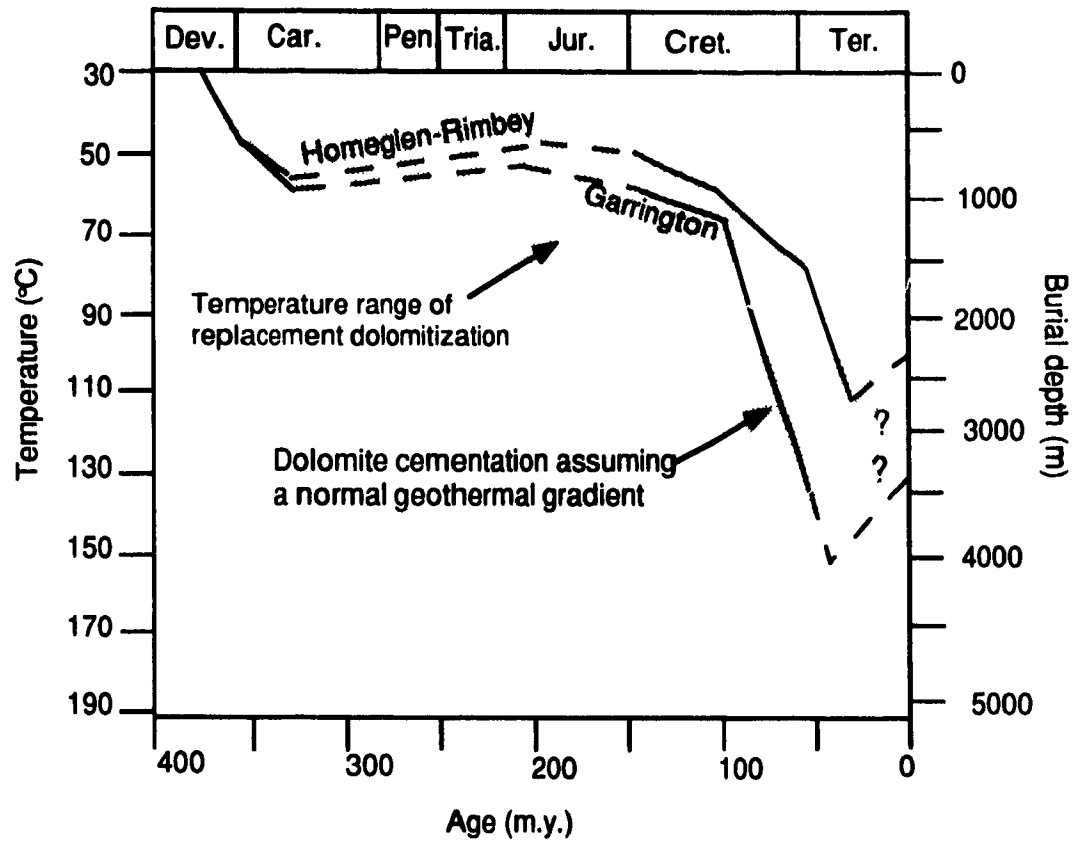
Replacement Dolomite-R2 overlaps and has slightly higher $^{87}Sr/^{86}Sr$ ratios (0.70818 to 0.7085) than values for Upper Devonian seawater (0.7080 to 0.7083) derived from the Burke et al. (1982) curve (Fig. 8). Mountjoy et al. (1992) reported similar values for secondary replacement dolomites from the Presqu'ile Barrier, the Rainbow, Rosevear, Miette, and Nisku buildups, and some fault and fracture controlled Wabamun dolomites. They concluded that the dolomitizing fluids were probably modified from Devonian seawater with small amounts of radiogenic ^{87}Sr being added during early compaction from adjacent or underlying clastics, or older carbonates. The strontium isotopic data for the Leduc replacement dolomites from the southern part of the Rimbey-Meadowbrook reef trend support this conclusion.

Origin of later-stage dolomite cements

The environment in which Dolomite-C1 precipitated is constrained by its relationship with stylolites and hydrocarbons, oxygen isotopic compositions, and fluid inclusion data. Dolomite-C1 is commonly distributed along stylolites (Plate 6c) and lines pores that are connected by stylolites indicating a possible link between pressure solution and dolomite cementation. Thus, dolomite cementation must have taken place in the burial environment during stylolitization at depths deeper than about 500 metres. Because crystal zonations of Dolomite-C1 occasionally contain specks of pyrite (Plates 7d and 7e), some Dolomite-C1 cementation appears to have continued during pyritization.

The progressive depletion in ^{18}O from replacement dolomites (-5.27 to -3.71 ‰PDB) to Dolomite-C1 (-7.05 to -3.96 ‰PDB) (Fig. 7b) probably reflects the different composition and temperature of the fluids responsible for dolomite cementation. Compared to replacement dolomites, Dolomite-C1 has slightly higher strontium isotopic ratios (Fig. 8) suggesting that they precipitated from slightly more radiogenic fluids. Measurements of primary fluid inclusions (Fig. 9a) indicate that Dolomite-C1 precipitated from brines with salinities (17.9 to 20.4 wt% NaCl equ.) about six times higher than seawater, similar to those present in Devonian subsurface strata today (Connolly et al., 1990). Homogenization temperatures

range from 98 to 121°C, with three inclusions yielding somewhat higher homogenization temperatures varying between 140 and 142°C. Dolomite-C1 would have formed during deep burial relative to the replacement dolomites at depths ranging from 2.3 to 3.7 km, during the Late Cretaceous to reach temperatures of 98 to 142°C (Fig. 11) assuming that: 1) the fluid inclusions are representative of the temperatures of precipitation of Dolomite-C1; 2) a normal geothermal gradient of 30°C/km; and 3) a surface temperature of 30°C. Since the generation of hydrocarbons occurred at depths of about 2800 m, or shallower if hydrocarbons were generated downdip (Deroo et al., 1977), the maximum depths at which Dolomite-C1 precipitated would have been 2800 m or less. This corresponds to temperatures less than 115°C. Therefore, fluid inclusions in Dolomite-C1 with homogenization temperatures greater than 115°C may be due to: 1) fluids hotter than those expected from the current geothermal gradient; or 2) an abnormally high geothermal gradient. In summary, based on the relationship between dolomite cements and stylolites, and assuming that T_h data represent true precipitation temperatures, Dolomite-C1 could have precipitated from saline hydrothermal fluids probably under intermediate to deep burial conditions (2000 to 2800 m) during the Cretaceous, or earlier if higher geothermal gradients existed (Fig. 11).

Petrographic evidence (Fig. 10; Plate 5a) shows that saddle dolomite (C2) cementation postdated Dolomite-C1 precipitation. The slightly more depleted oxygen isotopic values of Dolomite-C2 (-8.78 and -9.34‰PDB) compared to Dolomite-C1 (-7.05 to -3.96‰PDB) (Fig. 7a) suggest that saddle dolomite precipitated under higher temperatures, and/or from fluids with different isotopic compositions.

Origin of later-stage diagenetic phases

Thermochemical sulphate reduction (TSR) can explain, in part, the late-stage diagenesis (syn- and post- maturation of organic matters) in Leduc dolostones. TSR refers to high-temperature chemical reactions (>100°C) that occur between hydrocarbons (organic matter, carbohydrates, kerogen, crude oil,

bitumens, dissolved methane and other gaseous organic compounds) and aqueous sulphate in the presence of a catalyst. These temperatures would have been reached during the Cretaceous or possibly earlier if hot fluids were available (Fig. 11). The net reaction can be summarized by the following equation (Machel, 1987 a,b):

$$\text{hydrocarbons} + SO_4^{2-} \rightarrow \text{altered hydrocarbons} + \text{bitumen} + HCO_3^{1-} + H_2S\ (+CO_2?) + \text{heat}$$

Several intermediate stages, including thermal cracking and sulphurization of organic matter, and multistep reduction of sulphur species may complicate the above net reaction (Machel, 1987 a,b). The release of H_2S, and CO_2 with isotopically light carbon may result in (Krouse et al., 1988): 1) precipitation of late-stage cements such as blocky calcite and saddle dolomite with light carbon isotopic signatures (-2 to -20 ‰PDB); 2) precipitation of sulphur bearing minerals (including anhydrite, sulphides, and elemental sulphur); 3) replacement of anhydrite by calcite or dolomite; and 4) creation of local secondary porosity. These late-stage diagenetic products and evidence of dissolution have been recognised in several Devonian carbonate buildups of Western Canada (Eliuk, 1984; Krouse et al., 1988; Laflamme, 1990; Machel 1987 a,b; Reimer and Teare, 1992) and have been used as evidence to support TSR processes and reactions in the deeper parts of the basin. Potential TSR by-products observed in the study area are anhydrite cement, elemental sulphur, sulphides, bitumen, and blocky calcite cement (Fig. 10). Geochemical evidence for TSR includes the negative $\delta^{13}C$ values of two blocky calcite samples (-17.9 and -6.53 ‰PDB; Table 3b) that may have resulted from CO_2 generated by the oxidation of light hydrocarbon gases during TSR.

The amounts of anhydrite, blocky calcite, sulphides, and native sulphur are most abundant in the deepest part of the study area (below 3000 m) and gradually decrease updip. Only rare occurrences of anhydrite and calcite cement are found north of township 39 (above 3000 m) (Figs. 5 and 6). Concentrations of H_2S in gas and oil fields of the Bearberry and Caroline fields average 90 and 30% respectively

(Laflamme, 1990). In contrast, the Homeglen-Rimbey field that is located at shallower burial depths updip to the northeast, has an average mole percent of 1.4% H_2S equivalent (James, 1990). H_2S concentrations above 2 mole percent are generally considered to have resulted from thermochemical sulphate reduction (TSR) (Machel, 1987a,b; Krouse et al., 1988). Thus, the distribution of late-stage diagenetic minerals (anhydrite, blocky calcite, sulphides, and native sulphur), and the H_2S content of the reservoir gases suggest that the deepest part of the trend was more affected by TSR processes than its updip equivalent. This hypothesis, however, needs to be tested by further geochemical work, particularly sulphur isotopes of sulphides, anhydrite, and elemental sulphur in order to rule out other possible burial processes.

SUMMARY AND CONCLUSIONS

The paragenesis and petrographic data indicate that Leduc replacement dolomites postdate the deposition of submarine cements and the overlying Ireton Formation, and overlap with early stylolitization. These observations imply that replacement dolomitization originated in the burial environment at depths greater than about 500 metres. This interpretation is consistent with burial depths calculated from oxygen isotopes (500 to 1500 m). These estimates indicate that replacement dolomitization started during the Late Devonian to Early Carboniferous. Replacement Dolomite-R2 overlaps with and has slightly higher $^{87}Sr/^{86}Sr$ ratios (0.7082 to 0.7085) than the corresponding Devonian seawater (0.7080 to 0.7083) indicating that the dolomitizing fluids were probably modified from Devonian seawater with the addition of small amounts of radiogenic strontium from adjacent or underlying clastics, or older carbonates. The above assumes that these replacement dolomites have not been significantly modified since deposition. Only minor neomorphism is suggested by: 1) fine dolomite rhombs (30 to 60 μm) that are occasionally distributed interstitial to and within coarser dolomite crystals (60 to 250 μm) suggesting the recrystallization of fine crystals to coarser ones; 2) the occurrence of coarser replacement dolomite crystals near fractures, stylolites,

50

and pores that display irregular sometimes nonplanar crystal boundaries and exhibit weak undulose extinction; 3) the presence of bright and dull luminescent bands of replacement dolomites along fractures; and 4) replacement of crystal cores in Dolomite-R2 by zoned dolomite. Aside from these local zones of alteration, the textures of Leduc dolomites appear to represent dolostones that have not been modified geochemicaly since the time of their precipitation.

Later dolomite cements (C1 and C2) fill pores around dolomite clasts, in vugs, molds, and fractures. Dolomite-C1 precipitated out of saline (17.9 to 20.4 wt%NaCl equ.) hydrothermal (Th= 98 to 142°C) fluids that were slightly radiogenic ($^{87}Sr/^{86}Sr=$ 0.70830 to 0.70895) compared to Devonian seawater, under intermediate to deep burial conditions (2000 and 2800 m) during the Cretaceous or earlier if higher geothermal gradients existed. Saddle dolomite (C2) cementation occurred after Dolomite-C1 precipitation. The slightly more depleted oxygen isotopic values of saddle dolomite (-8.78 and -9.34‰PDB) compared to Dolomite-C1 (-7.05 to -3.96‰PDB) probably reflects a combination of the different compositions and temperatures of the fluids responsible for saddle dolomite cementation.

Evidence for thermochemical sulphate reduction (TSR) reactions during deep burial along the deepest part (>3000 m) of the Rimbey-Meadowbrook reef trend include: 1) the presence of late-stage blocky calcite cements with light carbon isotopic composition (-17.89 and -6.53 ‰PDB), anhydrite cement, native sulphur, and sulphides in the deepest part of the trend; 2) the scarcity of these phases in the updip part of the trend; and 3) the higher levels of H_2S observed in the deepest part of the reef trend (30 to 90%, Caroline and Bearberry fields respectively) compared to 1.4% in the shallowest part of the study area (Homeglen-Rimbey field).

CHAPTER 3

Reservoir characteristics and porosity evolution
in Upper Devonian Leduc dolomites,
southern Rimbey-Meadowbrook reef trend, Alberta

Eva Drivet and Eric W. Mountjoy

Department of Earth and Planetary Sciences
McGill University
Montreal, Quebec, Canada
H3A 2A7

ABSTRACT

Vertical and lateral heterogeneities are controlled by depositional cyclicity and diagenesis in dolostone reservoirs of the Upper Devonian Leduc Formation along the southern part of the Rimbey-Meadowbrook reef trend in Alberta. Stromatoporoid facies of the buildup margins are the best reservoirs, comprising the most vertically continuous intervals dominated by vuggy pores with high porosity and good permeability. Skeletal grainstones of the buildup interior comprise excellent reservoirs with intercrystalline pores having the best permeabilities of all facies/pore systems, and good porosity. The skeletal grainstones, however, form heterogeneous and complex reservoirs because they occur commonly as laterally discontinuous thin layers (5 to 50 cm) interbedded with non-porous facies.

Distribution of pore types is governed mainly by depositional facies. However, reservoir effectiveness is strongly affected by diagenesis that increased the heterogeneity of the Leduc reservoirs. Cementation (anhydrite, dolomite, calcite, and sulphur) decreased the porosity and is most extensive downdip from the Medicine River field below present burial depths of 3000 m. The effect of dolomitization on reservoir properties is evaluated by contrasting undolomitized Golden Spike buildups with dolomitized Homeglen-Rimbey buildups. Comparable facies units in Golden Spike limestones and Homeglen-Rimbey dolostones contain different pore types, have generally similar average porosity, but the average permeability in the dolostones is significantly higher. At the reservoir scale, dolomitization initially led to a decrease in porosity during early burial. However, dolostones tend to have better retained their porosity because limestones have been more affected by pressure solution. Burial dissolution events (syn- and post-shallow burial replacement dolomitization, stylolitization, and deep burial dolomite cementation) may have been induced by acidic fluids generated by mixing corrosion, maturation of organic matter, and thermochemical sulphate reduction.

INTRODUCTION

A series of subsurface Leduc carbonate buildups (Woodbend Group, Frasnian) are located along the southwest - northeast trending Rimbey-Meadowbrook reef trend that extends for 480 km in central Alberta (Fig. 1). These buildups are enclosed in basinal shales of the Ireton and Duvernay formations, and accumulated along the western edge of the Cooking Lake platform (Fig. 2). The fields studied include: Homeglen-Rimbey, Gilby, Medicine River, Sylvan Lake, Lanaway, Garrington, Bearberry, and Harmattan (townships 43 to 33, ranges 1 to 7 west of 5) over a distance of 130 km along the southern part of the Rimbey-Meadowbrook reef trend (Fig. 3). The burial depth increases southward from about 2300 m in the Homeglen-Rimbey area to about 3500 m for the Harmattan field. Chapter 2 provides a description of the diagenetic phases observed within these fields and attempts to constrain the origin of the dolomites. This paper examines the role of depositional and diagenetic processes in porosity development of Leduc dolostone reservoirs. The objectives are: 1) to develop a depositional framework for the Upper Leduc dolostones, and use it in conjunction with the diagenesis described in Chapter 2 to characterize the reservoir quality of these Leduc dolomites; and 2) to identify the main dissolution events, examine evidence for their origin (near-surface v.s. burial dissolution), and discuss potential processes capable of generating sufficient acidic fluids to account for the porosity observed.

METHODS

Cores from 35 wells through the Ireton, Duvernay, and Upper Leduc formations were logged and sampled for petrographic analysis (Table 1, Fig. 3). Cores and logs do not penetrate the Middle and Lower Leduc Formation, thus most samples come from the upper 60 metres of the Leduc buildups. Systematic observations (Table 6) were obtained for all cores examined. The depositional environments for the Homeglen-Rimbey field were reconstructed using facies descriptions and correlations along south-north (B-C') and west-east (D-D') cross sections (Figs. 13 and 14). Porosity was described following the classification

Table 6. Observations made from core.

1. Core number, box, depth	**6. Fractures**
	connection with pores
2. Matrix grain size	orientation (vertical, horizontal,
<0.01 mm	inclined)
0.01-0.12	visually estimated percentage
0.12 - 0.50	fracture density index
0.50 - 1.0	
1.0 - 2.0	**7. Breccia**
>2.0 mm	brecciated intervals, clast size,
	cement types
3. Visual estimate of percent porosity	
	8. Fossils
	Stromatoporoids, *Amphipora*,
4. Pore type	*Thamnopora*, *Stachyodes*,
intercrystalline	subspherical, tabular, massive,
vug	unidentified fragments, corals,
moldic	other fossils
fenestral-like	
interparticle	**9. Other variables**
	diagenetic cements (anhydrite,
5. Pore description	bitumen, sulphides, calcite,
Size range	dolomite), grain size of the
Dominant pore size	matrix
Pore shape	

scheme of Choquette and Pray (1970). Porosity and permeability (horizontal and vertical) core analysis data (Table 7a) were obtained mostly from the files of Home Oil and the Energy Resources Conservation Board (ERCB). Core analyses were performed from 1956 to 1990, and were derived from core plugs or whole core. For the most part, these measurements are representative of the matrix porosity and exclude large vugs, molds, and fractures. In the Homeglen-Rimbey field, the arithmetic and geometric permeability mean were calculated for each depositional unit, and for each facies/pore system using the program StatViewII (Feldman et al., 1987). The arithmetic mean of the permeability is the summation of the permeability values divided by the number of values. The geometric permeability means were obtained by calculating the means of the logarithmitic distribution. The arithmetic mean is most appropriate when intervals of homogeneous permeability (permeability blocks) follow a layer-cake arrangement, whereas the geometric mean is more representative of a random arrangement of permeability blocks (Wardlaw, 1990). These two averaging techniques are used in this study because in the Leduc dolostones, some porosity and permeability blocks are continuous laterally while others are randomly distributed.

The reliability of the core analyses was tested by comparing log and core measurements. Because gamma ray and neutron/density logs in the study area date mostly from the 1960's, these comparisons could only be done for well 11-29-43-01W5 for which modern logs are available within an interval of skeletal grainstones that mostly contains intercrystalline porosity. For the interval considered in 11-29, core analyses (13.4 %) yield similar porosities to those calculated from the density log (15%). McNamara et al. (1991) made similar comparisons for porosities of Leduc dolomites of the Westerose field (north of the study area) and also concluded that core analyses are generally comparable to log porosity for intervals with high matrix porosity. When the interval measured contains pores that are larger than the core diameter, such as large vugs, matrix core analyses underestimate the porosity by about 3 percent or more (McNamara et al., 1991). Porosity was visually estimated in cores using representative photos

of different Leduc pore types as a reference so that estimates would be as consistent as possible. These estimates were either lower (by about 1 to 3%) or about the same as the measured core analyses.

A number of factors contribute to overestimation of horizontal permeability (kh) measurements (McNamara and Wardlaw, 1991): 1) measurements are not made at overburden pressure and are not corrected for gas slippage; 2) vugs and fractures are large in relation to core size; and 3) additional fractures are induced by coring. Average values of Kh may be unrealistically low in cases when: 1) cores with the largest vugs and fractures were not recovered; 2) open fractures contributing to high permeability units in the subsurface were not adequately sampled; and 3) drilling mud invasion has restricted communication between pores (McNamara and Wardlaw, 1991). No attempt was made in this study to evaluate the net effect of these factors on core measurements of permeability.

DEPOSITIONAL FACIES AND PORE TYPES

Identification of the original carbonate textures and fossils is difficult in many Leduc dolostone cores because of strong modification by replacement dolomitization, leaching, and oil staining. Faint outlines of allochems, the shape and size of vugs and molds, and relict primary textures observed in cores and under diffused light microscopy, were used to construct a broad depositional facies framework for these dolomitized buildups, similar to the approach utilized in dolomitized outcrop equivalents of the Leduc Formation (e.g. McLean, 1992; Shields and Geldsetzer, 1992; McLean and Mountjoy, 1993 a,b). Cross sections B-C' (south-north) and D-D' (west-east), constructed using the top of the Calmar Formation as a datum, illustrate the facies distribution across the Homeglen-Rimbey field (Figs. 12 to 14). The Calmar Formation consists of about 10 meters of argillaceous siltstones (McCrossan et al., 1964) with a distinctive gamma/ray log response. Pore types, porosity and permeability charts have been included with the facies distribution to illustrate the relation between porosity and facies. Five main lithofacies have been recognized: 1) stromatoporoid; 2) skeletal grainstone;

57

Figure 12.   Structural map of the top of the Leduc Formation in the Homeglen-
Rimbey field showing 40 meter contour intervals.   Dashed lines represent poorly
constrained Leduc contours.   The oil-water contact is taken from Kirker (1959).

HOMEGLEN-RIMBEY FIELD

40 m contours - Leduc Formation

58
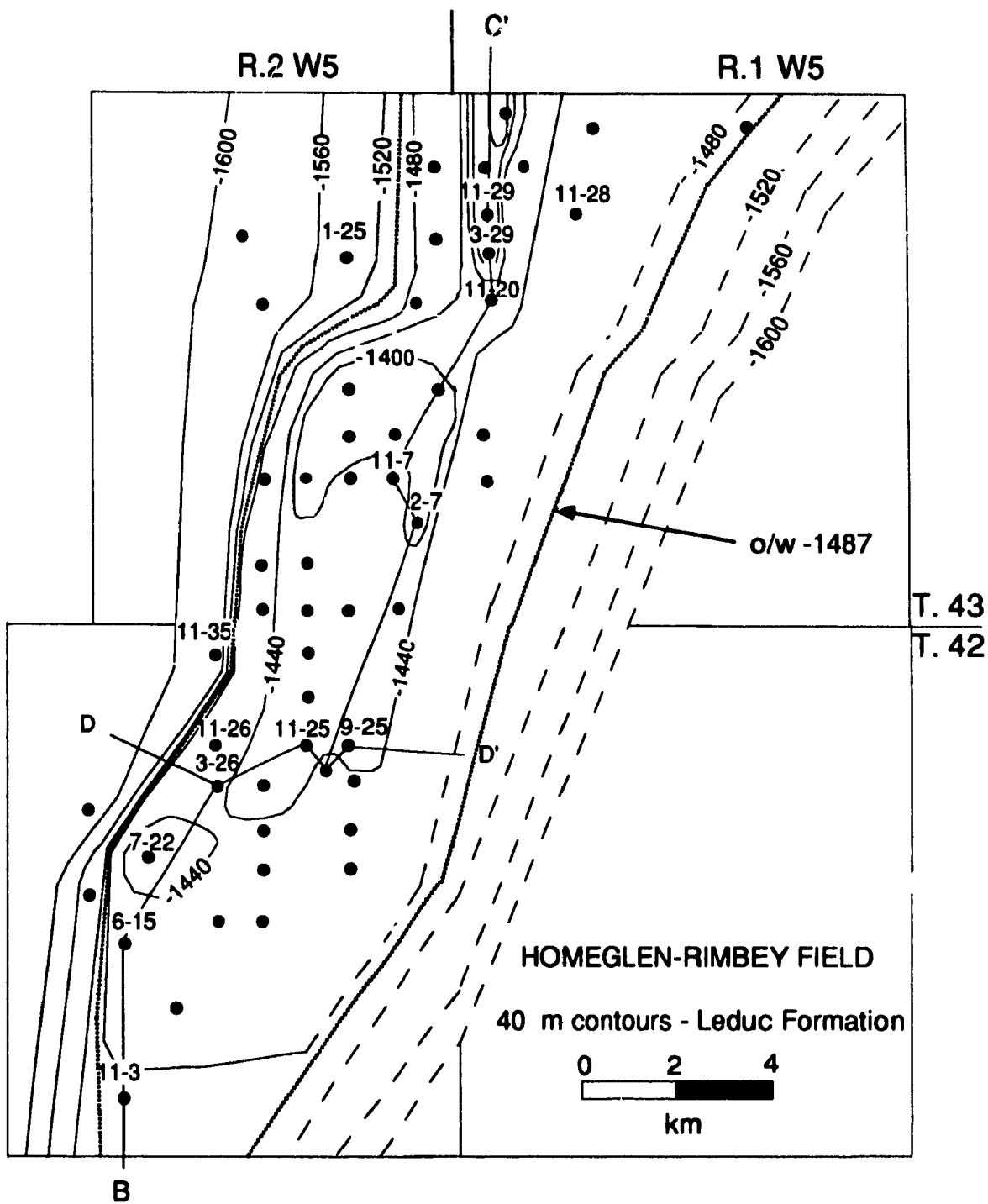
Figure 13. South-north (B-C') cross-section of Upper Leduc Formation along the Homeglen-Rimbey field showing depositional facies and pore types. Well locations are indicated in figures 3 and 12. The oil-water contact is taken from Kirker (1959). Datum: top of the Calmar Formation.

B ← 19 km → C'

Top of Calmar

Top of Leduc

86 m

102 m

11-03   06-15   03-26   11-25   02-07   11-07   11-20   03-29   11-29

20 m

Oil-Water contact

LEGEND

Pore types

■ Dense	
fn Fenestral	
vg Vuggy	
ic Intercrystalline	
bc Breccia	

Facies

■ Green shale	
☐ Stromomatolitic and planar dolostone	
▥ Dolomudstone	
☐ Carbonate sand	
▨ Amphipora facies	
⩗ Thamnopora facies	
∿ Stromatoporoid Facies	

59
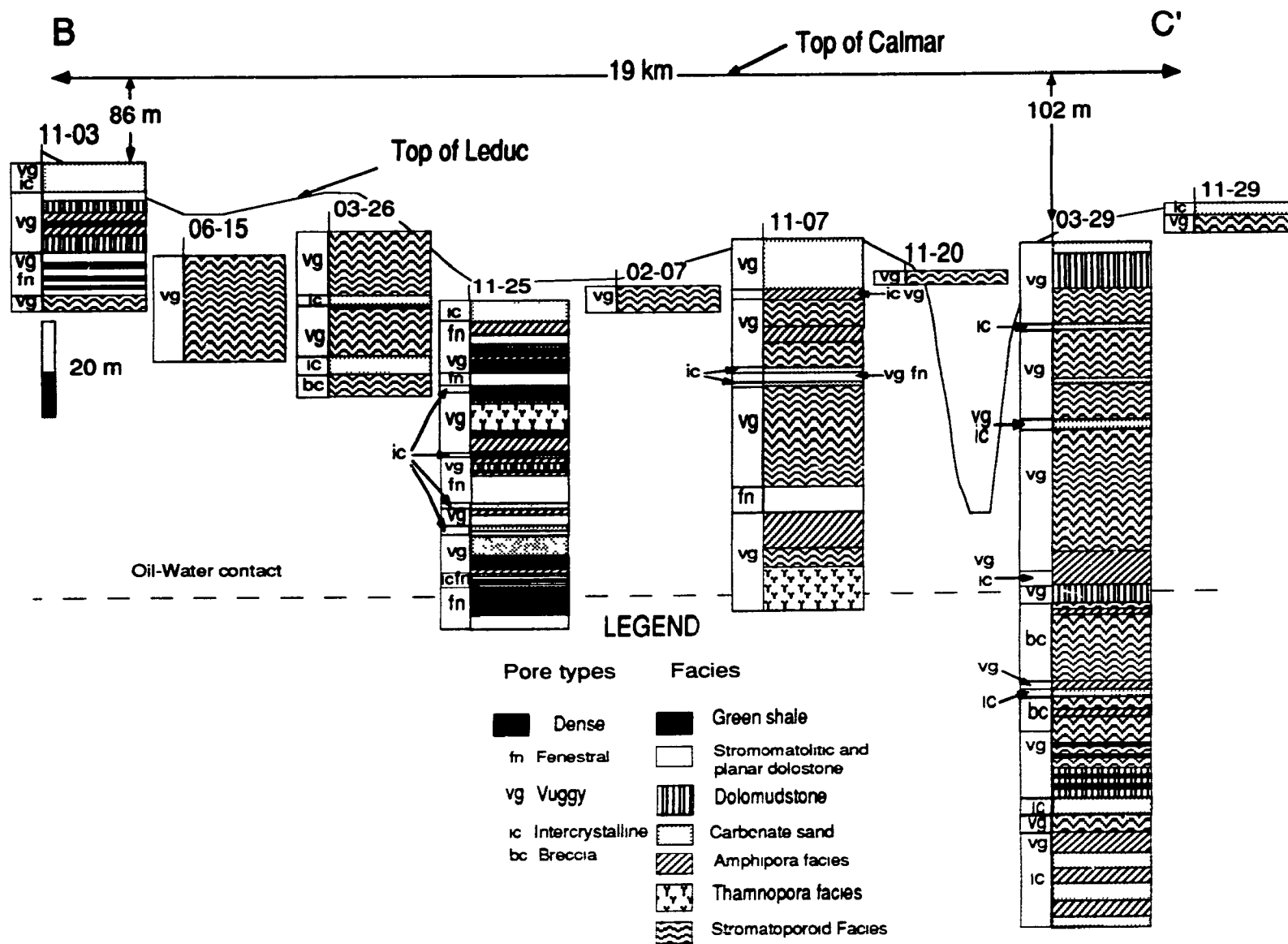
Figure 14. West-east (D-D') cross-section of Upper Leduc Formation along the Homeglen-Rimbey field showing depositional facies, pore types, percent porosity, and horizontal permeability from core analyses. Well locations are indicated in figures 3 and 12. The oil-water contact is taken from Kirker (1959). Datum: top of the Calmar Formation.

D   Top of Calmar   **D'**

2.8 km

98 m   104 m

Top of Leduc Formation

03-26   11-25   07-25   09-25

20 10 0   0 10 100 500 >1000

Pore types   Facies

■	Dense	■	Green shale
fn	Fenestral	□	Stromomatolitic and planar dolostone
vg	Vuggy	▥	Dolomudstone
ic	Intercrystalline	□	Carbonate sand
bc	Breccia	▨	Amphipora facies
		ᵛᵀᵛ	Thamnopora facies
		〰	Stromatoporoid Facies

10 m

Ø (%)   Kh (mD)

Oil-Water contact

Reef Margin   Reef interior   Reef Margin
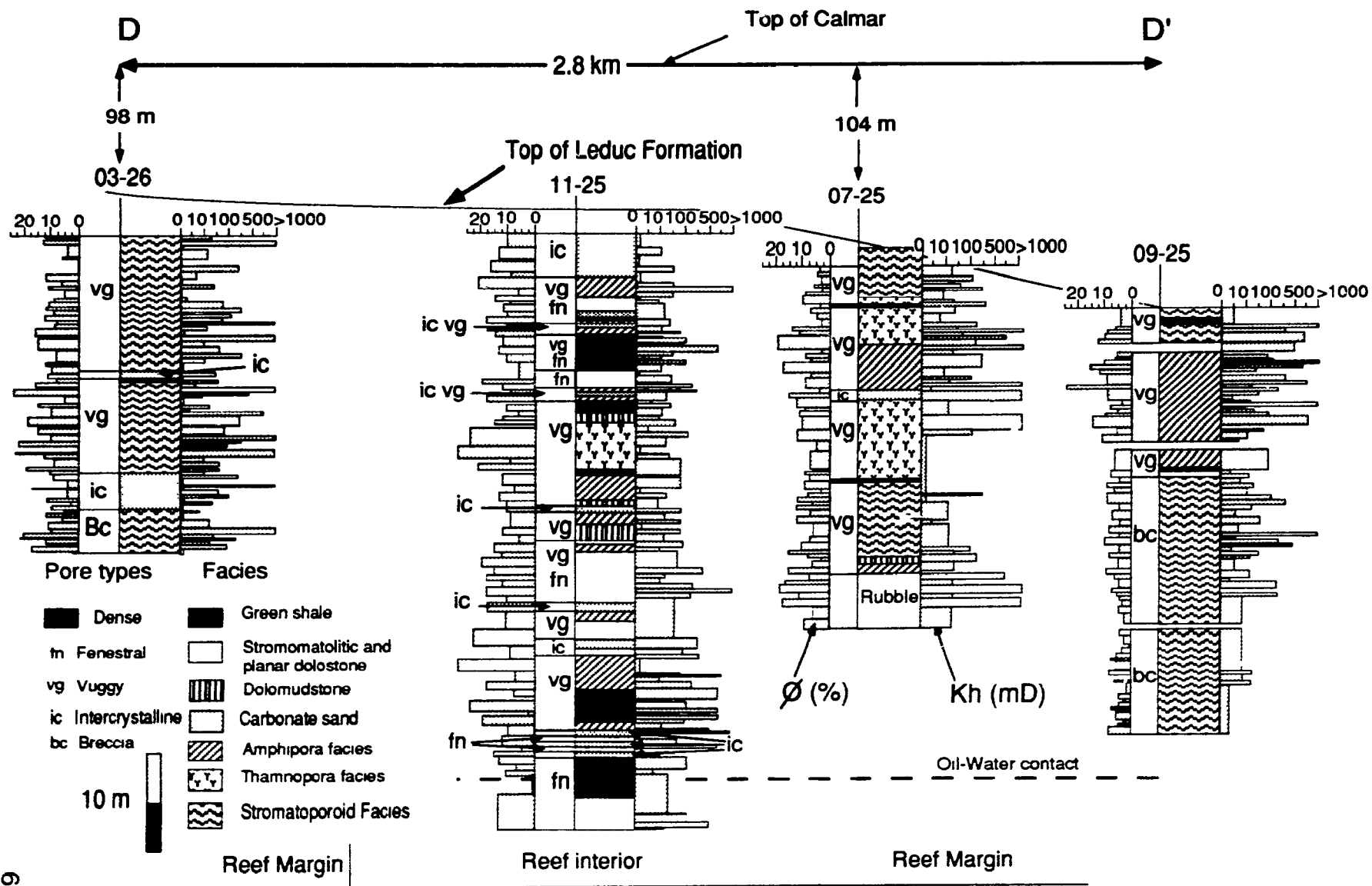
3) *Amphipora*; 4) stromatolitic; and 5) skeletal packstone facies. The main pore types observed are, in decreasing order of importance, vuggy, moldic, intercrystalline, and breccia. Porosity and permeability values for each facies and pore system are summarized in Table 7a.

Fabric selective porosity and lithofacies

The **stromatoporoid facies** consists of 1 to 20 m thick floatstones and rudstones comprised of bulbous or spherical-shaped vugs and molds, and/or relicts of stromatoporoids that range in diameter from 2 to 10 cm or more (Plates 8a and 8b). Relicts of accessory fossils include: *Amphipora*, *Thamnopora*, *Alveolites*, *Stachyodes*, and brachiopods (Plates 8c). Cross sections B-C' and D-D' reveal that the stromatoporoid facies is most abundant along the buildup margins and occurs locally in buildup interiors either as patch "reefs" or detritus. Large vugs and molds resulting from the dissolution of skeletal material are common. Primary intraparticle porosity (Plate 8d) is also important locally. Distribution of porosity is heterogeneous with strongly leached units alternating with intervals of little dissolution or extensive anhydrite infill. Some vugs are larger than the core diameter and thus may have unrealistically low horizontal permeability and porosity core analysis measurements. Despite this core analysis bias, and considering that core analysis underestimate large vuggy porosity by at least 3% (McNamara et al., 1991), stromatoporoid facies have the highest porosity and good horizontal and vertical permeability (Table 7a). This, combined with their relatively good vertical continuity, makes the stromatoporoid facies the best reservoir facies in the Homeglen-Rimbey buildup.

The **skeletal grainstone facies** is characterized by 5 to 50 cm, relatively coarse-grained, bedded and massive grainstones (Plates 8e to 8g). Dolomitization has obliterated much of the original textures, but a few cores reveal that most grains are skeletal fragments (Plate 8g). This is one of the most internally homogeneous facies, dominated by intercrystalline pores distributed as irregular narrow vertical burrow-like patches (about 1 to 2 cm wide), and as laterally

61

Table 7. A. Porosity-permeability values of different depositional facies and pore systems based on core analysis of selected intervals in the Homeglen-Rimbey field. Values for breccia porosity are derived from the entire study area. B. Porosity-permeability values of different depositional facies and pore systems of selected intervals in the Golden Spike limestones (McGillivray and Mountjoy, 1975; Walls and Burrowes, 1990). N: number of samples analyzed; Kh· horizontal permeability; Kv vertical permeability, Ar arithmetic average, Ge: geometric average, Min minimum, Max maximum.

7A)

Facies and pore types	N	Porosity			Kh (mD)		Kv (mD)		Kh/ Kv
		Ar	Min	Max	Ar	Ge	Ar	Ge	
Vuggy pores in stromatoporoid facies	201	9.52±4	2.0	24	196	0.51	26 7	5 39	43 3
Intercrystalline pores in skeletal grainstones	42	9.06±5	3.0	26	689	15 5	122	3 78	29.0
Intercrystalline and vuggy pores in stromatoporoid and *Amphipora* facies	130	7.99±3	0.0	19	192	7.35	35 0	6 40	75.3
Vuggy pores in *Amphipora* facies	173	8.64±4	2.0	26	232	6.34	28 7	2.11	547
Fenestral pores in stromatolitic facies	72	7.01±3	0.0	15	184	12.1	17.1	3.02	53 4
Vuggy pores in skeletal pakstone facies	106	5 85±3	0.0	14	10 3	2 81	2 26	0 53	22.4
Green shales	34	3.06±2	0.0	7 0	31.2	1.59	5.79	0 58	10 5
Breccia porosity	313	5.84±3	0.0	21	40.3	1.48	8.05	0 63	10.9

7B)

Facies type	Tabular stromatoporoid	Massive stromatoporoid and stromatoporoid rubble	Skeletal peloid sands	Algal laminites
Pore type	Interparticle	Interparticle, vugs, and molds	Interparticle	Fenestral
Porosity (mean)	5.5	10	12.5	7
Permeability (mean)	10	100	50	60

Plate 8.   EXAMPLES OF DEPOSITIONAL FACIES AND ASSOCIATED PORE
            TYPES IN THE UPPER LEDUC FORMATION: I

A)   Vuggy (V) porosity resulting from partial dissolution of
      stromatoporoids. Thin fractures connect the pores. 03-26-42-02W5,
      2442.4 m. Scale bar 5 cm.

B)   Relict of stromatoporoid (S) fossil. 11-07-43-01W5, 2328.2 m.

C)   Possibly relicts of *Stachiodes* (S) based on their size and shape,
      which are commonly observed in stromatoporoid facies. Some
      allochems are partially leached leading to the presence of vuggy
      porosity. 06-20-38-04W5, 3124.6 m. Scale bar in centimetres.

D)   Photomicrograph showing a cross-section of a rugose coral (C)
      containing intraclast porosity (I). This is a rare example of well
      preserved primary fabrics despite pervasive replacement
      dolomitization. These corals usually occur in the stromatoporoid
      facies. 01-30-39-03W5, 2993.2 m, plane-polarized light. Scale bar
      2.6 mm.

E)   Skeletal grainstone facies (SG) sharply underlain by a horizontal
      layer of dolomudstone (D). Alternating dense and porous vertical
      zones, underneath the dolomudstone, may represent the relicts of
      burrows. 11-25-42-02W5, 2386.6 m. Scale bar in centimetres.

F)   Photomicrograph illustrating that horizontal layers of dense (D) and
      intercrystalline porous (I) zones are also observed at the microscopic
      scale. The coarse, euhedral planar crystals of replacement dolomite
      in the porous intervals are classified as Dolomite-R3, whereas the
      finer, anhedral dolomite crystals in the dense layers are classified as
      Dolomite-R2. 03-29-43-01W5, 2441.1 m, plane-polarized light.
      Scale bar 3 mm.

G)   Example of skeletal grainstone facies where relicts of skeletal
      fragments (SF) are observed despite complete replacement
      dolomitization. In this example, porosity is from the partial dissolution
      of the skeletal fragments. 11-28-43-01W5, 2437.1 m. Scale bar 1
      cm.
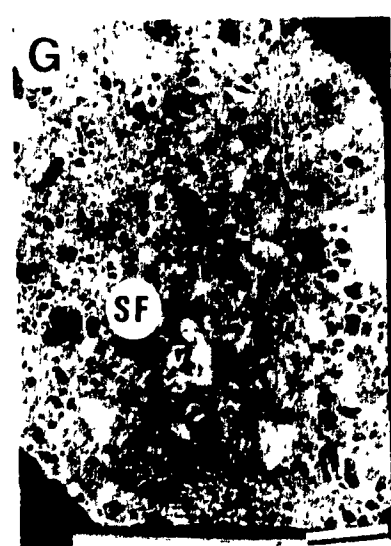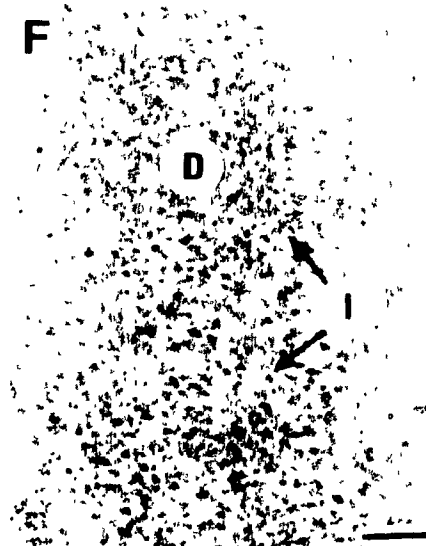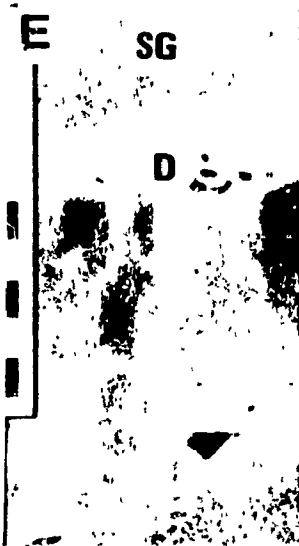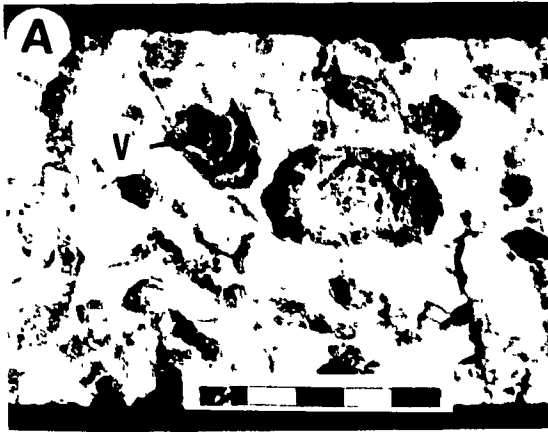
discontinuous horizontal layers (Plate 8e). As discussed later (see Figs. 17 and 18), several skeletal grainstone intervals can be correlated across the buildup interior, and a few also extend to the buildup margin. Commonly, grainstone layers displaying good intercrystalline porosity are in sharp contact and alternate with intervals of tight dolomudstones (Plate 8e). Alternation of porous and non-porous layers can also be observed at the microscopic scale (Plate 8d). In general, intercrystalline pores are associated with coarse, euhedral, and planar crystals of replacement dolomite. Because of the uniform crystal size of these dolomites (300 to 500 µm), the pores are polyhedral in shape, and extremely well sorted in size (Plate 3a) Core analysis for skeletal grainstones with abundant intercrystalline pores is a reliable approximation of the true porosity and permeability because matrix porosity predominates in these intervals. Of all the facies group, skeletal grainstones have the highest horizontal and vertical permeability, and are characterized by relatively high porosity (Table 7a) and thus comprise excellent reservoirs. However, at the buildup scale skeletal grainstones are thin, interbedded with denser facies, and laterally discontinuous resulting in the second best reservoir facies after the stromatoporoid facies. Vuggy and moldic pores resulting from extensive leaching of skeletal fragments (Plate 8g) are also present in skeletal grainstones, lowering the porosity and permeability compared to intervals with only intercrystalline porosity (Table 7a).

The **Amphipora facies** consists of 20 cm to 10 m thick beds of wackestones, packstones, and grainstones that contain abundant centimetre long cylindrical molds and grains, probably *Amphipora* (Plates 9a and 9b). *Amphipora* grainstones are usually observed in the buildup interior. *Amphipora* wackestones and packstones are most abundant in the buildup interior but also occur in the buildup margins. Vuggy and moldic porosity predominates with the pore size often reflecting the shape of original skeletal components (Plates 9a and 9b). Primary interparticle porosity is locally present in *Amphipora* grainstones (Plate 3e) but is volumetrically insignificant. In general, interparticle pores are partially to completely occluded by primary isopachous and fibrous submarine cements now replaced by

64

dolomites. Compared to stromatoporoid facies, *Amphipora* facies have slightly higher horizontal permeability, and similar porosity and vertical permeability (Table 7a). In addition, *Amphipora* facies are commonly interbedded with different sediments such as tight dolomudstones, and skeletal grainstones with beds alternating every 10 cm. This interbedding further increases the contrasts between horizontal and vertical permeability which is consistent with the high horizontal to vertical permeability ratio (Kh/Kv) observed in this facies (Table 7a)

The **stromatolitic facies** consists of 20 cm to 1 m thick beds of finely laminated dolomudstones, with occasionally crinkled laminations, and in some cases centimetre-scale stromatolitic structures (Plate 9c). This facies occurs in the buildup interior and is commonly interbedded with skeletal grainstones, and with a **dolomudstone facies** that represents 10 cm to 2 m thick beds of massive dolomite that lack relicts of allochems "Fenestral-like" pore in stromatolites are very common, but larger vugs, intercrystalline and moldic pores are also important. In contrast to all the facies described above, stromatolitic facies are characterized by relatively low porosity and good horizontal permeability with comparatively low vertical permeability (Table 7a).

Skeletal packstone facies occur in the buildup flanks. They are characterized by skeletal packstones composed of stromatoporoid and coral fragments (Plate 9d), interbedded with laminated mudstones and wackestone These deposits are porous with moldic and vuggy porosity resulting from the leaching of skeletal fragments, and are enclosed in low porosity flank mudstones and wackestones. Consequently, porosity and permeability generally are good within skeletal packstones but communication with the rest of the reservoir may be limited.

Green shales and associated dolomites comprise layers up to 20 cm thick that are interlaminated with the stromatolitic and dolomudstone facies in the buildup interior, and with stromatoporoid facies along the buildup margins (Plate 9e; Figs. 13 and 14). In a few cases, green shales and argillaceous dolostones can be correlated across parts of the buildup (see Fig. 18). Green shales also occur as

Plate 9. EXAMPLES OF DEPOSITIONAL FACIES AND ASSOCIATED PORE
TYPES IN THE UPPER LEDUC FORMATION: II

A) Moldic porosity probably after leaching of *Amphipora* (A) fossils. This
core is an example of an *Amphipora* wackestone that comprises the
Amphipora facies. 03-29-43-01W5, 2423.2 m.

B) Photomicrograph of moldic porosity (M) after partial dissolution of
probably *Amphipora* fossils. 11-07-43-01W5, 2341.5 m, plane-
polarized light. Scale bar 2.0 mm.

C) Finely laminated dolomudstone with fenestra-like pores comprising
the stromatolitic facies. 11-25-42-02W5, 2399.8 m.

D) Completely dolomitized skeletal intraclast packstone in a slump
deposit from the buildup flanks. Presence of stromatoporoid
fragments (S) suggests proximity to the shallower parts of the
buildup. Intraclast porosity predominates and is partially to
completely filled by dolomite and anhydrite cements. 11-28-43-
01W5, 2442.8 m. Scale bar 3 cm.

E) Green shaly (GS) layers are commonly observed near finely
laminated dolomudstones (LD). 11-25-42-02W5, 2391.5 m.

F) Green shales also fill geopetals (GI). 11-03-42-02W5, 2394.8 m.
Scale bar 7.0 mm.

G) Some vugs (V) are so irregular that the precursor fabric cannot be
recognized. 11-07-43-01W5, 2351.4 m.

66
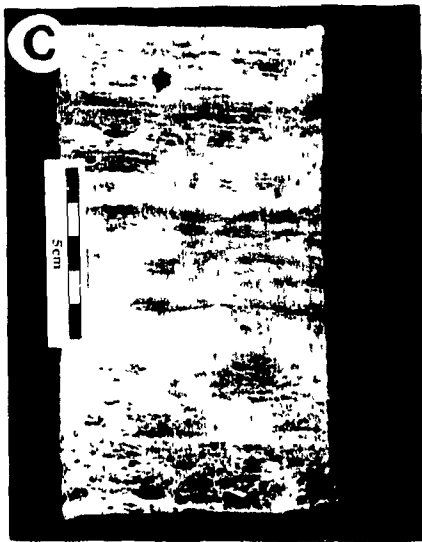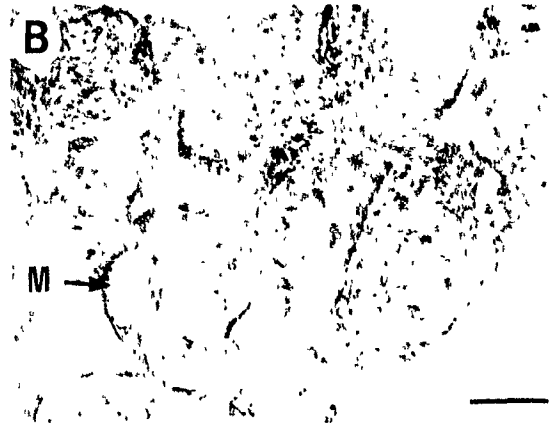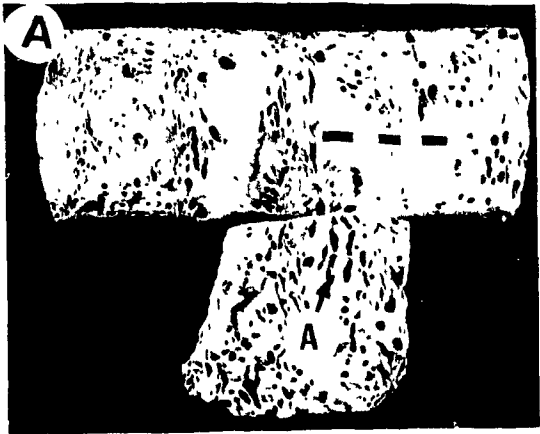
geopetal infills in interparticle and intraparticle pores in the buildup interior and margins (Plate 9f). Green shales are characterized by average porosity and permeability that are unexpectedly high, probably reflecting the presence of porous and permeable dolostones mixed with, or immediately adjacent to, these shaly intervals. Nevertheless, intervals containing green shales have low average vertical permeability, the lowest porosity (Table 7a), and thus act as efficient permeability barriers for vertical flow. Average horizontal permeability, however, is relatively good indicating that horizontal flow occur in horizons comprised of green shales.

Nonfabric selective porosity

Other pore types occurring in the Leduc dolomites include irregular vugs that commonly are large, randomly distributed and without indication of their precursor fabric (Plate 9g), and breccia porosity (Plates 10a to 10c). Brecciated intervals are comprised of replacement dolomite fragments cemented by dolomite and anhydrite with or without sulphides (Plates 10a to 10c). Fragments are typically rotated and have dropped from their original stratigraphic position. The sulphides occur as a layer of coarse crystals preferentially coating the tops of the dolomite fragments. The underside of fragments is coated either not at all or to a much lesser degree. This lining of the cavities by sulphides was first described by Oder and Hook (1950), and is a diagnostic texture of MVT deposits because it has not been reported in any other type of mineral deposit (Sangster, 1988).

This variety of breccia is observed in the Leduc dolostones but have not been reported in the Golden Spike and Redwater limestone buildups. In the Homeglen Rimbey field, breccias were only observed in buildup margin facies in wells 9-25, 3-29, and 3-26. They cannot be correlated east-west across the buildup, and are not associated with major surfaces of subaerial exposure (see Figs. 17 and 18). The volume of dolomite breccias increases to some extent downdip along the Rimbey-Meadowbrook reef trend with increasing burial depth (Fig. 15). Brecciated intervals are all completely cemented by dolomite and

Plate 10.   EVIDENCE FOR FRACTURING AND DISSOLUTION IN THE UPPER LEDUC FORMATION

A)   Breccia porosity is characterized by voids surrounding fragments of replacement dolomite (R2). These voids are completely occluded by dolomite cement (C1), and anhydrite (A). Thin geopetal layers of pyrite (P) occur on top of some fragments. Irregular fragments of matrix dolomite surrounded by anhydrite are corroded along the edges suggesting they were replaced by anhydrite. 03-29-43-01W5, 2382 m. Scale bar in centimetres.

B)   Fractures (F) observed in brecciated intervals crosscut replacement dolomite resulting in the presence of dolomite fragments (DF). In this particular example, the edges of the dolomite fragments are rimmed by a thin zonation of dolomite cement (C1) indicating that the fracturing event associated with the brecciation postdates replacement dolomitization and predates dolomite cementation. 11-06-36-03W5, 2982.4 m. Scale bar 9.6 mm.

C)   A rim of dolomite cement (C1) is offset by fractures (f) suggesting that a later fracturing event postdates dolomite cementation. 16-25-36-06W5, 3469.6 m. Scale bar 7.5 mm.

D)   Example of microfractures observed in the Harmattan field. 13-09-33-04W5, 3406.8 m. Scale bar 1.6 cm.

E,F) Paired plane light and cathodoluminescence photomicrographs of replacement dolomite clasts, dolomite cement (C1), and anhydrite (A) that occur in the breccias. Replacement dolomite (R2) and the edges of the dolomite cement (C1) appear to be partially dissolved indicating dissolution phases post-dolomitization and post-dolomite cementation. These events overlapped with replacement of the dolomite crystals by anhydrite, and anhydrite cementation. 06-20-38-04W5, 3134.3 m. Scale bar 230 μm.

G,H) Paired plane light and cathodoluminescence photomicrographs illustrating that dolomite cement (C1) observed in the breccia intervals is not always dissolved, as in Plates 10 e&f, suggesting that anhydrite (A) is predominantly a cement as opposed to a replacive phase. 03-29-43-01W5, 2382 m. Scale bar 230 μm.

I,J) Paired plane light and fluorescent photomicrographs showing a vug along a stylolite (S) that crosscuts replacement dolomite (R2). The crystals of replacement dolomite adjacent to the vug appear corroded under fluorescent light suggesting that they have been dissolved. This indicates that dissolution occurred after replacement dolomitization, syn- and/or post- stylolitization. 08-27-36-06W5, 3593 m. Scale bars for I and J are 200 and 75 μm respectively.
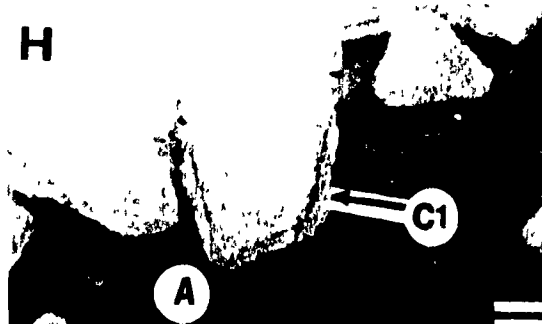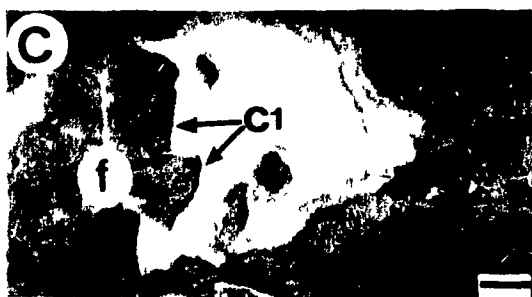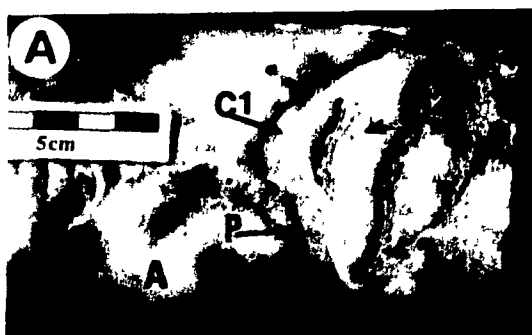
Figure 15. South-north cross-section A-B-C showing the presence and absence of anhydrite, dolomite cements (C1 and C2), pyrite, and breccia porosity. Based on estimates from logged cores, the occurrence of these diagenetic phases decreases northward updip along the Rimbey-Meadowbrook reef trend. North of the Medicine River field above present burial depths of about 3000 m, these diagenetic phases are rare to absent (e.g. wells 01-30, 03-26, 11-25, 07-25, and 11-07).

Top of Leduc

A

Lanaway

Medicine River

11-10 11-06 16-25 08-27 16-32 06-04 16-11 08-30 06-20 10-23

meters
0
20
40

Gilby

B

Homeglen-Rimbey

C

01-30 14-28 14-05 11-03 03-26 11-25 07-25 11-07 03-29 11-28

■ Anhydrite
■ Dolomite cements
▢ Sulphides
▨ Breccia porosity
▢ Lack the above features
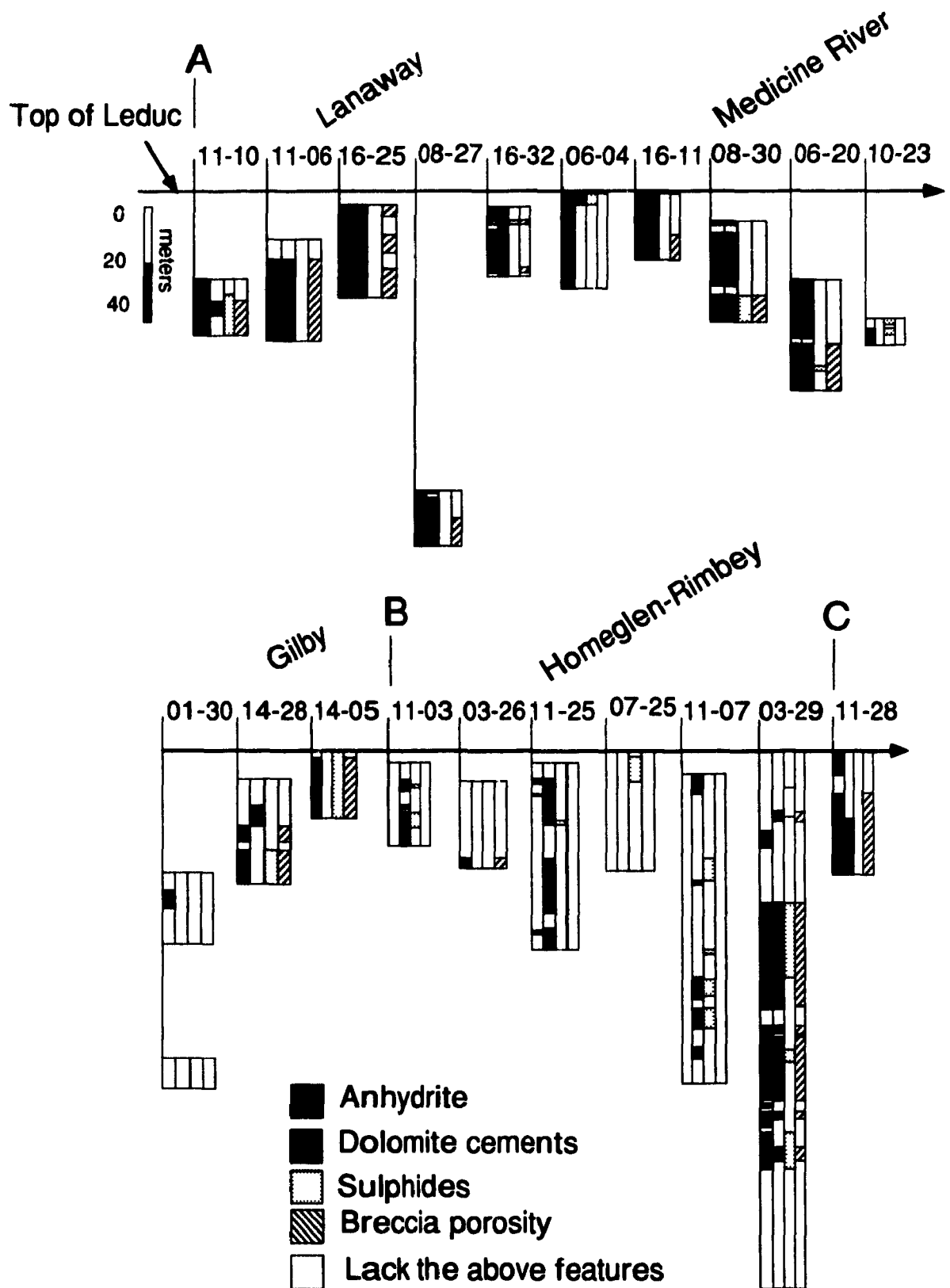
anhydrite cements (Plates 10a to 10c), and thus represent poor reservoirs with relatively low average porosity and permeabilities (Table 7a). The highest porosity values (up to 21%; Table 7a) in brecciated intervals are related to the presence of intercrystalline and pinpoint porosity in dolomite breccia clasts.

EVIDENCE FOR THE TIMING OF DISSOLUTION AND FRACTURING

Diagenesis in the dolomitized Leduc buildups is complex (Fig. 10; Chapter 2). Based on textural and crosscutting relationships the generalized paragenetic sequence may be summarized as: 1) early fibrous and isopachous calcite cementation; 2) several phases of stylolitization; 3) matrix replacement dolomitization overlapping with early stylolitization; 4) late-stage cementation by dolomite, anhydrite, calcite, and quartz; 5) bitumen emplacement; and 6) sulphur and sulphide precipitation. The distribution of pyrite, anhydrite and dolomite cements, and their common association with breccia porosity is shown along a south-north cross section (A-C) that covers the entire study area (Fig. 15). Of all the cements, anhydrite constitutes the most pervasive and volumetrically important, filling vugs, molds, fractures, and intraclast pores in dolomite breccias.

A total of four fracturing and three dissolution phases are observed in the Leduc dolostones and placed in the paragenetic sequence (Fig. 16):

Dissolution I- The presence of dolomitized matrix surrounding leached calcite allochems has been observed in partially dolomitized Leduc buildups (Mattes and Mountjoy, 1980; Marquez, pers. comm., 1992; Chouinard, 1993) and indicates preferential dolomitization of the matrix contemporaneous with and/or postdated by dissolution of the calcite remnants.

Fracturing and dissolution II- Evidence for fracturing and dissolution postdating replacement dolomitization is indicated by: 1) fracturing and brecciation of matrix dolomite as described in the previous section (Plates 10a to 10c); 2) corrosion of the edges of the replacement dolomite clasts (Plates 10e and 10f);and 3) corroded crystals o replacement dolomite crosscut by stylolites (Plates 10i and 10j).

Figure 16. Inferred porosity changes with respect to the paragenetic sequence, including dissolution phases. In the Homeglen-Rimbey field, the present average porosity of the buildup interior and margins are 7 and 10% respectively.

Paragenetic sequence in the Leduc dolostones and inferred porosity evolution

DIAGENETIC EVENT	EARLY → LATE	Porosity 0% — 30 to 50%
Isopachous calcite cementation		
Submarine cementation		
Dissolution I		
Stylolitization		
Replacement dolomitization		? ?
Fracturing and dissolution II		
Dolomite cementation		
Fracturing and dissolution III		
Anhydrite cementation and replacement		
Calcite cementation		
Quartz cementation		
Bitumen emplacement		
Fracturing IV		
Sulphur and sulphides emplacement		7 to 10%

Sea floor | Shallow Burial (< 500 m) | Intermediate Burial (500-2000 m) | Deep Burial (> 2000 m)

71

Fracturing and dissolution III- A later phase of fracturing and dissolution is indicated by dissolution along fractures that crosscut the rims of dolomite cement in brecciated intervals (Plates 10c, 10e, and 10f). This solution event postdates dolomite cement, but predates blocky calcite and anhydrite cements. It is volumetrically minor compared to the fracturing and dissolution events I and II.

Fracturing IV- Fractures filled with native sulphur, crosscut anhydrite cements (Plate 1e), and are rare.

Microfractures- Extensive hairline microfractures only occur in the Harmattan field (well 13-09), an isolated buildup that is not connected to the Rimbey-Meadowbrook reef trend (Fig. 1). They are filled with bitumen, radiate away from pores, and crosscut fractures filled with dolomite and anhydrite cements (Plate 10d). They are similar to those reported by Marquez et al. (1992) from the Strachan and adjacent buildups and are interpreted to have formed in these isolated reservoirs when trapped oil was converted to gas.

RESERVOIR CHARACTERIZATION

In this section, the depositional environments for the Upper Leduc Formation in the Homeglen-Rimbey are reconstructed on the basis of facies correlations (Figs. 17 and 18), and are used to subdivide the Leduc reservoir into depositional units. Facies distribution maps for two of these units show the distribution of porous and permeable zones (Fig. 20). The effect of diagenesis (including dolomitization) on porosity evolution is also discussed.

Interpretation of depositional environments

The facies identified from detailed core descriptions are correlated in the B-C' and D-D' cross sections of the Upper Leduc Formation in the Homeglen-Rimbey field (Figs. 17 and 18) based on the preserved dolomitized fauna, pore shapes, and on depositional models for Leduc limestone equivalents in the Golden Spike and Redwater buildups (McGillivray and Mountjoy; 1975; Reitzel et al., 1976; Wendte and Stoakes, 1982; Wendte et al., 1992). Five main depositional units

Figure 17A. Correlation of facies in Upper Leduc Formation along south-north cross-section B-C'. The oil-water contact is derived from Kirker (1959).

B

C'

Top of Calmar
19 km

86 m

102 m

11-03

E
D4
D3

06-15

03-26

Top of Leduc

11-29

11-07

03-29

E

11-25

02-07

E

11-20

D4

D

D2

D1

D3

20 m

C

D2

B

D1

C

Oil-Water contact

A

B

A

Facies

Green shale

Amphipora facies

Stromomatolitic and planar dolostone

Thamnopora facies

Dolomudstone

Stromatoporoid facies

Carbonate sand

B ← 19 km → Top of Calmar C'

Top of Leduc

Pore types

20 m

fn Fenestral
vg Vuggy
ic Intercrystalline
bc Breccia

Oil-Water contact

Ø (%)   Kh (ge,mD)

Figure 17B. South-north cross-section B-C' in Upper Leduc Formation showing calculated average porosity in the left column, and arithmetic average horizontal permeability in the right column for each depositional unit. Porosity and permeability data are based on core analysis. Horizontal permeability values for well 11-07 are not available.

Figure 18. Correlation of facies along west-east cross-section D-D' in Upper Leduc Formation. Calculated average porosity in percent is shown in the left column, and arithrnetic average horizontal permeability in millidarcies is given in the right column for each depositional unit. Porosity and permeability data are based on core analysis. The oil-water contact is derived from Kirker (1959).

D — D' cross-section showing Top of Calmar, Top of Leduc. 2.8 km across. Wells 03-26, 11-25, 07-25, 09-25. Vertical measurements 98 m and 104 m.

Facies:
- Green shale
- Stromatolitic and planar dolostone
- Dolomudstone
- Carbonate sand
- Amphipora facies
- Thamnopora facies
- Stromatoporoid facies

Pore Types:
- vg Vuggy & moldic
- ic Intercrystalline
- fn Fenestral
- bc Pores in dolomite breccia

10 m

Ø (%)   Kh (ge, mD)

Oil-Water contact

Rubble

Reef Margin | Reef interior | Reef Margin

10 to 50 metres thick (A to E, Figs. 17 and 18) are recognized mainly on the basis of abrupt vertical facies changes, and correlative green shale layers. In several wells, green shale layers are absent (e.g. 11-07; 06-15; 03-29) in some depositional units, possibly a result of: 1) poor core recovery; 2) non deposition and limited lateral extent; or 3) erosion. Where green shales are absent, depositional units are correlated using constant thicknesses. Green shale horizons are interpreted to be the products of storms that transported fine sediment from an adjacent basinal source based on their character and distribution:

1.   Green shales are interlaminated with stromatolitic facies (Plate 9e) implying they are depositional rather than due to solution of previous carbonates during exposure.

2.   Green shales occur as geopetal fillings (Plate 9f) in the buildup margins and interior suggesting marine deposition.

3.   Green shales are similar texturally and mineralogically to the subtidal green shales of the Ireton Formation that occur adjacent to the Leduc buildups.

4.   Cyclic repetition of green shales in the stratigraphic succession implies a repeated cycle of deposition.

Green shales in the Swan Hills reef complex at Judy Creek have similar characteristics and distribution and were also interpreted to be the product of storm (Wendte and Stoakes, 1982). The green shales are interpreted as time lines, assuming that they represent storm deposits.

Each depositional unit is comprised of one or more shallowing upward hemi-cycles, both in the buildup margin and interior, that are on the order of 10 to 20 m thick (Fig. 19). From bottom to top, the depositional hemi-cycles of the reef margin are represented by: 1) stromatoporoid floatstones or rudstones; 2) *Amphipora* wackestones and packstones; 3) skeletal grainstones; and 4) green shale horizons. Commonly, one or more of the four facies is missing or poorly developed. The hemi-cycles in the buildup interior differ from the ones in the buildup margin in that they are thinner, and contain fewer occurrence of

Figure 19. Schematic reconstruction of an ideal shallowing upward hemi-cycle in the buildup margin and buildup interior of the Leduc dolostones in the Homeglen-Rimbey field.

Ideal Hemi-Cycle

Buildup interior

10 to 20 m
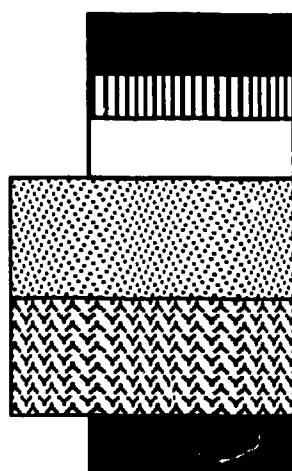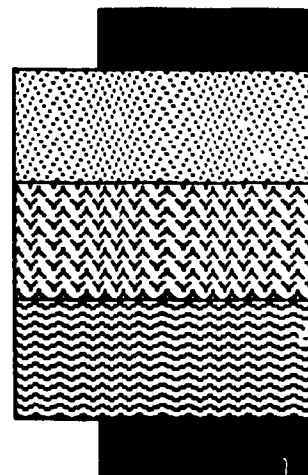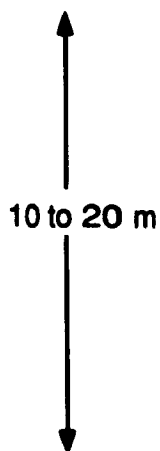
Buildup margin

Green shale

Dolomudstone

Stromatolitic and planar dolostone

Carbonate sand

Amphipora wackestone, packestone, grainstone

Stomatoporoid floastone, rudstone

stromatoporoid facies. They are characterised by three or more of the following, from bottom to top: 1) *Amphipora* grainstones; 2) skeletal grainstones; 3) stromatolitic and planar dolostones; 4) dolomudstones; and 5) green shales. These hemi-cycles are thicker than the meter-scale cycles reported in Leduc limestone buildups (Stoakes, 1992) and in the outcrop equivalent Leduc buildups of the Rocky Mountains (e.g. McLean, 1992; McLean and Mountjoy, 1993b). In part, this may result from the obliteration of some facies and their contacts by dolomitization, and continuous deposition of stromatoporoid and other facies along the buildup margins without obvious breaks. Similar conclusions have been reported for the Redwater and other buildups by Stoakes (1992).

Depositional units show a classic pattern of facies retrograding towards the buildup interior representing a transgression (units A, C, and E in Figs. 17 and 18), and prograding of facies representing a regression (units B and D in Figs. 17 and 18), similar to the interpretations for Golden Spike and Redwater Leduc limestone buildups by Wendte and Stoakes (1992). Unit A represents bulbous stromatoporoid banks alternating with thin intervals of skeletal grainstones in the buildup margins, with lagoonal deposits accumulating in the buildup interior (mostly green shales with thin layers of skeletal grainstones, and stromatolites). Unit B is characterized by stromatolite shoals (e.g. wells 11-25 and 11-07) suggesting a regression event. Locally, *Amphipora* grainstones were deposited between the stromatolite shoals. The stromatoporoid facies accumulated along the buildup margins of wells 7-25 and 9-25. Unit B is overlain by a green shale horizon in wells 7-25 and 9-25 (Fig. 18). Green shales and dolomudstones generally characterize the uppermost portions of shallowing upward cycles, a stage when sea level was relatively stationary and filling of the basin with shales from the north and northeast had become reestablished (Stoakes, 1980). This is overlain by unit C which lacks stromatolitic facies, and is comprised of relatively deeper water facies including mostly *Amphipora*, *Thamnopora*, and skeletal grainstones in the buildup interior and bulbous stromatoporoids along the buildup margins. Thus, unit C may represent a transgressive event. Unit D consists of stromatoporoid facies

78

(D2 and D4) along the buildup margins interlayered with thin skeletal grainstones (D1 and D3) that extended into the buildup interior (Figs. 17 and 18). Unit D differs from unit C by containing several layers of stromatolitic facies suggesting a regression event. Factors that terminated carbonate sedimentation are difficult to resolve. Unit E only occurs locally in wells 11-07 and 11-03 (Fig. 17). It consists predominantly of skeletal grainstones that may represent subtidal carbonate sand shoals deposited during the deepening event that marked the end of reef deposition in the Redwater and Golden Spike area (Stoakes, 1992).

Depositional controls on reservoir character

There is a good correspondence between pore type distribution and depositional facies (Figs. 17 and 18). Facies distribution maps (Fig. 20) of depositional units D3 and D2 outline the distribution of the porous and permeable zones. Because of the poor core control in many parts of this field, considerable interpretation was involved in constructing these maps. Contours were drawn to conform to the buildup morphology based on a structure map of the top of the Leduc Formation (Fig. 12). Wells with cores were assigned to reef positions (flank, margin, and interior) based on the lithofacies. Wells lacking core were positioned based on their location with respect to the structural contours. Contour line -1440 m is a rough approximate of the outer limit of the buildup interior. The outer limit of the buildup margins is indicated by the outer limits of the stromatoporoid facies.

The arithmetic average porosity and horizontal permeability were calculated for each depositional unit in each well along the cross sections (Figs. 17 and 18). Porosity in the margins is generally similar to or higher than the porosity in the buildup interior. One exception is well 09-25, where the porosity in depositional units A and B in the buildup margin is about 5% compared to 7-10% in the buildup interior. The presence of completely cemented breccia porosity in 09-25 within units A and B in part explains the lower porosity values. Based on the cross sections (Figs. 17 and 18) and facies distribution maps (Fig. 20), the Leduc dolostones are heterogeneous reservoirs with highly variable porosity and

Figure 20. Idealized facies distribution maps for depositional units D3 and D2 correlated in figures 17 and 18. The interpretations are based on the structural style of the area (Fig. 12) and the depositional model developed for the Golden Spike Leduc limestone (McGillivray and Mountjoy, 1975; Reitzel and others, 1976).
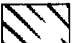
LEGEND

REEF INTERIOR

Skeletal grainstones

Algal laminites and shales

Mixture of skeletal grainstones,
Amphipora wackestones and
grainstones, green shales,
and dolomudstones.

REEF MARGIN

Stromatoporoid facies

Amphipora facies

REEF FLANK

—1400— Leduc structure contours

—1400— Poorly constrained Leduc contours
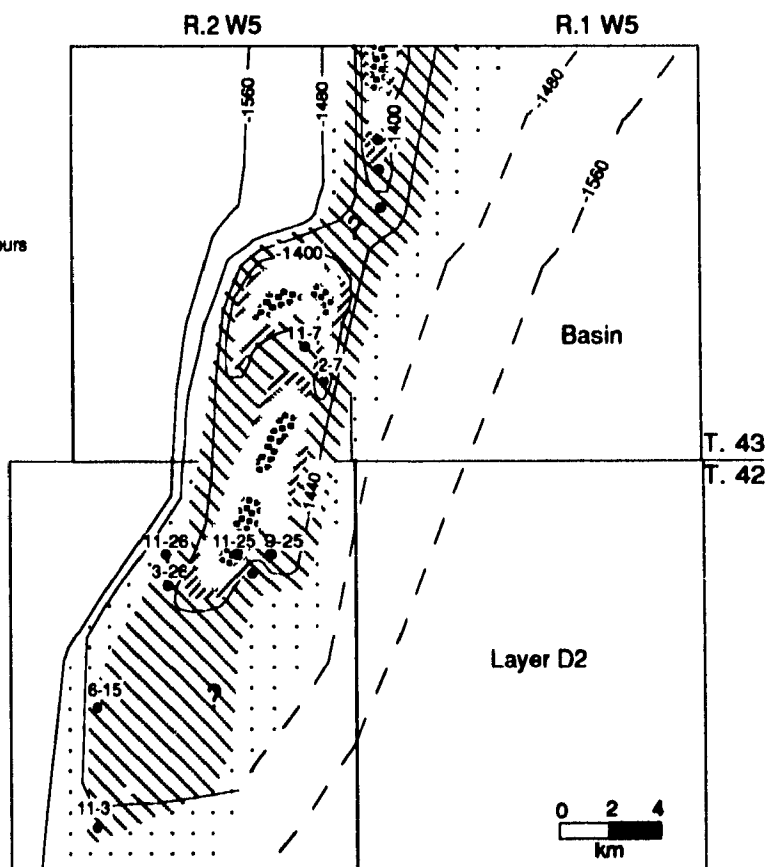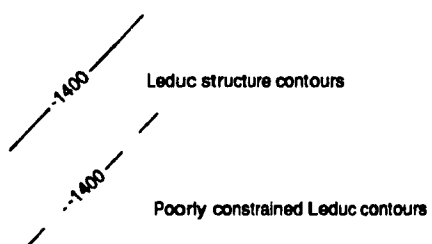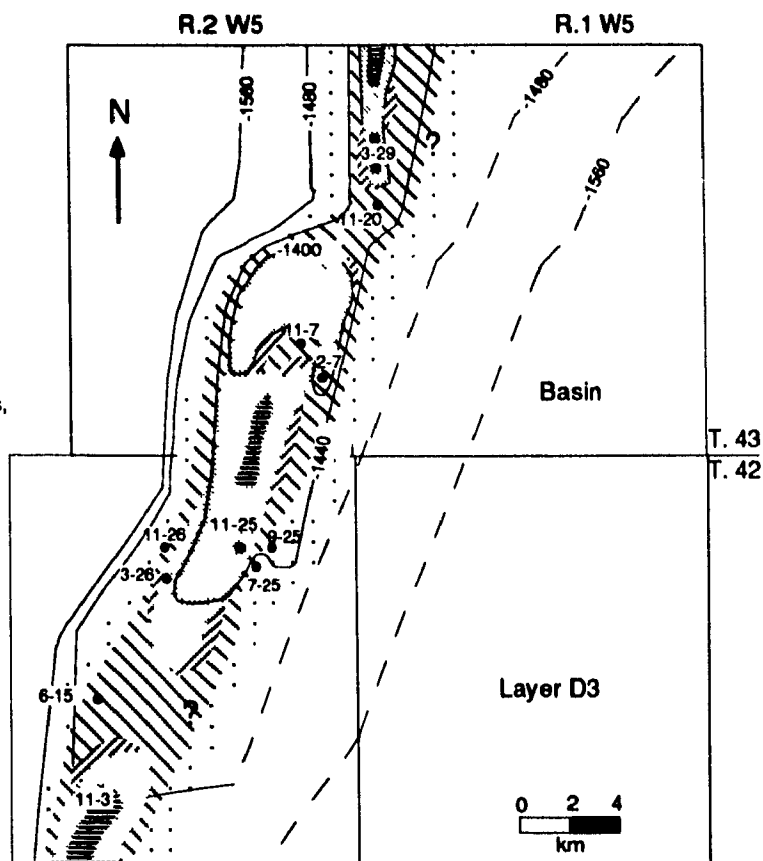
permeability. From the point of view of volume and vertical continuity, the best reservoir rocks are in the extensive vuggy stromatoporoid facies of the buildup margin facies which contains the greatest amounts of large vugs and are generally about 10 m thick. Average porosity core analyses are 9.52% (Table 7a). Probably a more realistic porosity would be about 13%, since core analysis underestimate porosity by at least 3% in intervals with large vugs (McNamara et al., 1991). Good intercommunication between the pores is indicated by the common occurrence of thin fractures that connect the pores (e.g. Plate 8a) which may explain the relatively high horizontal permeability in the stromatoporoid facies (Table 7a). Heterogenities of the reservoir character in the buildup margin are controlled by both depositional facies and diagenesis as indicated by: 1) the occasional occurrence of thin beds of porous and highly permeable skeletal grainstones, and dense and nonporous green shales interbedded with the stromatoporoid facies (Figs. 17 and 18); and 2) the presence of dolomite and anhydrite cements, both of which appear to be less abundant in the updip Homeglen-Rimbey field, but increase southward downdip in the study area (Fig. 5). Based on the depositional model of McGillivray and Mountjoy (1975) and Reitzel et al. (1976) for the Golden Spike limestones, the stromatoporoid facies in the Upper Leduc Formation tend to be laterally discontinuous and narrow. This was probably also true for the stromatoporoid facies in the Homgelen-Rimbey field since the carbonates in this area were depc ite.' under similar conditions.

The bui Jup interior is comprised of thin beds (centimetres in scale) of *Amphipora* grainstones alternating with skeletal grainstones, stromatolites, and dolomudstones resulting in vertical heterogeneities governed, for the most part, by depositional facies. Porosity and permeability, as a result, are variable. The skeletal sand flat deposits comprise the best reservoir facies in the buildup interior (Table 7a): they contain the highest horizontal and vertical permeability in the buildup complex, and exhibit good porosity. Prediction of the distribution of porous and permeable zones in skeletal grainstones must take into consideration that these horizons are relatively discontinuous both vertically and laterally because: 1)

they are thinly bedded and alternate with dense green shales and dolomudstones; and 2) they rarely extend to the buildup margins (Figs. 17 and 18). *Amphipora* and stromatolite facies of the buildup interior have slightly lower porosity and permeability, and occur as patches and lenses. Tight green shales and dolomudstones form local vertical permeability barriers that sometimes extend to the buildup margins. Patch reefs with vuggy porosity also occur in the reef interior. Permeability differs from one type of facies/pore system to another (Table 7a) indicating that permeability like porosity is controlled, in part, by depositional facies and diagenesis (see below).

Diagenetic controls on reservoir quality

In addition to mapping the porous and permeable facies, characterization of Leduc dolostone reservoirs must take into consideration diagenesis, particularly how cementation, dissolution, and dolomitization have affected the evolution of porosity and permeability. The paragenetic sequence of the Leduc dolostones and inferred porosity evolution are shown in Figure 16. In limestone Leduc buildups, early cementation decreased primary porosity and was followed by minor near-surface dissolution that enhanced primary pores and created some secondary porosity (Walls, 1977). These processes probably also took place in Leduc dolostones along the Rimbey-Meadowbrook reef trend which underwent a similar depositional and early diagenetic history. Mechanical and chemical compaction reduced both primary and secondary porosity. Later dissolution phases I and II, that occurred during and after replacement dolomitization and after early stylolitization, increased the porosity. The common occurrence of fractures that connect the pores (Plate 8a) suggests that permeability has been enhanced by fracturing. Porosity was gradually filled by late-stage cements including dolomite, anhydrite, and sulphur (Fig. 16). Because all the above porosity destruction and enhancement processes overlap, the distribution of final effective porosity in the Upper Leduc is difficult to predict and may, in some cases, be unrelated to the original depositional environment. Mapping of the distribution of the main cements

(Fig. 5), however, suggests that effective porosity at the reservoir scale decreases progressively downdip, especially south of Medicine River below present burial depths of 3000 m.

The effect of replacement dolomitization on porosity evolution is a complicated process, and may variously involve the preservation, enhancement, or destruction of pre-existing porosity (see review by Chilingarian et al., 1993, Mountjoy, 1994 in press). Porosity evolution during replacement dolomitization depends in part on the mechanism of dolomitization (Machel and Mountjoy, 1986). In theory, if the limestone is dolomitized by mole-for-mole replacement of calcium by magnesium, an approximate 13% volume reduction may result due to the greater density of the magnesium atom. The volume reduction creates up to 13% increase in porosity that may later be preserved, enlarged, or destroyed. If dolomitization occurred as volume-for-volume replacement (e.g. substitution of $MgCO_3$ for $CaCO_3$), a volume increase of 75 to 85% will result in porosity loss rather than gain (Lippmann, 1973). Dolomitization that involves no volume changes should theoretically lead to fabric and porosity preservation (Machel and Mountjoy, 1986).

Examples of two dolomite reservoirs with very different nature, porosity, and permeability are the Mississippian-hosted dolomites within the Upper Debolt Formation, and the Upper Devonian Wabamun dolostones (Packard, 1992). The former case is characterized by fabric retentive dolomites that probably originated from shallow seepage reflux model for dolomitization. It forms idiotopic planar-e fabrics with crystal sizes ranging from 1 to 20 μm, averaging 10μm, with high micro-intercrystalline porosity of up to 38% and permeability up to 75 mD. In contrast, Upper Devonian Wabamun Formation was dolomitized in a shallow to intermediate burial environment and is comprised of matrix dolomites with idiotopic-s fabric, and porosities that rarely exceed 5% (Mountjoy and Halim-Dihardja, 1991). These two examples illustrate that the dolomite crystal fabric, and the manner in which dolomitization took place are also important factors in controlling the reservoir quality.

The influence of dolomitization on reservoir properties, both at the facies and reservoir scale, is evaluated empirically by comparing the undolomitized Golden Spike buildup with the dolomitized Homeglen-Rimbey Leduc buildups, at present burial depths of about 1600 and 2300 m, respectively. The reservoir properties of the main facies/pore systems of the Homeglen-Rimbey buildups are summarized and compared with those of the Golden Spike buildup in Tables 7a and 7b. Information on the pore types, characterizing the facies in Golden Spike is derived from McGillivray and Mountjoy (1975) and Walls and Burrowes (1985, 1990). Interparticle pores predominate in the stromatoporoid facies and skeletal grainstones of Golden Spike and yield average porosity values as low as 5.5% (Table 7b), because of extensive submarine cementation in the buildup margins (McGillivray, 1975; Walls et al., 1979). Stromatoporoid facies and skeletal grainstones observed in Homeglen-Rimbey are comprised mostly of vuggy and intercrystalline porosity respectively. In contrast to Golden Spike, the stromatoporoid facies in Homeglen-Rimbey yield higher average porosity (10%) and permeability values (Tables 7a and 7b). Furthermore, the skeletal grainstones in Homeglen-Rimbey have similar average porosities to those of Golden Spike, but have much higher permeabilities (Tables 7a and 7b).

The different pore types within similar depositional facies in the Homeglen-Rimbey dolostones compared to the Golden Spike limestones indicates that dolomitization modified the pore types and their distribution. The higher porosity in the stromatoporoid facies of Homeglen-Rimbey is probably due to the greater abundance of vuggy pores resulting from dissolution that overlapped with replacement dolomitization, but may not necessarily be related to the process of dolomitization itself. The average porosities in Golden Spike and Homeglen-Rimbey fields for skeletal grainstones, stromatolite and skeletal packstone facies are similar. Despite different diagenetic and burial histories in each field, the present porosity for each facies types was not changed significantly. However, compared to the Golden Spike, the permeability is in general much greater in all facies from Homeglen-Rimbey. These high permeability values have resulted from

84

replacement dolomitization, since the abundance of fractures are similar in both fields.

At the reservoir scale, it is difficult to determine whether dolomitization decreased or increased porosity. Nevertheless, the effect of dolomitization on porosity evolution for Leduc dolostones are interpreted in Figure 21 based on several assumptions: 1) the initial porosity in all Leduc buildups was similar to porosities in modern reefs (30 to 50%); 2) cementation reduced porosity during near surface and early burial diagenesis; and 3) during early stages of burial (0 to 500 m) porosity is decreased mostly by mechanical compaction, whereas at burial depths greater than about 500 m, chemical compaction reduces porosity (Dunnington, 1967; Lind, 1993).

The present average porosity values for Golden Spike are 7% and 10% for the buildup margins and interior respectively (Walls and Burrowes, 1985). These values are reversed in the Homeglen-Rimbey field (10% in the buildup margin and 7% in the interior), in part due to the abundant submarine cements along the margins of the Golden Spike buildup. Although the Homeglen-Rimbey buildup has been buried 700 m deeper than the Golden Spike buildup, it contains higher porosity values in the buildup margins. In the buildup interior, however, the average porosity in the Homeglen-Rimbey dolomites is somewhat lower. With deeper burial downdip from the Homeglen-Rimbey field, Leduc limestones contain abundant stylolites and have their porosity is reduced to an overall average of 1.5% at about 3500 m (e.g. Strachan field D3B, Marquez, pers. comm., 1993), whereas the dolomite counterparts (Ricinus and Strachan field D3A) have fewer stylolites and have an average porosity of 6%. Compared to dolostones, the relatively larger reduction in porosity of limestones with increasing burial depth, concomitant with the greater number of stylolites (Marquez, pers. comm., 1993) indicate that dolomites are more resistant to chemical compaction than limestones, as has been shown for Pleistocene and Mesozoic rocks from south Florida (Schmocker and Halley, 1982). The slightly higher present porosity values in the margins of the Homeglen-Rimbey buildup and in the dolostones of Ricinus and

Figure 21. Comparison of inferred porosity changes with burial between the limestone Golden Spike buildup and the dolomite Homeglen-Rimbey buildups buried at about 1600 and 2300 m respectively. Initial porosity in both fields is assumed to have been about the same as the porosity observed in modern reefs (30 to 50%). The present average porosity values for the Golden Spike buildup margin and interior are 7% and 10% respectively (Walls and Burrowes, 1990). Based on core analysis, present average porosity values in the Homeglen-Rimbey buildup margin and interior are 10% to 7% respectively. The slightly higher porosity values in the Homeglen-Rimbey margins appears to be due to the greater abundance of vuggy porosity, whereas the buildup margins of Golden Spike are dominated by interparticle porosity partially to completely filled with submarine cements. Although the Homeglen-Rimbey dolostones have undergone deeper burial, they retained, in general, similar average porosity values as the shallower buried Golden Spike buildup, because dolomites are more resistant to chemical compaction than limestones.

Estimated porosity at time of deposition

30 to 50%

Golden Spike limestones

Homeglen-Rimbey dolomites

Mechanical compaction & cementation decrease porosity.

0 m

20 to 30%

20 to 30%

Undolomitized. Mechanical & chemical compaction & cementation decrease porosity.

Replacement Dolomitization. Porosity redistributed & decreased.

500

20 to 25%

15 to 20%

Chemical compaction & cementation decrease porosity progressively

1600

Little chemical compaction. Minor cementation. Little decrease in porosity.

7% 10% 7%

2300

10% 7% 10%

Strachan field D3A can also in part be explained by the greater abundance of vugs in dolomites than in Leduc limestones. If the assumptions and interpretations noted above are correct (Fig. 21), then replacement dolomitization decreased porosity during early burial. During later burial, the porosity in dolostone reservoirs appears to have been retained, while it has been progressively decreased in the limestones. This is probably because dolomites are more resistant to chemical compaction than limestones.

ORIGIN OF SECONDARY POROSITY

Two important questions in carbonate reservoir studies concern: 1) the extent to which porosity of a carbonate unit is affected by its residence time in the burial environment; and 2) the nature and types of pore fluids causing carbonate dissolution. It is critical, from an economic standpoint, to determine the diagenetic environments in which porosity originated. This, combined with a better knowledge of the dissolution processes involved, would improve our understanding of the origin and distribution of secondary porosity in Leduc dolostones. The occurrence of several phases of dissolution makes it difficult to resolve the origins of porosity and to determine which dissolution process affected a particular pore system. Later processes can partially or completely obliterate evidence of earlier events. This section attempts to constrain the environment of porosity formation (near-surface v.s. burial) in the Leduc dolostones based on the spatial relationships between porosity and diagenetic phases including stylolites, later-stage cements, and fractures. This is followed by a discussion on potential processes that may have generated sufficient acidic fluids to account for some of the secondary porosity observed in these Leduc reservoirs.

Environment and timing of porosity generation

In Golden Spike limestones, minor molds, small vugs, and fenestral pores are related to paleoexposure horizons and likely originated from early solution during subaerial exposure (Walls, 1977; Walls and Burrowes, 1985). Since the

87

Leduc buildups along the Rimbey-Meadowbrook reef trend had a similar depositional history, early dissolution during subaerial exposure probably also took place in the southern part of the Rimbey-Meadowbrook reef trend, forming minor amounts of moldic, vuggy, and fenestral porosity (Fig. 22).

At least three later phases of dissolution followed near surface dissolution (Fig. 16). In partially dolomitized intervals, dolomite preferentially replaced the matrix, leaving calcite remnants (Marquez, pers. comm., 1993; Amthor et al., 1993) that were dissolved during and/or after replacement dolomitization forming vuggy and moldic porosity (Dissolution I in Fig. 16). Because of the inferred environment and timing of replacement dolomitization (see Chapter 2), these vugs originated below depths of 500 m, sometime during or after the Late Devonian (Fig. 23).

Fracturing and dissolution stage II postdates replacement dolomitization, and predates dolomite cementation and thus must have occurred in the burial environment below depths of 500 m. Fracturing and dissolution stage II was partly responsible for brecciation of replacement dolomites that formed clasts of replacement dolomite rimmed by dolomite cement (Plates 10a to 10c). The presence of corroded crystals of replacive Dolomite-R2 along a pore transected by a stylolite (Plates 10i and 10j) suggests that dissolution II increased the existing vuggy porosity and overlapped and/or postdated stylolitization, further supporting a deeper burial origin.

Fracturing and dissolution stage III postdates dolomite cement in the brecciated intervals and late-stage fractures (Fig. 16; Plates 10c, 10e, and 10f). Fluid inclusion data from these dolomite cements indicate precipitation temperatures ranging between 98 and 142°C (Chapter 2) suggesting that fracturing and dissolution stage III originated in a deeper burial setting during the Cretaceous, assuming a normal geothermal gradient, or earlier if the hot fluids involved were derived from a hydrothermal source (Fig. 23).

Figure 22. Schematic diagram illustrating four possible origins of vuggy and moldic porosity: 1) dissolution of calcite allochems prior to replacement dolomitization in the near surface environment; 2) solution of calcite allochems during replacement dolomitization in the shallow burial environment; 3) dissolution of calcite remnants following replacement dolomitization in the shallow to intermediate burial environment; and 4) dissolution of replacement dolomites and dolomite cements following replacement dolomitization and dolomite cementation in the shallow to deep burial environment. All four processes occurred in the Leduc dolostones (see text for explanations).

FOUR POSSIBLE ORIGINS FOR MOLDIC AND VUGGY POROSITY

1 Dissolution of allochems during and soon after deposition

2 Dissolution of calcite remnants syngenetic with dolomitization Shallow burial

3 Dissolution of calcite remnants after dolomitization Shallow burial

4 Dolomitization of matrix and allochems

Dolomitization

Dissolution of replacement dolomite and dolomite cements Burial

Limestone

Dolomite

Leached allochem

Figure 23. Inferred timing of dissolution and fracturing phases I to IV with respect to the main diagenetic events and the burial history of the Leduc Homeglen-Rimbey and Garrington buildups.

Burial Plot

Dissolution I pre-replacement dolomitization

Homeglen-Rimbey

Garrington

Dissolution II syn-replacement dolomitization

Dissolution III post-dolomite cementation (related to acidic fluids?)

Dissolution IV (TSR related ?)

Temperature (°C): 30, 50, 70, 90, 110, 130, 150, 170, 190

Burial depth (m): 0, 1000, 2000, 3000, 4000, 5000

Age (m.y.): 400, 300, 200, 100, 0

Dev. | Car. | Pen. | Tria. | Jur. | Cret. | Ter.
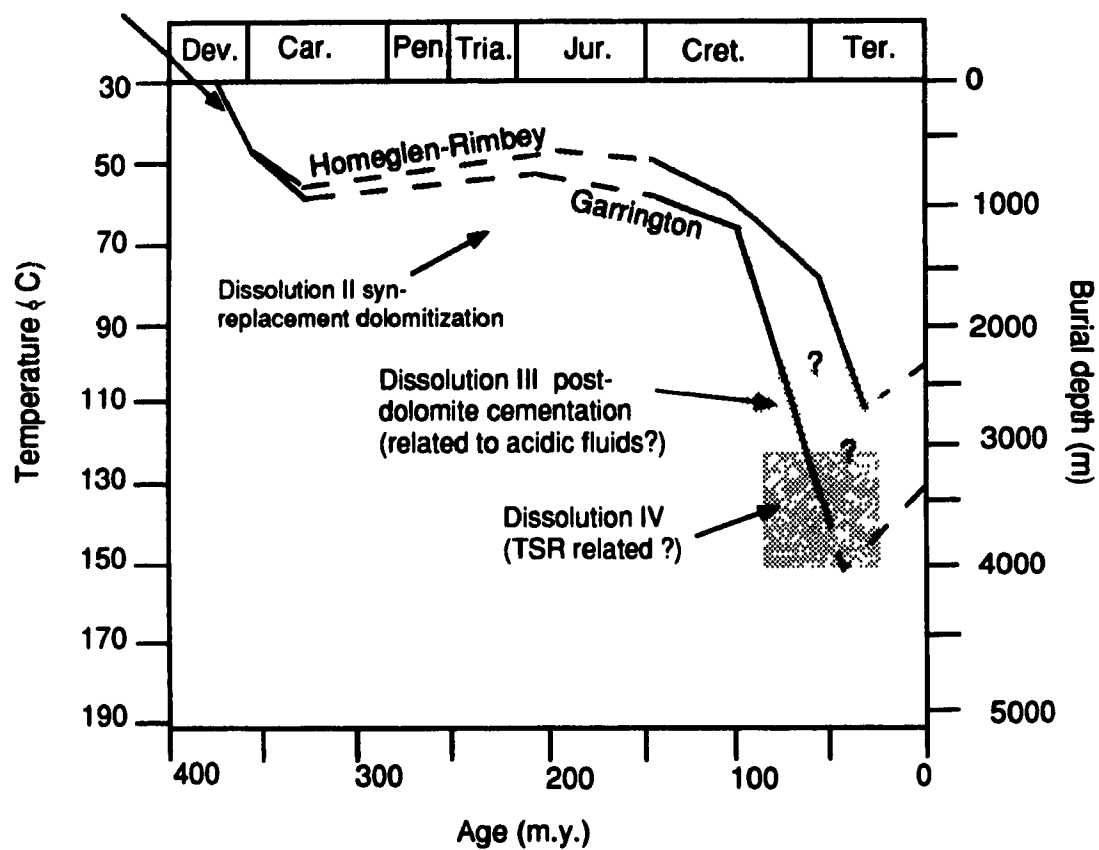
Fluids causing dissolution

The generation of acidic fluids is an important factor in controlling dissolution and secondary porosity development in carbonates (Mazzullo and Harris, 1992). Several processes may have provided acidic fluids in the burial environment in Leduc buildups. Mixing of two solutions that are both in equilibrium with respect to carbonate minerals but have different pCO_2, temperatures, salinity, degree of calcite saturation, and/or pH may result in undersaturation with respect to $CaMg(CO_3)_2$, leading to carbonate dissolution (mixing corrosion). For example, the presence of microstalactitic cements in Golden Spike suggests that mixing of vadose and phreatic waters may have been responsible for near surface dissolution in the Leduc Formation (Walls and Burrowes, 1990). Hutcheon suggested that in the western Canada foreland basin, small fractions of relatively low-salinity waters from Mesozoic rocks may have been added to greater proportions of the saline water from Palaeozoic rocks. The resulting mixture would become undersaturated with respect to dolomite and calcite and favours burial dissolution of carbonates in the subsurface. Based on the geochemistry of the oils, Devonian formations (including the Leduc) along the Rimbey-Meadowbrook reef trend have been sealed from overlying strata (Creaney and Allan, 1992). This sealing effect does not favour mixing corrosion as outlined by Hutcheon (1992), and thus carbonate dissolution in the Leduc dolomites probably resulted from other processes.

Burial dissolution of carbonate strata by reaction with meteoric fluids charged with carbonic and organic acids probably did not affect the Leduc reservoirs significantly since there is no textural and geochemical evidence to support extensive meteoric recharge in the Leduc dolostones, although they were probably exposed briefly from time to time. During burial at temperatures between 90 and 150°C (Mazzullo and Harris, 1992), the release of hydrogen ions during silicate hydrolysis of clay minerals lowers the pH of the formation waters and may induce dissolution. These acidic fluids would likely have been neutralized in situ, at least partially, because the Ireton and Duvernay shales surrounding the Leduc

buildups are carbonate rich. However, some of these fluids may have been funnelled updip along the Rimbey-Meadowbrook reef trend and potentially caused carbonate dissolution.

Maturation of organic matter produces CO_2, H_2S, and kerogen that may combine with water to generate carbonic, sulfuric, and organic acids respectively. Acidic fluids produced in these ways may also have contributed to creating porosity in the Leduc Formation. Fluid inclusions with high homogenization temperatures (up to 142°C) indicate that hydrothermal fluids precipitated the Leduc dolomite cements (Chapter 2). As these hot fluids rise and cool, the temperature of the system decreases thereby increasing the saturation level of dissolved carbonates and causing dissolution (Qing, 1991).

Evidence for thermochemical sulphate reduction (TSR) was presented in Chapter 2, including high levels of H_2S (30 and 90% in the Caroline and Bearberry fields respectively), and the common occurrence in the deepest part of the trend (below present burial depth of 3000 m) of late-stage blocky calcite cement with light carbon isotopic composition (-17.9 to -6.53 ‰PDB), sulphides, and sulphur. These minerals of presumed TSR origin become less abundant northward with decreasing burial depths (Chapter 2), which correlates with the general decrease northward in brecciation and H^2S(Fig. 15). During hydrocarbon maturation (Late Cretaceous) organic and carbonic acids would have been generated by the thermal cracking and oxidation of hydrocarbons, or when TSR acids would have been released during sulphide formation (Machel, 1987 a,b). Both organic maturation and TSR may have created and enhanced secondary porosity, and locally in some areas could have caused considerable solution and brecciation in the southern part of the Rimbey-Meadowbrook reef trend. However, this idea needs to be tested by more detailed regional mapping of late brecciation, since similar dolomite breccias have been reported updip in the Westerose, Bonnie-Glen, and Leduc buildups (Amthor et al., 1993). Thus, some breccias may have formed prior to the generation of acidic solutions by TSR reactions, possibly as a result of dissolution by organic acids.

In addition to dissolution, TSR reactions may have been responsible for precipitating late-stage cements such as anhydrite, dolomite, and calcite. However, whether TSR related reactions overall created, or both created and destroyed porosity is uncertain. Attempts to mass balance these reactions suggest that TSR processes do not appear to produce an overall major change in porosity (Machel, pers. comm., 1992). However, these reactions are capable of both dissolving carbonates and precipitating reaction products and, thus, locally creating considerable porosity in places, but also decreasing porosity by precipitating cements, such as extensive anhydrite, in other parts of a reservoir. Clearly more examples need to be studied where the lateral variations in, and amounts of, late-stage porosity and TSR products can be assessed and mass balanced.

CONCLUSIONS

This study describes in detail the reservoir characteristics of Leduc dolostones along the southern part of the Rimbey-Meadowbrook reef trend and includes a discussion of the origin of secondary porosity. The main conclusions are:

1. The facies and their hemi-cyclic stacking in Leduc buildups control the vertical and lateral distribution of the different pore types. The best reservoir quality in the Homeglen-Rimbey field occurs along the reef margins in the stromatoporoid facies which comprises the most vertically continuous intervals containing high porosity and good permeability. In the buildup interior, the best reservoir quality is found in the skeletal grainstones that exhibit good intercrystalline porosity, and the highest permeability in the entire Upper Leduc buildup. Compared to the stromatoporoid facies of the buildup margins, however, skeletal grainstones comprise more complex reservoirs because they are thin bedded (as thin as 5 cm), laterally discontinuous, and alternate with frequent layers of dense shales and dolomudstones.

2. Post-depositional processes extensively modified the primary porosity and permeability increasing the complexity of these Leduc reservoirs. Comparisons between undolomitized Leduc buildups and dolomitized equivalents along the Rimbey-Meadowbrook trend suggest that at the facies scale, dolomitization modified the distribution and types of the porosity and increased permeability. At the reservoir scale, porosity is better preserved in Leduc dolostones than in limestones probably because the dolostones are more resistant to chemical compaction. Cementation, particularly by anhydrite, and to a lesser extent by dolomite, calcite, and sulphur, gradually decreased the porosity especially in the deeply buried part

of the Rimbey-Meadowbrook reef trend at depths of more than 3000 m. Porosity reduction by cementation was offset by at least four dissolution phases that overlapped with replacement dolomitization. This resulted in effective secondary porosity unrelated to depositional facies making it difficult to predict its occurrence and distribution.

3. Processes causing burial dissolution that may have provided sufficient acidic fluids at different times include mixing corrosion, maturation of organic matter, and thermochemical sulphate reduction. The amount of porosity and cements created by these processes is difficult to quantify.

CHAPTER 4

GENERAL CONCLUSIONS

The Upper Devonian Leduc Formation along the southern part of the Rimbey-Meadowbrook reef trend has undergone diagenetic alteration in submarine, subaerial, and subsurface environments. Isopachous and fibrous submarine cements are best observed in Leduc limestone buildups, and are still recognizable along the southern part of the Rimbey-Meadowbrook reef trend despite dolomitization. Subsurface diagenesis includes: dolomitization, stylolitization, several phases of fracturing and dissolution, dolomite cementation, precipitation of anhydrite, quartz, calcite, bitumen, and elemental sulphur.

Six types of dolomites are identified: four are replacement dolomites, and two are dolomite cements. Replacement dolomites postdate deposition of the overlying Ireton Formation and early submarine cementation, overlap with stylolitization, and are characterized by $\delta^{18}O$ values of -5.27 to -3 71‰PDB that suggest minimum precipitation temperatures of 45°C, or paleodepths of at least 500 m. Thus, replacement dolomitization probably took place in a shallow burial environment beginning in the Late Devonian or later. Strontium isotopic ratios of replacement dolomites (0.70818 to 0.70912) overlap with, and are somewhat higher than, the corresponding Devonian seawater (0.7080 to 0.7083), suggesting that the dolomitizing fluids were probably modified from Devonian seawater with small amounts of radiogenic strontium being added from adjacent or underlying clastics, or older carbonates.

Replacement dolomites may also have been subjected to neomorphism affecting their isotopic composition. Neomorphism appears to have taken place locally near fractures, pores, and stylolites as indicated by: 1) fine crystals of replacement dolomites (30 to 60 μm) that are occasionally distributed interstitial to and within coarser dolomite crystals (60 to 250 μm); 2) the occurrence of coarser replacement dolomite crystals near fractures, stylolites, and pores that display irregular sometimes nonplanar crystal boundaries with undulose extinction; 3) the presence of bright and dull luminescent bands of replacement dolomites along fractures; and 4) dolomite crystals that selectively replace the cloudy cores of

Dolomite-R2 crystals. However, based on the scarcity of these neomorphic textures, recrystallization of the replacement dolomites or an earlier precursor dolomite appears to have been insignificant.

There are two types of dolomite cements; C1: coarse-crystalline planar-e(s), and C2: very coarse-crystalline nonplanar. Dolomite-C1 postdates replacement dolomitization, and precipitated near and along stylolites. $\delta^{18}O$ values (-7.05 to -3.96‰PDB), and fluid inclusion data indicate that Dolomite-C1 precipitated out of hydrothermal brines under intermediate to deep burial depths. Dolomite-C2 postdates Dolomite-C1 and is comparatively depleted in ^{18}O, reflecting the different composition and temperature of the fluids responsible for Dolomite-C2 cementation.

The presence of blocky calcite cement with light $\delta^{13}C$ values, anhydrite cement, free sulphur, sulphides, anhydrite, and the high mole percent H_2S (30 to 90 mol%) in the deeply buried reservoirs are supportive of TSR reactions. The amount of TSR related cements and the mole percent of H_2S decrease northward along the Rimbey-Meadowbrook reef trend suggesting that TSR was most prevalent in the deepest part of the reef trend, below burial depths of about 3000 m.

Depositional environment, dolomitization, and later diagenesis are major factors controlling the reservoir character and quality. The distribution of porous and permeable zones in the Homeglen-Rimbey dolostone reservoirs is variable and heterogeneous and is controlled both by the depositional facies and the later diagenesis. The reef margins are comprised mostly of thick beds (5 to 20 m thick) of stromatoporoid facies dominated by vuggy pores. These intervals comprise the best reservoir because they are the most vertically continuous, and are characterized by high average porosity and permeability. Skeletal grainstones in the buildup interior have good reservoir quality with intercrystalline pores having the highest average permeabilities of all the facies and good porosity. Compared to the stromatoporoid facies, skeletal grainstones comprise more complex reservoirs because they are thin bedded (5 to 50 cm), laterally discontinuous, and alternate with dense shales and dolomudstones.

The reservoir quality is controlled by diagenesis, in particular, cementation, dissolution, and dolomitization. In decreasing importance, anhydrite, dolomite, calcite, and native sulphur late-stage cements gradually reduced the porosity, and are most extensive south of the Medicine River field below present burial depths of about 3000 m. Cementation was offset to some extent by three main phases of burial dissolution that took place during and after dolomitization, stylolitization and later-stage cements. These late dissolution events originated in the burial environment and were generated by acidic fluids that may have been produced by mixing corrosion, maturation of organic matter, and various TSR reactions.

The effect of dolomitization on porosity evolution is complex. Based on comparison with Leduc limestone buildups (Golden Spike), dolomitization modified the type and distribution of the pores, and increased the permeability. At the reservoir scale, dolomitization probably decreased porosity initially, but later during progressive burial, the porosity was largely retained in dolomites because they are less affected by chemical compaction than limestones.

FUTURE RESEARCH

This dissertation provides the background for several future research projects. Preliminary work on fluid inclusions suggests that it is possible to obtain measurements from primary or pseudo-primary fluid inclusions in replacement dolomites. More work in this area would further constrain the origin of the replacement dolomites. The geochemical and microthermometric data could be plotted vertically and laterally along the Rimbey-Meadowbrook reef trend, which combined with more extensive geochemical modelling would potentially elucidate the extent to which neomorphism has affected the Leduc dolomites, and the pathways of the dolomitizing fluids.

Regional facies and porosity correlations updip and downdip of the Homeglen-Rimbey field would improve our understanding of the character of these dolomitized reservoirs, and would indicate whether the reservoir properties established for the Homeglen-Rimbey field are representative of the Leduc

dolomites along the Rimbey-Meadowbrook reef trend. The primary obstacle in correlating the facies and reservoir character, however, is the difficulty of recognizing primary facies in partially to completely dolomitised strata. A more detailed study of the pore geometry using SEM microscopy, particularly determining sorting and skewness, spatial arrangement, and orientation of the pore size and pore throats, and roughness of pore walls, would improve our knowledge of the reservoir character of each facies/pore system in these dolomites.

REFERENCES

Amthor, J.E., Mountjoy, E.W., and Machel, H.G., 1993. Subsurface dolomites in Upper Devonian Leduc formation buildups, central part of Rimbey-Meadowbrook reef trend, Alberta, Canada. Bulletin of Canadian Petroleum Geology, v. 41, p. 69-185.

Amthor, J.E., Mountjoy, E.W., and Machel, H.G., submitted. Regional-scale porosity and permeability variations in Upper Devonian Leduc buildups: implications for origin and distribution of porosity in carbonates. American Association of Petroleum Geologists, Bulletin.

Andrichuk, J.M., 1958. Cooking Lake and Duvernay (Late Devonian) sedimentation in Edmonton area of central Alberta, Canada. American Association of Petroleum Geologists, Bulletin, v. 42, p. 2189-2222.

Berner, R.A., 1978. Rate control of mineral dissolution under earth surface conditions. American Journal of Sciences, v. 278, p. 1235-1252.

Burke W.H., Denison R.E., Hetherington E.A., Koepnick R.B., Nelson H.F., and Otto J.B., 1982. Variation of seawater $^{87}Sr/^{86}Sr$ throughout Phanerozoic time. Geology, v. 10, p. 516-519.

Burrowes, O.G., 1977. Sedimentation and diagenesis of back-reef deposits, Miette and Golden Spike buildups, Alberta. Unpublished M.Sc. thesis, McGill University, 207 p.

Carpenter, S.J. and Lohmann, K.C., 1989. $\delta^{18}O$ and $\delta^{13}C$ variations in Late Devonian marine cements from the Golden Spike and Nevis reefs, Alberta, Canada. Journal of Sedimentary Petrology, v. 59, p. 792-814.

Chilingarian, G.V., Mazzullo, S.J., and Rieke, H.H., 1993. Carbonate reservoir characterization: a geologic - engineering analysis, part I, Elsevier, 639 p.

Choquette P.W., and Pray L.C., 1970. Geologic nomenclature and classification of porosity in sedimentary carbonates. American Association of Petroleum Geologists, Bulletin, v. 54, p. 207-250.

Chouinard, H., 1993. Lithofacies and diagenesis of the Cooking Lake platform carbonates, Alberta basin subsurface, Canada. Unpublished M.Sc. thesis, McGill University, 101 p.

Coniglio, M., and Williams-Jones, W.E., 1992. Diagenesis of Ordovician carbonates from the north east Michigan Basin, Manitoulin Island area, Ontario:

evidence from petrography, stable isotopes, and fluid inclusions. Sedimentology, v. 39, p. 813-836.

Connolly, C.A., Walter, L.M., Baadsgaard, H., and Longstaffe, F.,J., 1990. Origin and evolution of formation waters, Alberta Basin, Western Canada, Sedimentary Basin. I. Chemistry. Applied Geochemistry, v. 5, p. 375-395.

Craig, H., 1957. Isotopic standards for carbon and oxygen and correction factors for mass-spectrometric analysis of carbon dioxide. Geochemica et Cosmochimica Acta, v. 12, p. 272-374.

Creaney, S., and Allan, J., 1992. Petroleum systems in the Foreland Basin of Western Canada. in: Foreland basins and fold belts. Macqueen, R.W., and Leckie, D.A. (eds.). American Association of Petroleum Geologists, Memoir 55, p. 279-308.

Deroo, G., Powell, T.G., Tissot, B., McGrossan, R.G., and Haquebard, P.A., 1977. The origin and migration of petroleum in the Western Canada Sedimentary Basin, Alberta - a geochemical and thermal maturation study. Geological Survey of Canada Bulletin 262, 136 p.

Dickson, J.A.D., 1965. A modified staining technique for carbonates in thin sections. Nature, v. 205, p. 587.

Dickson, J.A.D., 1991. Disequilibrium carbon and oxygen isotopic variations in natural calcite. Nature, v. 353, p. 842-844.

Drivet, E., and Mountjoy, E.W., 1993. Porosity variations in Upper Devonian Leduc dolomites, central Rimbey-Meadowbrook reef trend, Alberta. American Association of Petroleum Geologists, annual meetings abstracts, p. 93.

Dunnington H.V., 1967. Aspect of diagenesis and shape change in stylolitic limestone reservoirs. 7th World Petroleum Congress Proceedings, Mexico City, v. 20, p. 339-352.

Eliuk L.S., 1984. A Hypothesis for the origin of hydrogen sulphide in Devonian Crossfield dolomite, Wabamun Formation, Alberta, Canada. in: Carbonates in subsurface and outcrop. Eliuk, L.S., Kaldi, J., and Watts, N. (eds.). Canadian Society of Petroleum Geologists, Core Conference.

Feldman, D.S., Gagnon, J., Hofmann, R., and Simpson, J., 1987. Statviewll The solution for data analysis and presentation graphics. 247 p.

Folk, R.L., 1962. Spectral subdivision of limestone types. in: Classification of

carbonate rocks. Ham W.E. (ed.). American Association of Petroleum Geologists, Memoir 1, p. 62-64.

Friedman, I., and O'Neil, J.R., 1977. Data of geochemistry, 6th edition, Chapter KK. Compilation of stable isotope fractionation factors of geochemical interest, United States Geological Survey Professional Paper 440-KK, p. 1-12.

Gregg, J.M., Howard, S.A., and Mazzullo, S.J., 1992. Early diagenetic recrystallization of Holocene (<3000 years old) peritidal dolomites, Ambergis Cay, Belize. Sedimentology, v. 39, p. 143-160.

Gregg, J.M., and Shelton, K.L., 1990. Dolomitization and dolomite neomorphism in the back reef facies of the Bonneterre and Davies formations (Cambrian) southeastern Missouri. Journal of Sedimentary Petrology, v. 60, p. 549-562.

Gregg, J.M., and Sibley, D.F., 1984. Epigenetic dolomitization and the origin of xenotopic dolomite texture. Journal of Sedimentary Petrology, v. 54, p. 908-931.

Hollister, L.S., Crawford, M.L., Roedder, E., Burruss, R.C., Spooner, E.T.C., and Touret, J., 1981. Pratical aspects of microthermometry. *in:* Fluid inclusions: applications to petrology. Hollister, L.S., and Crawford, M.L. (eds.). Mineralogical Association of Canada, p. 278-304.

Hudson, M.J.P., and Anderson, T.F., 1989. Ocean temperatures and isotopic compositions through time. Transactions of the Royal Society of Edinburgh, Earth Sciences, v. 80, p. 183-192.

Hutcheon, I., Abercombie, H., and Krouse, H.R., 1990. Inorganic origin of carbon dioxide during low temperature thermal recovery of bitumen: chemical and isotopic evidence. Geochemica et Cosmochimica Acta, v. 54, p. 165-171.

Hutcheon, I., 1992. The chemical systematics of carbonate mineral dissolution. *in:* Subsurface dissolution porosity in carbonates - recognition, causes and implications. American Association of Petroleum Geologists - Canadian Society of Petroleum Geologists short course notes, part 1: p. 1-17.

James, A.T., 1990. Correlation of reservoired gases using the carbon isotopic compositions of wet gas components. American Association of Petroleum Geology, Bulletin, v. 74, p. 1441-1458.

Kaufman, J., Hanson, G.N., and Meyers, W.J., 1991. Dolomitization of the Devonian Swan Hills Formation, Rosevear field, Alberta, Canada. Sedimentology, v. 38, p. 41-66.

Kirker, R.J.., 1959. Homeglen-Rimbey field. *in:* Oil Fields of Alberta- a Reference volume by the Alberta Society of Petroleum Geologists. White, R.J., Pow, J.R., Axford, D.W., et al., (eds.). p. 130-131.

Klovan, J.E., 1964. Facies analysis of the Redwater reef complex, Alberta, Canada. Bulletin of Canadian Petroleum Geology, v. 12, p. 1-100.

Krouse, H.R., Viau, C.A., Eliuk, L.S., Ueda, A., and Halas, S., 1988. Chemical and isotopic evidence of thermochemical sulphate reduction by light hydrocarbon gases in deep carbonate reservoirs. Nature, v. 333, p. 415-419.

Kupecz, J.A., and Land L.S., 1991. Late-stage dolomitization of the Lower Ordovician Ellenburger group, West Texas. Journal of Sedimentary Petrology, v. 61, p. 551-574.

Kupecz, J.A., Montañez, I.P., and Gao, G., 1992. Recrystallization of dolomite with time. *in:* Carbonate microfacies. Springer Verlag (ed.). p. 187-194.

Laflamme A., 1990. Replacement dolomitization in the Upper Devonian Leduc and Swan Hills Formations, Caroline area, Alberta Canada. Unpublished M.Sc. thesis, McGill University, 138 p.

Land L.S., 1980. The isotopic and trace element geochemistry of dolomite: the state of the art. *in:* Concept and Models of Dolomitization. Zenger D.H., Dunham J.B., and Ethington R.L. (eds.). Society of Economic Paleontologists and Mineralogists Special Publication, No. 28, p. 87-110.

Land L.S., 1983. The application of stable isotopes to studies of the origin of dolomite and to the problems of diagenesis of clastic sediments. *in:* Stable Isotopes in Sedimentary Geology. Arthur, M.A., Anderson, T.F., Kaplan, I.R., Veizer J., and Land L.S. (eds.). Society of Economic Paleontologists and Mineralogists Short Course, No. 10, p. 4-1 to 4-22.

Land L.S., 1985. The origin of massive dolomite. Journal of Geological Education, v. 33, p. 112-125.

Lee, Y.I. and Friedman, G.M., 1987. Deep-burial dolomitization in the Ordovician Ellenburger Group carbonates, western Texas and southeastern Mexico. Journal of Sedimentary Petrology, v. 57, p. 544-557.

Lind I., 1993. Stylolites in chalk from Leg 130, Ontong Java Plateau. *in:* Berger, W.H., Kroenke, J.W., Mayer, L.A., et al. (eds.). Proceedings of the Ocean Drilling Program, Scientific Results, v. 130, p. 445-451.

Lippmann, F., 1973. Sedimentary carbonate minerals. Springer, Berlin, 228 p.

Lundergard, P.D., and Land, L., 1989. Carbonate equilibria and pH buffering by organic acids - response to changes in pCO2. Chemical Geology, v. 74, p. 277-287.

Machel, H.G., 1987a. Saddle dolomite as a by-product of chemical compaction and thermochemical sulphate reduction. Geology, v. 15, p. 936-940.

Machel, H.G., 1987b. Some aspect of diagenetic sulphate-hydrocarbon redox reactions. in: Diagenesis of Sedimentary Sequences. Marshall, J.D. (ed.). Geological Society of London Special Publication, No 36, p. 15-28.

Machel, H.G., 1990. Burial diagenesis, porosity and permeability development of carbonates. in: The development of porosity in carbonate reservoirs. Canadian Society of Petroleum Geologists short course notes, p. 2.1-2.18.

Machel, H.G. and students, 1991. The Bonnie Glen - Acheson area. Unpublished report,   University of Alberta, 3 p.

Machel H.G., and Anderson J.H., 1989. Pervasive subsurface dolomitization of the Nisku formation in Central Alberta. Journal of Sedimentary Petrology, v. 59, p. 891-911.

Machel, H.G., and Mountjoy, E.W., 1986. Chemistry and environments of dolomitization - A reappraisal. Earth Science Reviews, v. 23, p. 175-222.

Machel, H.G., and Mountjoy, E.W., 1987. General constraints on extensive pervasive dolomitization and their application to the Devonian carbonates of western Canada. Bulletin of Canadian Petroleum Geology, v. 35, p. 143-158.

Marquez, X., 1993. Sedimentological and diagenetic controls on pore systems in a dolomitized reservoir; a case study: Ricinus West gas field, Alberta. American Association of Petroleum Geologists, p. 145.

Marquez, X., (in progress). Reservoir Geology of Leduc Strachan and Ricinus buildups in the deep Alberta basin. Ph.D. thesis, McGill University.

Marquez, X.,Mountjoy, E.W., and Amthor, J., 1992. Microfracturing in deeply buried carbonate buildups: Upper Devonian Strachan and Ricinus reservoirs, Alberta. American Association of Petroleum Geologists - Canadian Society of Petroleum Geologists annual meetings abstracts, p. 81.

Mattes, B.W., and Mountjoy, E.W., 1980. Burial dolomitization of the Upper

Devonian Miette buildup, Jasper National Park, Alberta. *in:* Concepts and models of dolomitization. Zenger, D.H., Dunham, J.B., and Ethington, R.L. (eds.). Society of Economic Paleontologists and Mineralogists Special Publication, No. 28, p. 259-297.

Mazzullo, S.J., 1992. Geochemical and neomorphic alteration of dolomite: a review. Carbonates and Evaporites, v. 7, p. 21-37.

Mazzullo, S.J., and Harris, P.M., 1992. Mesogenetic dissolution: its role in porosity development in carbonate reservoirs. American Association of Petroleum Geologists, Bulletin, v. 76, p. 607-620.

McCrossan, R.G., and Glaister, R.P., 1964. Geological history of Western Canada. 2nd edition, 232 p.

McLean, D.J., 1992. Upper Devonian buildup development in the southern canadian Rocky Mountains: a sequence stratigraphic approach. Unpublished Ph.D. thesis, McGill University, 245 p.

McLean, D. and Mountjoy, E.W., 1993a. Stratigraphy and depositional history of the Burnt Timber Embayment, Fairholme Complex, Alberta. Bulletin of Canadian Petroleum Geology, V. 41, p. 290-306.

McLean, D. and Mountjoy, E.W., 1993b. Upper Devonian buildup-margin and slope development in the southern Canadian Rocky Mountains. Geological Society of America Bulletin, v. 105, p. 1263-1283.

McNamara, L.B., and Wardlaw, N.C., 1991. Geological and statistical description of the Westerose reservoir, Alberta. Bulletin of Canadian Petroleum Geology, v. 39. p. 332-351.

McNamara, L.B., Wardlaw, N.C., and McKellar, M., 1991. Assessment of porosity from outcrops of vuggy carbonate and application to cores. Bulletin of Canadian Petroleum Geology, v. 39, p. 260-269.

McGillivray J.G., and Mountjoy E.W., 1975. Facies and related reservoir characteristics Golden Spike reef complex, Alberta. Bulletin of Canadian Petroleum Geology, v. 23, p. 753-809.

Montañez, I.P., and Read, J.F., 1992. Fluid-rock interaction history during stabilization of early dolomites, Upper Knox Group (Lower Ordovician), U.S. Appalachians. Journal of Sedimentary Petrology, v. 62, p. 753-778.

Mountjoy, E.W., 1994, (in press). Dolomitization and the character of hydrocarbon

reservoirs: Devonian of Western Canada. *in:* Quantitative Diagenesis, NATO short course notes, Klower Academic Publication. Rarker, A., and Sellword, B.W., (eds.).

Mountjoy E.W., and Amthor, J.E., 1994. Has burial dolomitization come of age? Some answers from the Western Canada Sedimentary Basin. B. Purser, M. Tucker, and D. Zenger (eds.). International Association of Sedimentologists, Special Publication, No. 21, p. 203-229.

Mountjoy E.W. and Halim-Dihardja, M., 1991. Multiple phase fracture and fault-controlled burial dolomitization, Upper Devonian Wabamun Group, Alberta. Journal of Sedimentary Petrology, v. 61, p. 590-612.

Mountjoy E.W., Qing H., and McNutt R.H., 1992. Strontium isotopic composition of Devonian dolomites, Western Canada Sedimentary Basin: Significant sources of dolomitizing fluids. Applied Geochemistry, v. 7. p. 59-75.

Oakes, C.S., Bodnar, R.J., and Simonson, J.M., 1990. The system $NaCl-CaCl_2-H_2O$: I. The ice liquidus at 1 atm total pressure. Geochimica et Cosmochimica Acta, v. 54, p. 603-610.

Oder, C.R.L., and Hook, J.W., 1950. Zinc deposits in the southeastern states, in: Symposium on mineral resources of the south eastern United States: Knoxville, Tennessee. Snyder, F.G., (ed.), University of Tennessee Press, p. 72-87.

Packard, J.P., 1992. A tale of two dolomites, Canadian Society of Petroleum Geologists Reservoir, abstract, v.19, no.9, p. 1-2.

Qing, H., 1991. Diagenesis of Middle Devonian Presqu'ile dolomite, Pine Point NWT and adjacent subsurface. Unpublished Ph.D. thesis, McGill University, 287p.

Qing, H., and Mountjoy, E.W., 1989. Multistage dolomitization in Rainbow buildups, Middle Devonian Keg River, Alberta, Canada. Journal of Sedimentary Petrology, v. 59, p. 114-126.

Qing, H., and Mountjoy, E.W., 1990. Petrography and diagenesis of the Middle Devonian Presqu'ile Barrier: implications on formation of dissolution vugs and breccias at Pine Point and adjacent subsurface, District of MacKenzie. *in:* Current Research, part D, Geological survey of Canada, Paper 90-1D, p. 37-45.

Qing, H., and Mountjoy, E.W., 1992. Large scale fluid flow in the Middle Devonian Presqu'ile Barrier, Western Canada Sedimentary Basin. Geology, v. 20, p. 903-906.

Reimer, J.D., and Teare, M.R., 1992. Deep burial diagenesis and porosity modification in carbonate rocks by thermalorganic sulphate reduction and hydrothermal dolomitization: TSR-HTD. *in:* Subsurface dissolution porosity in carbonates - recognition, causes and implications. American Association of Petroleum Geologists - Canadian Society of Petroleum Geologists short course notes, p. 1-26.

Reitzel, G.A., Davidson, G., Callow, G.O., and Bates, D.R., 1976. Golden Spike D3-A pool oil depletion study, Calgary. Imperial Oil Ltd., Producing Department, Western Region, Report IPRC-5ME-76.

Sangster, D.F., 1988. Breccia-hosted lead-zinc deposits in carbonate rocks. *in:* Paleokarst. James, N.P., and Choquette, P.W., (eds.), Springer-Verlag. p. 102-116.

Shields, M.J., and Geldsetzer, H.H.J., 1992. The MacKenzie margin, Southesk-Cairn carbonate complex: depositional history, stratal geometry and comparison with other Late Devonian platform-margins. Bulletin of Canadian Petroleum Geology, v. 40, p. 274-293.

Schmocker, J.W., and Halley, R.B., 1982. Carbonate porosity versus depth: a predictable relation for South Florida. American Association of Petroleum Geologists, Bulletin, v. 66, p. 2561-2570.

Sibley, D.F., and Gregg, J.M., 1987. Classification of dolomite rock textures. Journal of Sedimentary Petrology, v. 57, p. 967-975.

Stoakes, F.A., 1980. Nature and control of shale basin fill and its effect on reef growth and termination: Upper Devonian Duvernay and Ireton formations of Alberta, Canada. Bulletin of Canadian Petroleum Geology, v. 28, p. 234-410.

Stoakes, F.A., 1992. Woodbend megasequence. *in:* Devonian-Early Mississippian carbonates of the Western Canada sedimentary basin: a sequence stratigraphic framework. Wendte, J.C., Stoakes, F.A., and Campbell, C.V. (eds.). Society of Economic Paleontologists and Mineralogists Special Publication Short Course, No. 28, p. 183-206.

Tucker, M.E., and Wright, V.P., 1990. Carbonate sedimentology. Blackwell, London, 482 p.

Walls R.A., 1977. Cementation history and porosity development, Golden Spike reef complex (Devonian), Alberta. Unpublished Ph.D., McGill University, 307p.

Walls, R.A., and Burrowes O.G., 1985. The role of cementation in the diagenetic history of Devonian reefs, western Canada. *in:* Carbonate cements. Schneidermann, N. and Harris, P.M. (eds.). Society of Economic Paleontologists and Mineralogists Special Publication, No. 36, p. 185-220.

Walls, R.A., and Burrowes O.G., 1990. Diagenesis and reservoir development in Devonian limestone and dolostone reefs of Western Canada. *in:* The development of porosity in carbonate reservoirs. Bloy, G.R., and Hadley, M.G. (eds.). Canadian Society of Petroleum Geologists short course, section 5, p. 1-17.

Walls, R.A., Mountjoy, E.W., and Fritz, P., 1979. Isotopic composition and diagenetic history of carbonate cements in Devonian Golden Spike reef, Alberta. Geological Society of America Bulletin, v. 90, p. 963-982.

Wardlaw, N.C., 1990. Characterization of carbonate reservoirs for enhanced oil recovery. Proceedings 1st technical symposium on enhanced oil recovery, Tripoli, Libya, paper no. 90-01-05, p. 85-105.

Werre, R.W., Jr., Bodnar, R.J., Bethke, P.M., and Barton, P.B., 1979. A novel gas-flow fluid inclusion heating/freezing stage, Geological Society of America, Abstracts with programs, v. 11, p. 539.

Wendte, J.C., 1974. Sedimentation and diagenesis of the Cooking Lake platform and Lower Leduc reef facies, Upper Devonian Redwater, Alberta. Unpublished Ph.D. thesis, University of California, Santa Cruz, 222 p.

Wendte, J.C., 1992. Platform evolution and its control on reef inception and localization. *in:* Devonian-Early Mississippian carbonates of the Western Canada sedimentary basin: a sequence stratigraphic framework. Wendte, J.C., Stoakes, F.A., and Campbell C.V. (eds.). Society of Economic Paleontologists and Mineralogists Short course, No. 28, p. 41-87.

Wendte, J.C., and Stoakes, F.A., 1982. Evolution and corresponding porosity distribution of the Judy Creek reef complex, Upper Devonian, central Alberta. *in:* Canada's great hydrocarbon reservoirs. Cutler, W.G. (ed.). Canadian Society of Petroleum Geologists Core Conference, p. 63-81.

Zenger, D.H., Dunham, J.B., and Ethington, R.L., 1980. Concepts and models of dolomitization. Society of Economic Paleontology and Mineralogy Special Publication, No. 28, 320 p.

APPENDIX I

MICROTHERMOMETRIC DATA FOR FLUID PRIMARY INCLUSIONS IN DOLOMITES FROM THE LEDUC FORMATION, SOUTHERN RIMBEY-MEADOWBROOK REEF TREND, CENTRAL ALBERTA

Appendix 1. Microthermometric data for fluid inclusions in Dolomites from the Upper Leduc Formation along the southern part of the Rimbey-Meadowbrook reef trend. The majority of the fluid inclusions studied are liquid primary inclusions within Dolomite-C1 and where indicated may be possibly from Dolomite-R2. Weight percent NaCl values are calculated according to the equations in Oakes et al. (1990).

Well (Depth)	Chip #	HOST	Tf	Te	TmICE	Th	Weight % NaCl
08-30-38-04W5	1,1	Dol-C1	-69			105	
(3159.4 m)	1,2	Dol-C1	-69		-17.1	100	19.6
	1,3	Dol-C1	-69	-43	-16.9	121	19.5
	1,4	Dol-C1	-69		-17.3	107	19.7
	2,1	Dol-C1	-70		-17.3	116	19.7
	2,4	Dol-C1	-69			107	
	2,5A	Dol-C1	-68		-16.8	105	19.4
	2,6	Dol-C1	-73		-17.8	118	20.1
	2,7	Dol-C1	-66		-17	116	19.5
	2,8	Dol-C1				103	
	2,9	Dol-C1				119	
	2,11	Dol-C1	-56		-16.8	98	19.4
Mean			**-67.8**		**-17.1**	**110**	**19.6**
11-03-42-02W5	1,1	Dol-C1	-69.6		-18.2	140	20.3
(2390.2 m)	1,2	Dol-C1	-69.2			142	
	1,3	Dol-C1	-69.4		-18.3	121	20.4
	2,1	Dol-C1				110	
	2.1a	Dol-C1				125	
	2,2	Dol-C1				123	
	2,2a	Dol-C1	-66		17.9	112	20.1
	2,3	Dol-C1	-66			119	
	2,4	Dol-C1	-68		-17.5	112	19.9
	2,5	Dol-C1	-68.5		-18.3	120	20.4
		Dol-C1	-68.3		-17.6	116	19.9
Mean			**-65.9**		**-17.9**	**-122**	**20.2**

Well (Depth)	Chip #	HOST	Tf	Te	TmICE	Th	Weight % NaCl
03-29-43-01W5	1.1	Dol-C1	-61		-14.7	123	17.9
(2381.0 m)	1.2	Dol-C1	-66		-15.4	129	18.4
	1.2a	Dol-C1	-65		-15	126	18.2
	1.3	Dol-C1	-64		-15.2	129	18.3
	1.4						
	1.5	Dol-C1	-62		-14.9	114	18.1
	1.6	Dol-C1	-66		-14.7	140	17.9
	1.7	Dol-C1	-62			119	
Mean			**-64**		**-15.0**	**126**	**18.1**
03-29-43-01W5	2.1	Dol-R2 or -C1	-69		-17	122	19.5
2381.0 m	2.2	Dol-R2 or -C1					
	2.3	Dol-R2 or -C1	-70		-17.4	115	19.8
	2.4	Dol-R2 or -C1	-70		-17.3	117	19.7
	2.5	Dol-R2 or -C1					
	2.6	Dol-R2 or -C1	-68		-17.2	100	19.7
	2.6A	Dol-R2 or -C1	-69.2		-17	105	19.5
	2.7	Dol-R2	-71		-17.4	118	19.8
Mean			**-69**		**-17.2**	**113**	**19.7**

APPENDIX II

PALEOTEMPERATURE ESTIMATES
OF REPLACEMENT DOLOMITE PRECIPITATION

Appendix 2. Calculations of paleotemperature of replacement dolomite precipitation, assuming temperature of Devonian seawater= 25°C, $\delta^{18}O_{calcite}$= -3‰PDB, and isotopic equilibrium between calcite and sea water.

Equations (1), (2), and (3) are used to estimate the oxygen isotopic composition of sea water ($(^{18}O/^{16}O)_{water}$).

(1) 10^3 lnα= 2.78 X 10^6 (T)$^{-2}$(°K) - 2.89 for calcite (Friedman and O'Neil, 1977)

(2) α= $\dfrac{(^{18}O/^{16}O)_{calcite} \quad + 1000}{(^{18}O/^{16}O)_{fluid} \quad +1000}$ <-Upper Devonian fossils and submarine cements with $\delta^{18}O$ values of -3.0 ‰PDB.
                                                    <-solve

(3) $\delta^{18}O_{calcite} - \delta^{18}O_{fluid} \cong 10^3$ lnα

Combining equations (1) and (3):

(4) $\delta^{18}O_{calcite} - \delta^{18}O_{fluid} \cong 2.78$ X 10^6 (T)$^{-2}$(°K) - 2.89 = 28.4

$\delta^{18}O_{fluid} \cong \delta^{18}O_{calcite} - 28.4$

$\delta^{18}O_{calcite} = -3.0‰PDB = 27.8‰SMOW$ using:

$\delta^{18}O_{(SMOW)} = 1.031 \ \delta^{18}O_{(PDB)} + 30.86$

$\delta^{18}O_{fluid} \cong 27.8 - 28.4 \cong -0.6‰SMOW$

Use the $(^{18}O/^{16}O)_{fluid}$ estimated above, the measured $(^{18}O/^{16}O)_{dolomite}$ and solve for T with equations (5) and (6).

(5) 10^3 lnα= 2.78 X 10^6 (T)$^{-2}$(°K) + 0.91 (Land, 1985)

(6) α= $\dfrac{(^{18}O/^{16}O)_{dolomite} \quad + 1000}{(^{18}O/^{16}O)_{fluid} \quad + 1000}$ <-measured
                                           <-estimated from equ'n (1), (2), and (3)

Combine equations (5) and (6):

T = $[2.78$ x $10^6/((10^3$ln$\alpha) - 0.91)]^{1/2}$

For $\delta^{18}O_{dolomite}$= -3.71‰PDB, T= 52°C.

Some problems associated with this method

1. One important assumption in this approach is that the temperature of Devonian sea water was 25 °C. However, the presence of Devonian black shale in the "shallow" Alberta basin suggests anoxic condition and deposition in stratified waters. Therefore the waters in the basin may have been warmer and temperatures may have been as warm as 30 to 35°C. Using 35°C as opposed to 25 °C affects significantly the paleotemperature and paleodepth estimations.

2. The oxygen isotopic signature of Devonian brachiopods and submarine cements may have been subjected to postdepositional alteration which obscures or obliterates the original isotopic record (see Hudson and Anderson 1989 for criteria used to recognise unaltered material).

3. Dickson (1991) documented sector zoned calcite with $\delta^{18}O$ differing by up to -1‰ from one zone to another. This data suggest that calcite may not necessarily precipitate in isotopic equilibrium with sea water. The differences in oxygen isotopic composition from one zone to another (as documented so far) are not large enough to affect significantly our interpretations. However it is an important effect to keep in mind since one assumption of this method is that calcite is in isotopic equilibrium with sea water.